CHNICAL REPORT STANDARD TITLE PAGE

1. Report No.	2. Government Accession No.	3. Recipient's Catalog No.
FHWA/AZ-84/194-I		

4. Title and Subtitle	5. Report Date
STATIC AND DYNAMIC BEHAVIOR OF MONOTUBE SPAN-TYPE SIGN STRUCTURES Volume I - Final Report	May, 1984 6. Performing Organization Code

7. Author(s)	8. Performing Organization Report No.
M. R. Ehsani, S. K. Chakrabarti and R. Bjorhovde	

9. Performing Organization Name and Address	10. Work Unit No.
Arizona Transportation and Traffic Institute College of Engineering University of Arizona Tucson, Arizona 85721	11. Contract or Grant No. HPR-1-23(194)
12. Sponsoring Agency Name and Address Arizona Transportation Research Center Arizona Department of Transportation Arizona State University Tempe, Arizona 85281	13. Type of Report and Period Covered FINAL June 83 - May 84 14. Sponsoring Agency Code

15. Supplementary Notes Prepared in cooperation with the U.S. Department of Transportation, Federal Highway Administration, from a study of Monotube Span-Type Sign Structures. The opinions and conclusions are those of the authors and not necessarily of the Federal Highway Administration.

16. Abstract

The report presents the results of the first major investigation into the static and dynamic behavior characteristics of monotube span-type sign structures. Detailed static and dynamic stresses and deflections have been determined for an actual 100 ft span sign structure, utilizing 2- and 3-dimensional finite element modeling. Parametric studies have also been made, where the effects of column stiffness, beam stiffness, span, and sign location and size were examined. It is shown that in-plane and out-of-plane analyses can be conducted independently, and that stresses for tubular members can be determined by vector addition. Static in-plane deflections generally govern the design, but do not satisfy the current AASHTO requirement of $d^2/400$, where d=depth of sign in feet. Structural resonance is found for a very narrow range of wind speeds, assuming no damping and sustained wind over a prolonged period. Design recommendations are made on the basis of stress and deflection computations for simple planar frames. Cambering is recommended for structures where gravity load deflections may be aesthetically undesirable.

Volume II - Appendices, 61 pages

17. Key Words	18. Distribution Statement
Monotube; sign structures; single span; behavior; static; dynamic; stresses; deflections; design criteria; evaluating criteria.	No restrictions. This document is available to the public through the National Technical Information Service, Springfield, VA 22161.

19. Security Classif. (of this report)	20. Security Classif. (of this page)	21. No. of Pages	22. Price
Unclassified	Unclassified	105	

Form DOT F 1700.7 (8-69)

ACKNOWLEDGMENTS

The investigation described in this report was funded by the Arizona Department of Transportation in cooperation with the Federal Highway Administration under Project No. HPR-1-23 (194).

The authors would like to thank Dr. R. H. Wortman and R. A. Jimenez of the Department of Civil Engineering at the University of Arizona. Dr. Wortman was of significant help during the initial stages of the project, and Dr. Jimenez assisted in the administration of the project as the Director of the Arizona Transportation and Traffic Institute.

The continuous support and helpful suggestions of the Arizona Department of Transportation personnel, in particular Messrs. Frank R. McCullagh, Roger Hatton, Rudolf Kolaja, Jamal Sarsam, James Pyne, and Mike Sarsam are gratefully acknowledged.

The cooperation and hospitality of Valmont Industries, Inc. and especially those of Mr. Tom Sanderson during the visit to their manufacturing facilities located at Valley, Nebraska are appreciated.

Professor H. A. Kamel of the Department of Aerospace and Mechanical Engineering at the University of Arizona and his associates were helpful in resolving many problems associated with the use of the computer program GIFTS.

Thanks are also due Carole Goodman, who did an excellent job in typing the report.

TABLE OF CONTENTS
VOLUME I

		Page No.
1.	INTRODUCTION	1
2.	SCOPE AND OBJECTIVES	5
3.	PREVIOUS AND RELATED STUDIES	7
4.	STATIC BEHAVIOR OF MONOTUBE STRUCTURES	9
	4.1 Description of Typical Structure	9
	4.2 Modeling of the Structure	9
	4.3 Computer Program	15
	4.4 Loads on the Structure	18
	4.5 Results of the Static Analysis	20
5.	DYNAMIC BEHAVIOR OF MONOTUBE STRUCTURES	31
	5.1 Description of Typical Structure	31
	5.2 Modeling of the Structure	31
	5.3 Computer Program	31
	5.4 Loads	33
	5.5 Dynamic Behavior: Free Vibration of the Monotube Structure	37
	5.6 Dynamic Behavior: Forced Vibration of the Monotube Structure	46
	5.7 Correlation of Wind Speed and Maximum Amplitude	51
6.	PARAMETRIC STUDIES	54
	6.1 Choices of Parameters	54
	6.2 Results for Individual Structures	57
	6.3 Significance of Parameters	74
7.	DEVELOPMENT OF DESIGN RECOMMENDATIONS	77
	7.1 General Introduction	77
	7.2 Static versus Dynamic Behavior	77
	7.3 Two- vs. Three-Dimensional Analysis	80
	7.4 Proposed Analysis Procedure	82
	7.5 Simplified Criteria for Structural Evaluation	83
8.	CONCLUSIONS AND RECOMMENDATIONS	85
	8.1 Conclusions	85
	8.2 Recommended Future Studies	88
	REFERENCES	90

LIST OF FIGURES
VOLUME I

		Page No.
Fig. 1.1	Typical Monotube Sign-Support Structure	2
Fig. 1.2	Beam-to-Column Connection for a Sign-Support Structure	2
Fig. 1.3	Drawing of Monotube Structure	3
Fig. 4.1	Monotube Structure Used as a Base Model for Study	10
Fig. 4.2	Typical Beam-to-Column Connection	11
Fig. 4.3	Typical Base Detail for Monotube Structure	12
Fig. 4.4	Detail of Traffic Sign Support Bracket	13
Fig. 4.5	Discretized Model of Monotube Structure for Computer Analysis	14
Fig. 4.6	Typical Beam Splice Detail for Monotube Structure	16
Fig. 4.7	Details of Beam-to-Column Connection Element for FEM Modeling	17
Fig. 4.8	Global and Displacement Coordinates for Monotube Structures	21
Fig. 4.9	Components of the Static Displacement for Node No. 16 (i.e., at Midspan of Beam)	26
Fig. 5.1	Discretization for Dynamic Loads and Masses Due to Signs	32
Fig. 5.2	Relationship between Strouhal Number, S, and the Logarithm of Reynolds Number, R	34
Fig. 5.3	X-Y Elevation View of Mode 1 for 2D Natural Vibration	41
Fig. 5.4(a)	Isometric View of Mode 1 for 3D Natural Vibration	42
Fig. 5.4(b)	Z-Y Elevation View of Mode 1 for 3D Natural Vibration	43
Fig. 5.4(c)	X-Z Plane View of Mode 1 for 3D Natural Vibration	44
Fig. 5.4(d)	X-Y Elevation View of Mode 1 for 3D Natural Vibration	45
Fig. 5.5	Dynamic (Vortex Shedding) Loads on Monotube Structure for Wind Speed of 15 MPH	49
Fig. 5.6	Displacement Histories for Nodal Points 16, 18, 23 and 17, Due to a Wind Speed of 15 MPH	50
Fig. 5.7	Maximum Vertical Dynamic Deflections at Midspan of Beam for Different Wind Speeds	52
Fig. 6.1	Overall Dimensions for Base and Eight Parametric Models	55
Fig. 6.2	Discretized Model of Monotube Structure for Span Model 1	58
Fig. 6.3	Discretized Model of Monotube Structure for Span Model 2	59
Fig. 6.4	Maximum Vertical Dynamic Deflections at Midspan of Beam for Different Wind Speeds for Column Model #1	71
Fig. 6.5	Maximum Vertical Dynamic Deflectins at Midspan of Beam for Different Wind Speeds for Beam Model #1	72
Fig. 6.6	Maximum Vertical Dynamic Deflections at Midpsan of Beam for Different Wind Speeds for Span Model #1	73
Fig. 7.1	Beam Splice Detail to Achieve Suitable Chamber	79

LIST OF TABLES
VOLUME I

		Page No.
Table 4.1	Static Nodal Loads for Different Cases of Loading (lbs)	19
Table 4.2	Static Displacements (in) and Rotations (rad) Due to D + I + W (1) Load Combination	22
Table 4.3	Static Deflections for Different Load Combinations (in)	24
Table 4.4	Static Forces Due to D + I + W (1) Load Combinations	27,28
Table 4.5	Maximum Bending Stresses (1) (ksi)	30
Table 5.1	Natural Frequencies and Periods for Monotube Structure	40
Table 6.1	Member Cross-Sectional Data for Column and Beam Models	56
Table 6.2	Member Cross-Sectional Data for Span Models	60
Table 6.3	Comparison of Static Deflections and Bending Stresses Between the Base Model and the Column Models	61
Table 6.4	Comparison of Static Deflections and Bending Stresses Between the Base Model and the Beam Models	63
Table 6.5	Comparison of Static Deflections and Bending Stresses Between the Base Model and the Span Models	64
Table 6.6	Comparison of Static Deflections and Bending Stresses Between the Beam Model and the Sign Models	66
Table 6.7	Natural Frequencies and Periods for All Monotube Structure Models	67-69
Table 6.8	Static and Dynamic (Wind Vortex Shedding) Deflections At Midspan	75

TABLE OF CONTENTS
VOLUME II

		Page No.
Appendix A:	Natural Mode-Shape Data for Basic Monotube Structure	1
Appendix B:	Numerical Evaluation of a Monotube Structure	22
Appendix C:	Background of the $d^2/400$ - Requirement of AASHTO	56

LIST OF FIGURES
VOLUME II

		Page No.
Table A.1	Displacements and Rotations for Natural Mode No. 1 (2-D) . .	2
Table A.2	Displacements and Rotations for Natural Mode No. 2 (2-D) . .	3
Table A.3	Displacements and Rotations for Natural Mode No. 3 (2-D) . .	4
Table A.4	Displacements and Rotations for Natural Mode No. 4 (2-D) . .	5
Table A.5	Displacements and Rotations for Natural Mode No. 5 (2-D) . .	6
Table A.6	Displacements and Rotations for Natural Mode No. 6 (2-D) . .	7
Table A.7	Displacements and Rotations for Natural Mode No. 7 (2-D) . .	8
Table A.8	Displacements and Rotations for Natural Mode No. 8 (2-D) . .	9
Table A.9	Displacements and Rotations for Natural Mode No. 9 (2-D) . .	10
Table A.10	Displacements and Rotations for Natural Mode No. 10 (2-D). .	11
Table A.11	Displacements and Rotations for Natural Mode No. 1 (3-D) . .	12
Table A.12	Displacements and Rotations for Natural Mode No. 2 (3-D) . .	13
Table A.13	Displacements and Rotations for Natural Mode No. 3 (3-D) . .	14
Table A.14	Displacements and Rotations for Natural Mode No. 4 (3-D) . .	15
Table A.15	Displacements and Rotations for Natural Mode No. 5 (3-D) . .	16
Table A.16	Displacements and Rotations for Natural Mode No. 6 (3-D) . .	17
Table A.17	Displacements and Rotations for Natural Mode No. 7 (3-D) . .	18
Table A.18	Displacements and Rotations for Natural Mode No. 8 (3-D) . .	19
Table A.19	Displacements and Rotations for Natural Mode No. 9 (3-D) . .	20
Table A.20	Displacements and Rotations for Natural Mode No. 10 (3-D). .	21
Table B.1	Data on Elements	24
Table B.2	Static Forces and Moments by Computer Analysis	28
Table B.3	Static Deflections	29
Table B.4	Maximum Static Bending Stresses (ksi) by Computer Analysis	31
Table B.5	Static Forces and Moments by Simplified Analysis	51
Table B.6	Maximum Static Bending Stresses (ksi) by Simplified Analysis	53
Table B.7	Static Deflections by Simplified Analysis	55
Table C.1	Comparison of the Calculated Frequencies with AASHTO's Suggested Values	58

LIST OF FIGURES
VOLUME II

		Page No.
Figure B.1	Simplified Model for In-Plane Bending	32
Figure B.2	Dead Loads on the Simplified Model	33
Figure B.3	Ice Loads on the Simplifed Model	33
Figure B.4	Dead Loads on the Simplified Model for Deflection	41
Figure B.5	Ice Loads on the Simplified Model for Deflection	42
Figure B.6	Simplified Model for Out-of-Plane Bending	44

The contents of this report reflect the views of the authors who are responsible for the facts and the accuracy of the data presented herein. The contents do not necessarily reflect the official views or policies of the Arizona Department of Transportation or the Federal Highways Administration. This report does not constitute a standard, specification, or regulation. Trade or manufacturer's names which may appear herein are cited only because they are considered essential to the objectives of the report. The U. S. Government and the State of Arizona do not endorse products or manufacturers.

1. INTRODUCTION

For many years, truss-type structures have been successfully used to support traffic signs and other implements spanning over the highways. These structures typically consist of two columns supporting a truss or a tri-chord element, which spans accross the width of the road. The traffic signs are fastened to the truss at various locations above the traffic lanes.

The methods of design of highway sign structures are based on the requirements of AASHTO's Standard Specifications for Structural Supports for Highway Signs, Luminaires and Traffic Signals (1), revised in 1978 and 1979, and one of its predecessors, the AASHTO 1968 Specifications for the Design and Construction of Structural Supports for Highway Signs.

The Specifications have guidelines which limit the static deflection of truss span-type structures to an empirical value of $d^2/400$, where d is the depth of the sign in feet. It is clear that this is incomplete at best. For any sign support structure, if the static deflection is found to be excessive, the designer can specify a deeper sign (i.e., larger d), and thus satisfy the code requirements. In brief, the current AASHTO guidelines are for the most part limited to a requirement that the design be based on rational engineering judgment and principles.

Although the performance of the truss structures in general has been satisfactory, they are expensive to fabricate and, in most cases, the application of the deflection criterion has resulted in structures which are not economical, compared to the available pre-engineered structures. Therefore, due to the growing number of needed sign support structures, the trend has been shifting toward the use of monotube structures which are more economical and aesthetically pleasing.

The monotube structures consist of linearly tapered steel tubes with a constant wall thickness. Figure 1.1 shows a typical monotube sign support structure. As indicated in this figure, the columns are a one-piece tapered member with a larger cross section at the base. The beam consists of two tapered elements, connected such that the largest cross section is at the middle of the span. The beams are attached to the top of the columns by a simple connection, such as the one shown in Figure 1.2. Figure 1.3 shows a drawing of a monotube structure with the details of the connection of the beam elements at the midspan.

The Specifications do not address the design of monotube structures adequately and, in the case of cantilever structures in particular, the design is based entirely on "engineering judgment". In addition, there

Fig. 1.1 Typical Monotube Sign-Support Structure (Courtesy of Valmont Industries, Inc., Valley, Nebraska)

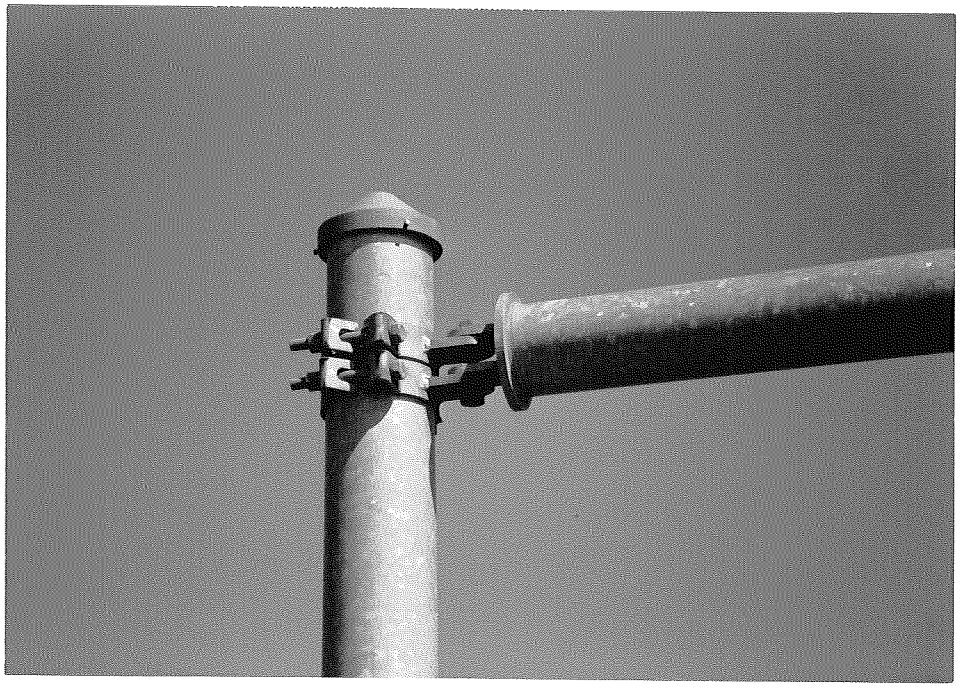

Fig. 1.2 Beam to Column Connection for a Sign-Support Structure (Courtesy of Valmont Industries, Inc., Valley, Nebraska)

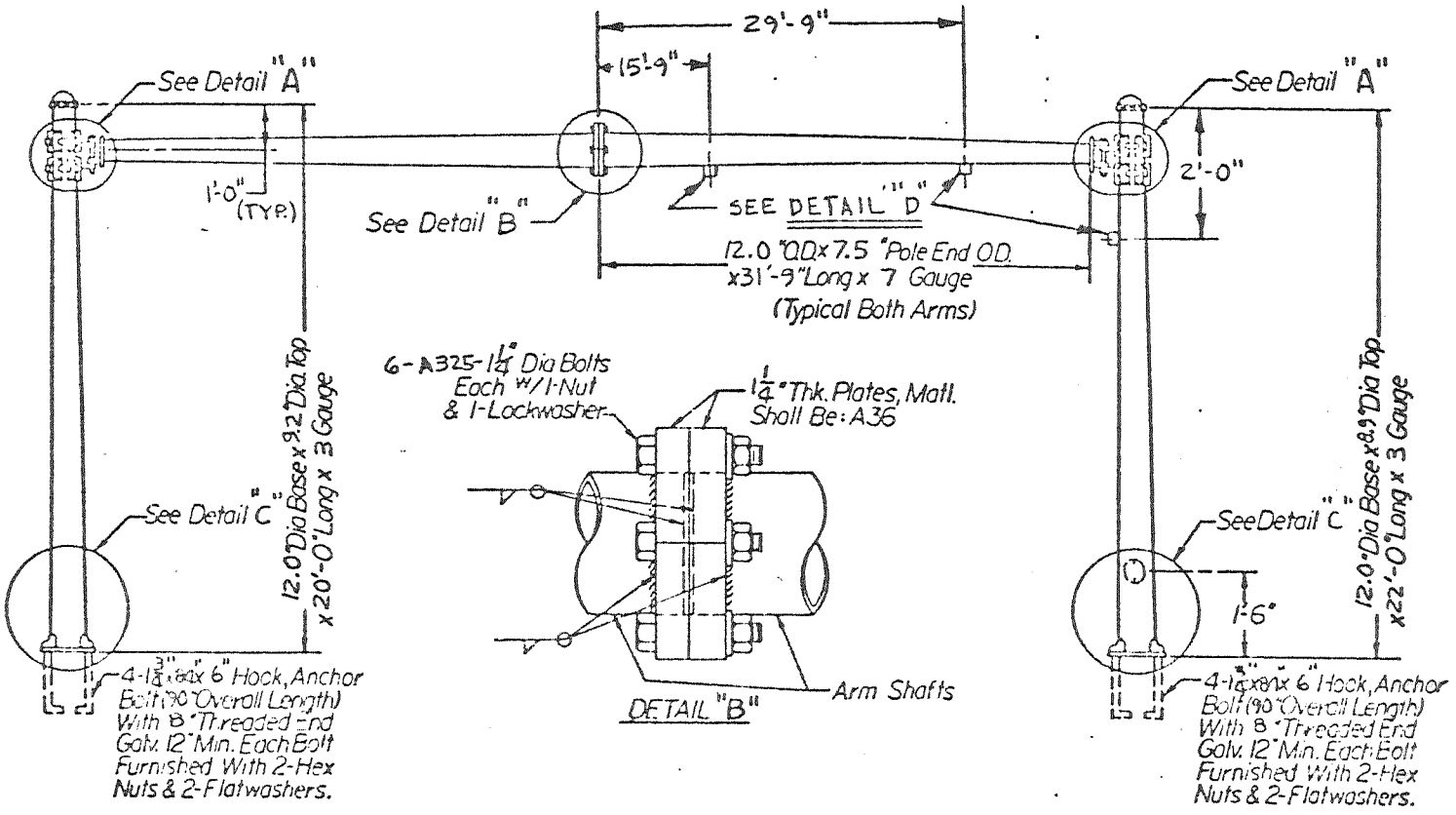

Fig. 1.3 Drawing of Monotube Structure (Courtesy of Valmont Industries, Inc., Valley, Nebraska)

are no guidelines for the design of structures supporting luminaires and traffic signals.

The lack of detailed and adequate design criteria can partly be attributed to a sparsity of research and engineering data on the behavior and strength of such structures. This is due to the complexity of the topic, which involves a need for an understanding of the response of the structure to wind loads (i.e., aerodynamic behavior of a light-weight structure), the influence of material types and cross sectional shapes of the monotubes, and the long-term service characteristics of the structure. The latter subject addresses the question of fatigue as well as the uses and re-uses of the structures. In particular, it is common practice to move a sign from one location to another, thereby changing the service conditions of the structure significantly. It is not known to what degree this form of usage changes the operating characteristics of the sign structure; conjecture can estimate that the cumulative effect of fatigue damage, for example, may be substantial.

The manufacturers of monotube structures, each having their own design procedures, produce such structures using sections which vary considerably both in material as well as cross sectional properties. As a result of this, the transportation authorities are faced with the problem of "accepting" or "rejecting" different designs without any rational guidelines to rely upon.

2. SCOPE AND OBJECTIVES

The primary objective of this study is to develop an appropriate analytical model which will enable the design engineers to provide a rational evaluation of the performance of monotube sign support structures. The study is limited to structures for which the beam elements are supported at both ends. Therefore, cantilever-type structures are excluded from consideration.

The effects of static and dynamic loading of the structures due to gravity and wind loads are examined in detail. Although in some cases fatigue may govern the behavior problems of this kind are not addressed in this study due to time limitations.

The scope of the study is given by the following five categories:

1. Survey and Review of Existing Structures and Design Methods

   a. Types of structures and materials.
   b. Fabrication practices.
   c. Design practices and criteria (e.g., which design specifications are used).
   d. Literature dealing with related structures and their strength and behavior.
   e. Any special subjects (e.g., unique base details, etc.).

2. Evaluation of Current Methods

   Evaluate current design philosophies and criteria, and compare them with existing specifications, such as AISC and AISI.

3. Development of Analytical Model

   Develop analytical model for the support structure with consideration of:

   a. Structural strength, including material and similar criteria.
   b. Stiffness (deflection).
   c. Dynamic characteristics, including thoe of the wind load and the response of the structure.

4. Model Evaluation

   Evaluation of model performance and comparison with current design methods.

5. Development of Design Criteria

Develop new design criteria, in light of findings in Sections (2), (3) and (4).

3. PREVIOUS AND RELATED STUDIES

Over the past fifteen years, a number of studies have been carried out dealing with the behavior of sign support structures. Each of these investigations concentrated on a certain aspect of the problem, which, although helpful in formulating the analysis of monotube structures, do not directly address the behavior of monotube sign support structures.

A few studies have examined the effects of wind on the structures, and the measurement of such parameters as the drag coefficient for different cross sections (2, 3, 4, 5, 6). Hay (4) compared the results of wind tunnel tests with field measurements on a full-scale sign gantry, and developed simple guidelines for approximating the wind forces on these structures. Zell (5) instrumented two sign support structures under service conditions, and concluded that for a typical structure, vehicle-induced gust loads do not appreciably reduce the life expectancy of the structure. Fung (6) provided a complete treatment of the determination of the forcing function as a result of vortex shedding, and the relationship between the wind speed and the vortex shedding frequency. A detailed discussion of this subject is presented in Chapter 5.

Studies have also been carried out on the structural properties and the feasibility of utilizing different materials in the construction of sign support structures. Although limited information is available which deals directly with sign support structures (7, 8), there are several references which address the design of structures made with tubular sections (9, 10, 11, 12). The work of Sherman (9) in producing design criteria for such nenbers, and the study to develop a design guide for outdoor advertising signs (10) are of significance. Similarly, the design specifications of the American Institute of Steel Construction (AISC) (11), and the American Iron and Steel Institute (AISI) (12) offer design criteria that are of direct use. There are otherwise available a number of papers and reports dealing with the behavior of tubular members; the lists of references given in the Commentary of Reference (10) are important in this respect.

A number of studies have dealt with the behavior of different types of structures subjected to wind, such as the work on wind-induced vibrations in antenna members by Weaver (13). However, the majority of the related studies deal with truss-type or tri-chord sign support structures (14, 15, 16). Kumar, et al. (14) analyzed two tri-chord structures subject to different wind velocities. They considered the vortex-shedding excitation of the structures under moderate wind velocities and the drag forces under severe gusts. Although they did recommend design procedures for truss-type structures, their main effort dealt with the evaluation of the Stockbridge damper to reduce the maximum displacement of the structure under vortex-shedding conditions.

Pelkey (17) studied the behavior of long span monotube structures that had been in place for two or three years, and concluded that for this category of structures, the $d^2/400$ limitation of AASHTO (1) can be relaxed. However, the study was very limited and no specific recommendations were made.

More recently, researchers have been concentrating on the effects of fatigue on these structures. Several studies by the departments of transportation in Kansas and California have either been completed (18, 19, 20, 21) or are currently in progress (22).

It is clear that as far as the monotube sign support structures are concerned, little information is available. However, due to the potential economies of these structures, it is imperative that concise guidelines be developed. This was the ultimate goal of the research work that is presented in this report.

4. STATIC BEHAVIOR OF MONOTUBE STRUCTURES

4.1 Description of Typical Structure

In order to make the study more realistic, it was decided to consider an existing monotube sign support structure as the base model. The Arizona Department of Transportation personnel provided the investigators with the shop drawings for a recently constructed sign support structure. It is located on the west-bound University Drive at the intersection of University Drive and Hohokam Expressway in Phoenix, Arizona.

Details of the dimensions of this structure are shown in Figure 4.1. The structure was designed in accordance with AASHTO Specification for Structural Supports of Highway Signs, Luminaries and Traffic Signals (1). The columns are linearly tapered circular tubes, with the largest diameter at the base of the column. Due to the site topography, the columns were constructed in different lengths in order to obtain the same elevation at the top of the columns. The beam is 100 feet long and is spliced at the approximate third points, in addition to at the middle of the span. The splices were designed such that the beam had its largest diameter at the midspan and tapered linearly to the ends of the span.

The beam-to-column connection is shown in Figure 4.2. It provides some moment resistance for in-plane bending, and essentially zero resistance for out-of-plane bending. Details of the column-base and the foundation are shown in Figure 4.3. It is reasonable to assume that the column is fully fixed at the base. The location of the traffic signs can be seen in Figure 4.1, and a typical sign bracket detail is illustrated in Figure 4.4.

4.2 Modeling of the Structure

The structure that is shown in Figure 4.1 was idealized and modeled for a finite element analysis. It was discretized in accordance with the guidelines of the computer program GIFTS (23), which was used in analyzing the structure. A detailed description of the program is given in the next section of the report.

The entire frame was discretized as an assembly of thirty beam elements, as shown in Figure 4.5. In order to analyze the frame in three-dimensional (3-D) space, each beam element was allowed to have three translational degrees of freedom at each node (i.e., displacements in the x, y and z directions) as well as three rotational degrees of freedom at each node (i.e., rotations about the x, y and z axes). The x, y and z axes, as indicated in Figure 4.5, are considered to be the global axes for the finite element analysis.

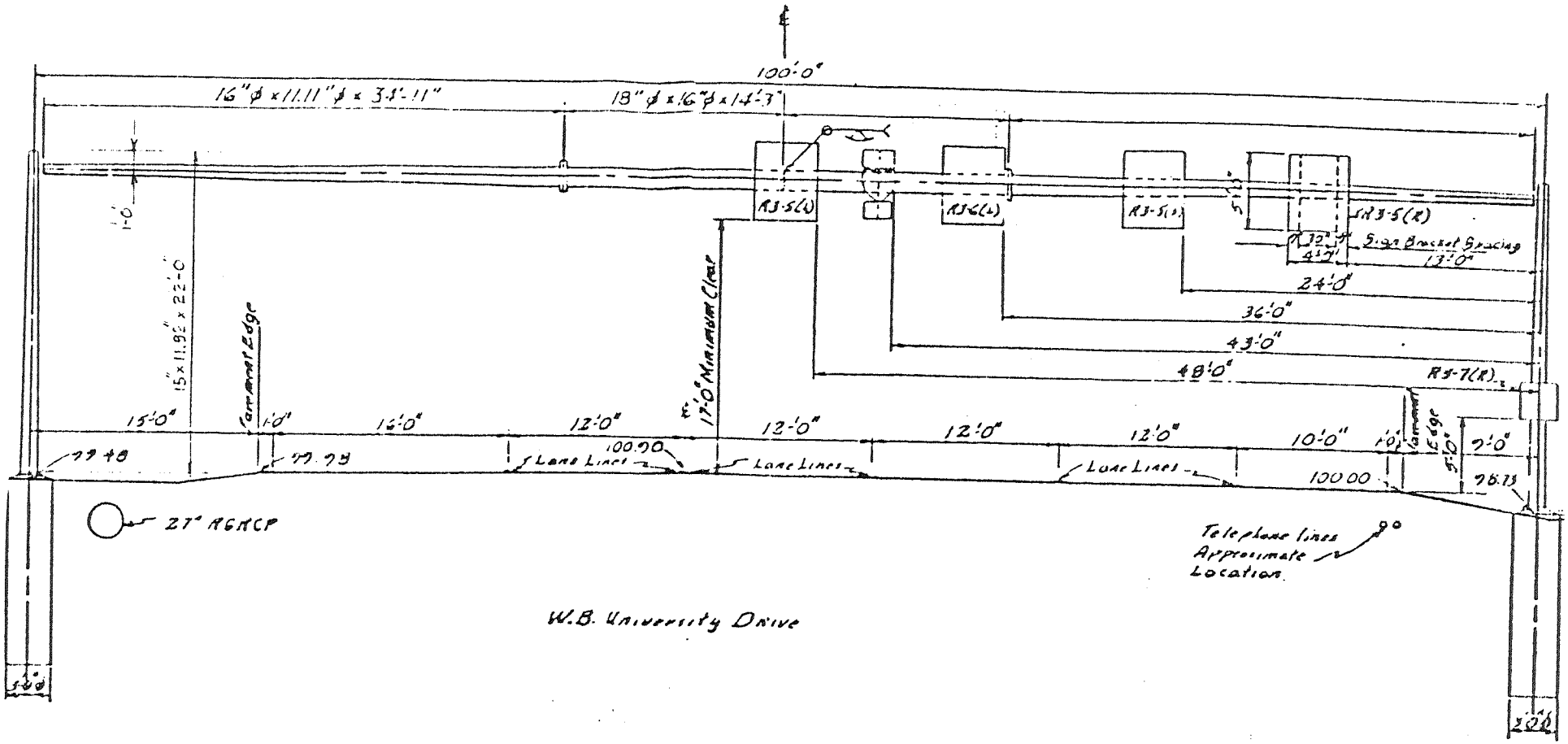

Fig. 4.1 Monotube Structure Used as Base Model for Study

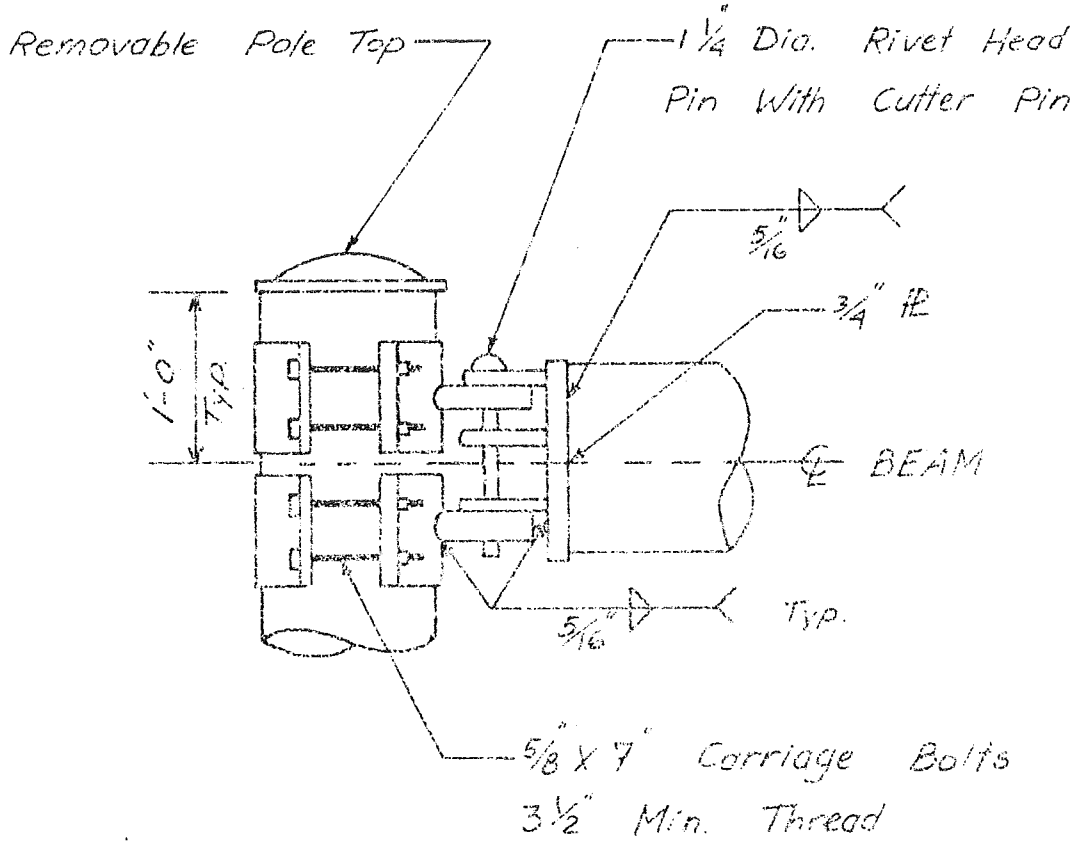

BEAM CLAMP DETAIL

Fig. 4.2 Typical Beam-to-Column Connection

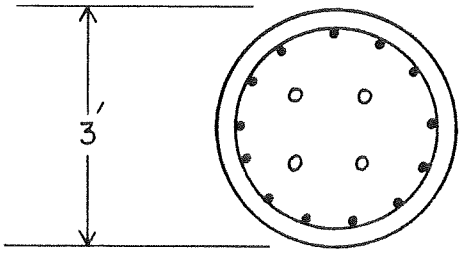

SECTION A–A

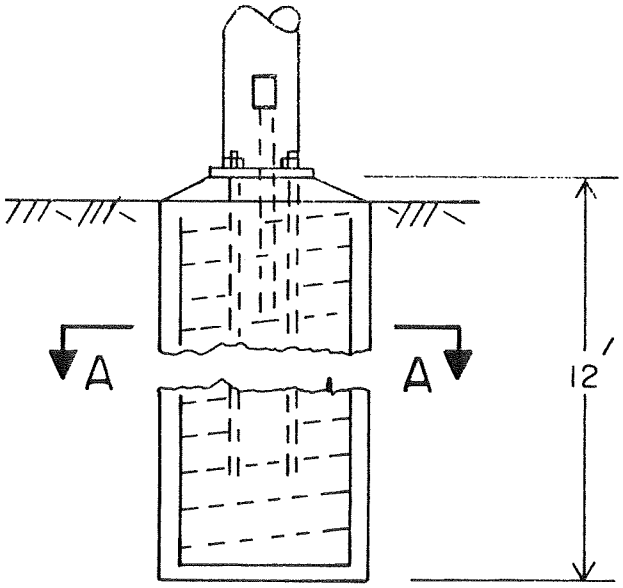

ELEVATION

Fig. 4.3 Typical Base Detail for Monotube Structure

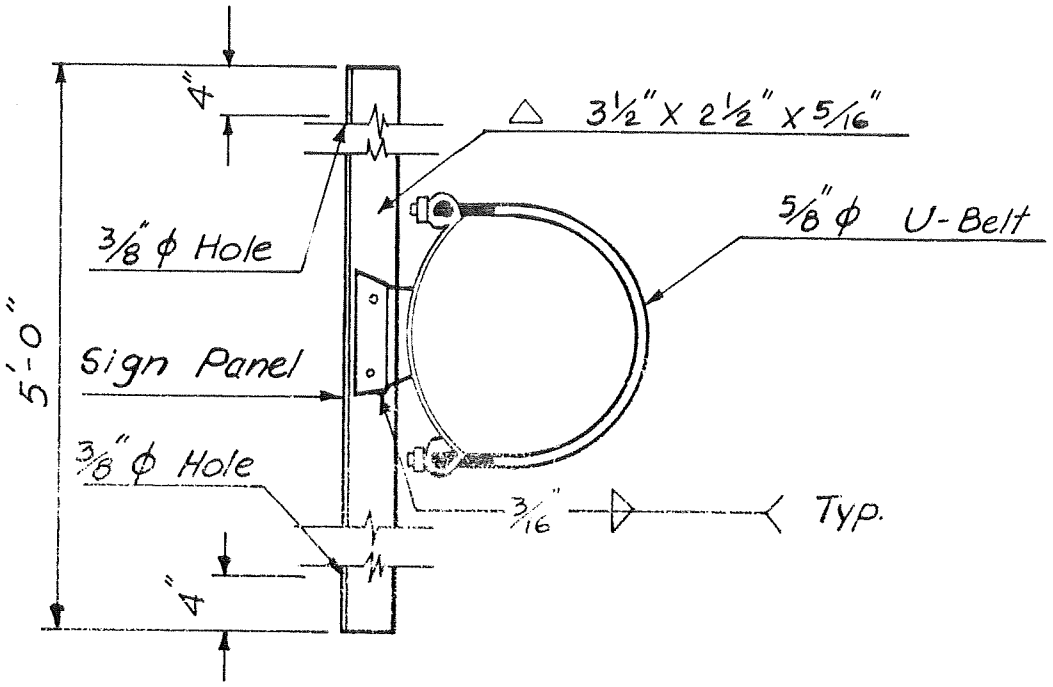

SIGN BRACKET
(Without Sign Light)

Fig. 4.4 Detail of Traffic Sign Support Bracket

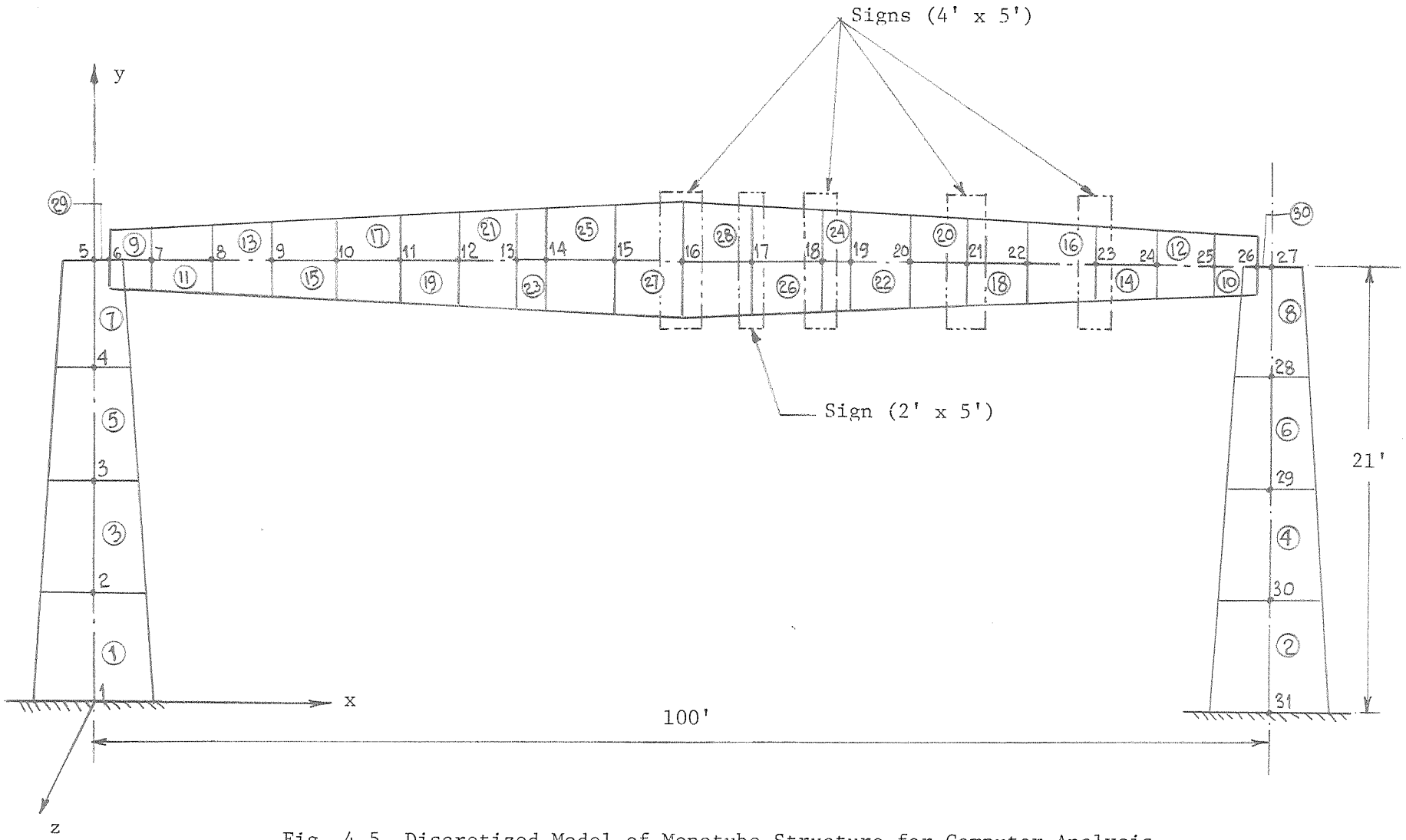

Fig. 4.5 Discretized Model of Monotube Structure for Computer Analysis

The program cannot accept elements with a varying cross section such as that of the tapered members used in monotube structures. Based on this limitation, the structure was modeled with a number of elements where the cross section of each was assumed to be constant and equal to the average of the cross sections at the two ends of that element. It is noted that, considering the large number of elements used for the analysis, this simplification will not result in any appreciable error. The wall thickness of the tubes was taken as 3/16-inch, which was the specified minimum wall thickness on the shop drawings.

The column base was considered to be fully fixed against all translational and rotational degrees of freedom. The beam splices shown in Figure 4.6 were assumed to provide full continuity between the adjoining members.

The most complicated element to model was the beam-to-column connection. The capacity of the connection in transferring shear forces depends on its cross sectional area, while its capacity in transferring bending moments is proportional to the moment of inertia. It was decided to model the connection as a short beam, having a rectangular cross section. The cross sectional area of the actual connection was used as the cross sectional area for the connection model. This assured comparable behavior in shear between the real connection and the connection model. Because the actual connection has almost no resistance in bending about the y-axis (out-of-plane), the connection rectangle had its longer side along the y-axis, as shown in Figure 4.7. The ratio of the dimensions of the rectangular connection model and its length along the x-axis was selected such that the z-axis bending stiffness of the actual connection and the model were approximately the same.

In selecting the elements for the beam, a node was always assumed at the centroid of each of the traffic signs, such as nodes number 16, 17, 18, 21 and 23 in Figure 4.5. It was assumed that the signs were connected to the beam at these points, and therefore the weight of the signs would be applied to the beam at these nodes.

4.3 Computer Program

After investigating a number of alternatives, it was decided to use the computer program GIFTS (Graphics-Oriented Interactive Finite Element Analysis Time-Sharing System) (23) for the analysis of the structure. This program, which has been developed at the University of Arizona, is a finite element pre- and post-processing and analysis package which may be implemented and run on a variety of minicomputers and time-sharing systems. It may be used with a graphics terminal, usually a storage tube device, or with an ordinary alphanumeric terminal. For this study,

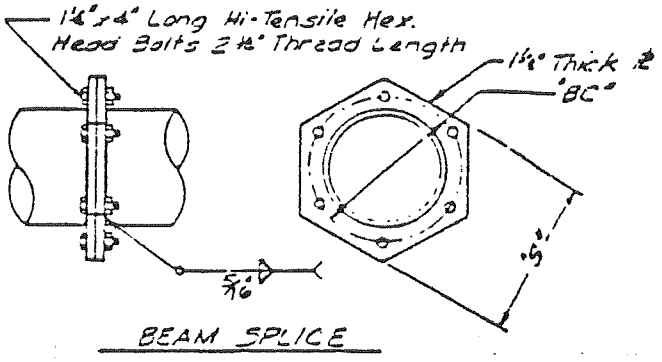

BEAM SPLICE DATA				
* Beam Size Thickness	Dia	"BC"	"S"	"T"
3/16"	16"	19"	20¼"	1⅛"

* Minimum

Fig. 4.6 Typical Beam Splice Detail for Monotube Structure

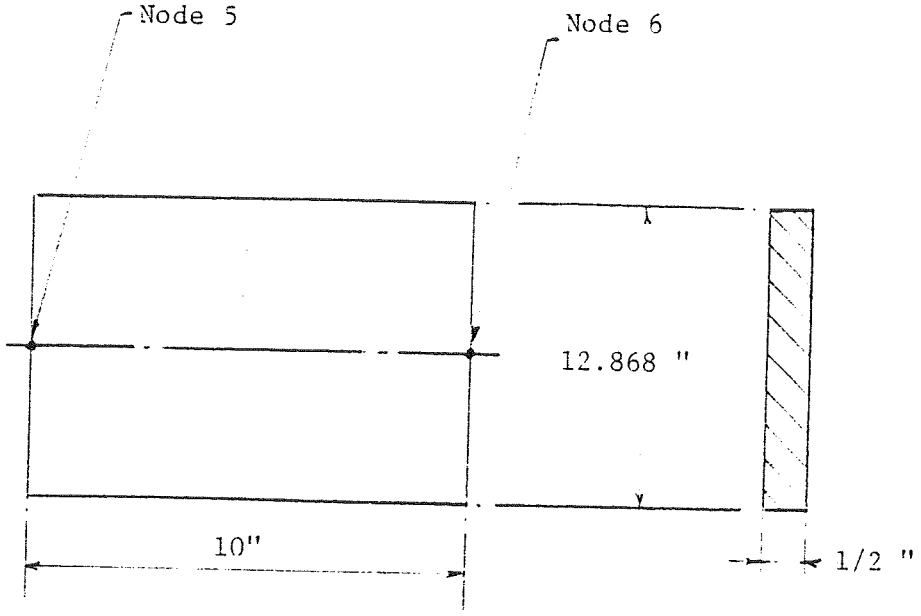

Fig. 4.7 Details of Beam-to-Column Connection Element for FEM Modeling

the program was run on the Data General Eclipse S-230 computer in the Department of Aerospace and Mechanical Engineering at the University of Arizona.

GIFTS is not a single program, but rather a group of fully compatible programs (modules), constituting a program library. Each module can be used for a specific function, such as stiffness matrix computation and assembly, or for a class of operations, such as load and boundary condition generation. GIFTS can handle different loads and loading cases on the structure, subjected to given boundary conditions for computation of stresses and deflections at all nodal points.

4.4 Loads on the Structure

The structure was analyzed for the static loads resulting from the self weight of the structure, ice loads, and wind pressure. A more detailed description of each loading case is given below.

4.4.1 Dead load. The weight of each element was calculated assuming a specific weight of 490 pounds per cubic foot for steel. The weight of each element was then equally divided between the two end nodes. The weights of the signs were calculated assuming that they weigh 10 pounds per square foot of surface area. These weights were assumed to act on the structure at the nodes where the beams support the signs, as discussed in Section 4.2. The nodal loads due to the dead load of the structure are listed in Table 4.1.

4.4.2 Ice load. In accordance with the Specifications (1), ice loads of 3 pounds per square foot of the actual area of the structural members and the signs was assumed to act on the structure. The ice loads were also divided among all nodes based on the tributary area of each node. The ice loads acting at each node are given in Table 4.1.

4.4.3 Wind load. Based on Specifications (1), the structure was analyzed for a maximum wind velocity of 70 miles per hour, blowing perpendicular to the plane of the frame, i.e., along the road. The statically equivalent wind loads have been computed as nodal loads, based on the tributary areas of the monotube members and the signs, in accordance with the Specifications (1). Considering the asymmetry of the structure with respect to the location of the traffic signs, the wind loads resulting from the wind blowing in two opposite directions were considered. Wind load (Case 1) corresponds to the wind blowing in the +z direction, and wind load (Case 2) corresponds to the wind blowing in the -z direction. The nodal loads resulting from the wind speed of 70 miles per hour are also listed in Table 4.1.

TABLE 4.1.
STATIC NODAL LOADS FOR DIFFERENT CASES OF LOADING (lbs)

Node No.	Dead Load[1,2]	Ice Load[2]	Wind Load (Case 1)[3]	Wind Load (Case 2)[4]
1	76	30	24.43	24.43
2	148	59	47.62	47.62
3	140	56	51	51
4	132	53	53.4	53.4
5	73	27	28.2	28.2
6	56	20	21.2	21.2
7	107	43	42.82	42.82
8	123	49	49.3	49.3
9	136	54	54.8	54.8
10	151	60	60.6	60.6
11	150	60	60.2	60.2
12	148	59	59.4	59.4
13	112	44	45	45
14	136	54	54.5	54.5
15	205	82	82	82
16	410	204	566.40	566.40
17	305	142	335	335
18	336	174	536.9	536.9
19	112	44	45	45
20	148	59	59.4	59.4
21	350	180	542.6	542.6
22	151	60	60.6	60.6
23	323	174	537.2	537.2
24	123	49	49.3	49.3
25	107	43	42.82	42.82
26	56	20	21.2	21.2
27	78	27	28.2	28.2
28	132	53	53.4	53.4
29	140	56	51	51
30	148	59	47.62	47.62
31	76	30	24.43	24.43

NOTES:

1. Dead Load includes loads due to the weight of the signs supported at applicable nodes.
2. Dead Loads and Ice Loads are applied in the -y direction (see Fig. 4.5).
3. Wind Load (Case 1) is applied horizontally at each node in the +z direction (see Fig. 4.5).
4. Wind Load (Case 2) is applied horizontally at each node in the -z direction (see Fig. 4.5).

A comprehensive static load analysis of the structure was carried out for which the following six loading combinations were considered:

1. Dead Load
2. Dead Load + Ice Load
3. Dead Load + Wind Load (Case 1)
4. Dead Load + Wind Load (Case 2)
5. Dead Load + Ice Load + Wind Load (Case 1)
6. Dead Load + Ice Load + Wind Load (Case 2)

All of these load combinations are realistic cases for the monotube structures. Due to the relative magnitude of the dead load versus the ice load, for example, the performance of the structure under pure self-weight is important. This applied both to sustained stress levels as well as the question of dead load deflections.

The governing gravity load combination will be No. 2 in the above listing, although ice load is not a realistic criterion in certain geographical areas. The two wind load cases are both valid for design, although Nos. 5 and 6 are extreme cases of combinations (i.e., dead load plus full ice load plus sustained wind of 70 mph). The importance of these will be discussed in detail in Chapter 7. However, it is noted that the allowable stresses for load combinations 3 to 6 are increased by 33-1/3% over those for static design (9, 11, 12).

4.5 Results of the Static Analysis

The static analysis of the structure was carried out for the different loading combinations specified in the previous section of this chapter. The output of the computer program GIFTS for the static analysis consists of the displacements and the stress-resultants for each node in the structure. Although the structure is symmetrical with respect to the overall geometry, member cross sections, column base supports, beam-to-column connections and splices, the asymmetric placement of the signs, which were located only on one-half of the span, as shown in Figure 4.1, results in asymmetrical displacements and stresses. It is noted that in addition to the dead load of the structure, which is affected by the asymmetric placement of the signs, the equivalent wind forces and the loads caused by the formation of ice on the structure also become asymmetric.

4.5.1 Static deflections. The nodal displacements and rotations are given with reference to the global ones x, y and z, and the sign convention for the displacments is shown in Figure 4.8. The deflection components in each of the x, y and z directions are defined as u, v and w, as shown in Figure 4.8. The nodal displacements and rotations for the case of dead plus ice plus wind load are in Table 4.2, as an example

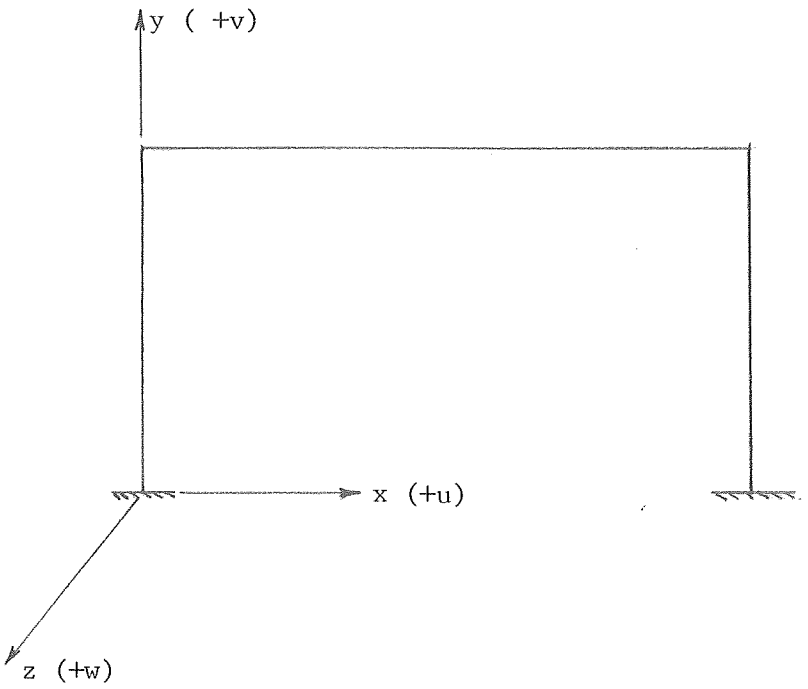

Fig. 4.8 Global and Displacement Coordinates for Monotube Structure

Table 4.2

Static Displacements (in.) and Rotations (rad.)
due to D + I + W(1) Load Combination

Node No.	Displacements (in)			Rotations (rad)		
	u	v	w	θ_x	θ_y	θ_z
1	0.000E-01	0.000E-01	0.000E-01	0.000E-01	0.000E-01	0.000E-01
2	-6.627E-02	-8.004E-04	1.020E-01	3.024E-03	-2.212E-04	1.724E-03
3	-1.923E-01	-1.589E-03	3.783E-01	5.510E-03	-4.799E-04	1.845E-03
4	-2.582E-01	-2.365E-03	7.883E-01	7.245E-03	-7.850E-04	-2.485E-04
5	-9.813E-02	-3.132E-03	1.276E 00	7.936E-03	-1.149E-03	-5.405E-03
6	-9.827E-02	-6.527E-02	1.457E 00	9.811E-03	-2.947E-02	-6.924E-03
7	-9.896E-02	-5.556E-01	2.925E 00	9.834E-03	-2.901E-02	-1.223E-02
8	-9.974E-02	-1.402E 00	4.625E 00	9.858E-03	-2.738E-02	-1.550E-02
9	-1.005E-01	-2.372E 00	6.203E 00	9.879E-03	-2.499E-02	-1.643E-02
10	-1.012E-01	-3.443E 00	7.753E 00	9.897E-03	-2.179E-02	-1.567E-02
11	-1.020E-01	-4.422E 00	9.082E 00	9.913E-03	-1.829E-02	-1.375E-02
12	-1.026E-01	-5.165E 00	1.006E 01	9.925E-03	-1.506E-02	-1.147E-02
13	-1.031E-01	-5.765E 00	1.085E 01	9.936E-03	-1.183E-02	-9.896E-03
14	-1.034E-01	-5.989E 00	1.115E 01	9.940E-03	-1.034E-02	-7.660E-03
15	-1.041E-01	-6.426E 00	1.176E 01	9.951E-03	-6.466E-03	-4.352E-03
16	-1.047E-01	-6.626E 00	1.209E 01	9.960E-03	-2.751E-03	-1.160E-03
17	-1.054E-01	-6.390E 00	1.215E 01	9.969E-03	1.189E-03	2.166E-03
18	-1.060E-01	-6.298E 00	1.190E 01	9.980E-03	5.781E-03	5.899E-03
19	-1.063E-01	-6.118E 00	1.172E 01	9.984E-03	7.655E-03	7.363E-03
20	-1.069E-01	-5.592E 00	1.114E 01	9.994E-03	1.190E-02	1.051E-02
21	-1.075E-01	-4.894E 00	1.031E 01	1.001E-02	1.639E-02	1.351E-02
22	-1.082E-01	-3.890E 00	9.054E 00	1.002E-02	2.155E-02	1.632E-02
23	-1.090E-01	-2.747E 00	7.460E 00	1.004E-02	2.650E-02	1.793E-02
24	-1.097E-01	-1.666E 00	5.743E 00	1.006E-02	3.037E-02	1.760E-02
25	-1.105E-01	-6.847E-01	3.828E 00	1.009E-02	3.301E-02	1.452E-02
26	-1.112E-01	-8.514E-02	2.149E 00	1.011E-02	3.380E-02	8.909E-03
27	-1.113E-01	-3.715E-03	1.928E 00	1.198E-02	1.488E-03	7.259E-03
28	1.470E-01	-2.789E-03	1.191E 00	1.096E-02	1.017E-03	1.515E-03
29	1.454E-01	-1.863E-03	5.713E-01	8.332E-03	6.215E-04	-1.071E-03
30	5.503E-02	-9.345E-04	1.539E-01	4.565E-03	2.865E-04	-1.367E-03
31	0.000E-01	0.000E-01	0.000E-01	0.000E-01	0.000E-01	0.000E-01

of the computer output. Similar results were obtained for all loading cases.

In order to analyze the static deflection results, four significant points on the structure were examined. These are given by nodes number 16, 18, 23 and 27, as shown in Figure 4.5. Point 27 is significant because it defines the top of the column, and node 16 is located at the middle of the span for the beam. It was expected that for most loading cases, the maximum static deflection would occur at this point. Points 18 and 23 were selected to study the variation of the displacements in the beam due to the asymmetric placement of the signs. The static deflections at the four points for the different loading combinations are given in Table 4.3.

It is noted that regardless of the load combination to which the structure was subjected, the static analysis of the structure was always carried out in three-dimensional space. The following conclusions can be made on the basis of the results given in Table 4.3.

(i) In the cases where the wind loads are excluded, such as the load combinations of dead load only and dead load plus ice load, the out-of-plane component of the deflection (i.e., w) is zero. In other words, the displacements of the frame occur entirely in the x-y plane, as expected.

(ii) The out-of-plane deflection of the frame, which is due to the wind load, is not affected by the magnitude of the applied gravity loads which act in the plane of the frame. This is to be expected for the level of gravity load and the type of structure that is being considered. As shown in Table 4.2, the w-component of the deflection is exactly the same for the loading combinations of dead plus wind loads and dead plus ice plus wind loads.

(iii) The in-plane deflection of the frame is not affected by the presence of the wind load. That is, the u- and v-components of the deflection for the loading cases of dead load only or dead load plus wind load are equal. Similarly, the u- and v-components of the deflection for the loading cases of dead plus ice load are identical to those for the case of dead plus ice plus wind load.

(iv) The displacement of the beam is primarily occurring in the plane of and in the same direction as the applied load. As shown in Table 4.3, the u-component of the deflection for points 16, 18 and 23 is at least one order of magnitude smaller than the deflections in the other directions. In other words, effects such as in-plane motion of the column are insignificant.

TABLE 4.3.
STATIC DEFLECTIONS FOR DIFFERENT LOAD COMBINATIONS (inches)

Load Combinations	Node Point	u	v	w
D	16	-0.065	-4.556	0.0
	18	-0.066	-4.320	0.0
	23	-0.068	-1.877	0.0
	27	-0.069	-0.003	0.0
D+I	16	-0.105	-6.626	0.0
	18	-0.106	-6.298	0.0
	23	-0.109	-2.747	0.0
	27	-0.113	-0.004	0.0
D+W(1)	16	-0.065	-4.556	12.090
	18	-0.066	-4.320	11.900
	23	-0.068	-1.877	7.460
	27	-0.069	-0.003	1.928
D+I+W(1)	16	-0.105	-6.626	12.090
	18	-0.106	-6.298	11.900
	23	-0.109	-2.747	7.460
	27	-0.113	-0.004	1.928

(v) The displacement of the top of the column (nodal point 27), primarily occur in the u-direction (in-plane horizontal) when wind forces are not included. This is due to the bending of the beam in the x-y plane, which causes the top of both columns to bend towards the middle of the span. However, when wind loads are considered, the deflection of the columns is primarily in the direction of the wind, i.e., the z-direction.

(vi) The out-of-plane deflection of the beam, i.e., in the z-direction, due to the statically equivalent loads corresponding to a wind velocity of 70 miles per hour is approximately twice the in-plane deflection of the beam due to the combined gravity loads.

Based on parts (i), (ii) and (iii) discussed above, it is concluded that for the service condition for which the structure responds elastically, the displacements from different cases of in-plane and out-of-plane loading can be combined to obtain the final deformed

configuration of the frame. In order to clarify this point, the process of displacement at the midspan of the beam is demonstrated in Figure 4.9. In this figure, the u-component of the deflection has been ignored due to its relatively small magnitude compared to the v- and w-components. Due to the dead plus ice load, point 16 will move 6.626 inches in the negative v-direction (vertically downwards). The equivalent static wind load for a wind speed of 70 mph causes the point to move 12.09 inches horizontally in the direction of the wind, i.e., the +w-direction. Thus, the total displacement of point 16 is equal to the length of the line AA', or

$$\sqrt{(6.626)^2 + (12.090)^2} = 13.78 \text{ in.}$$

An important observation is made with respect to the magnitude of the static deflection of point 16 compared to the allowable $d^2/400$ limit, as required by the current Specification (1). The signs that were attached to the structure that has been used for this study were five feet deep. This leads to an allowable maximum deflection of (5) $d^2/400 = .063$ ft. = 0.75 in. at the midspan of the beam. This is an order of magnitude smaller than the actual maximum static deflection of approximately 4.56 inches (for dead load). It is obvious that considering the stiffness and the span of these structures for a typical situation, the $d^2/400$ limitation cannot be satisfied for monotube single span sign structures.

The large out-of-plane deflection of the beam, discussed in (vi) above, is partly due to the type of the beam-to-column connection that is used, since it does not provide any resistance to bending out-of-plane. It is also noted that this deflection occurs under extreme loading combinations which include that due to a wind speed of 70 mph. As discussed in Chapter 5.4, the equivalent wind loads and the resulting deflections are proportional to the square of the wind speed. Therefore, under a more common wind speed of 20 miles per hour, the out-of-plane deflection of the beam will be approximately $12.09 \cdot (20/70)^2 = 0.99$ inches, which is roughly 1/1200 times the span length. These concepts, as well as the problems of realistic wind speeds and durations, will be discussed in detail in Chapter 6.

4.5.2 Static Stresses. Program GIFTS produces stress resultants at each node in terms of the local axes for that element. These include forces which are given in units of pounds and bending moments which are given in units of inch-pounds. The structure was analyzed for the different loading combinations listed in Section 4.4. The nodal forces for the case of dead plus ice plus wind load are listed in Table 4.4. As far as the analysis of the stress resultants is concerned, two significant points were selected and their stresses studied in detail.

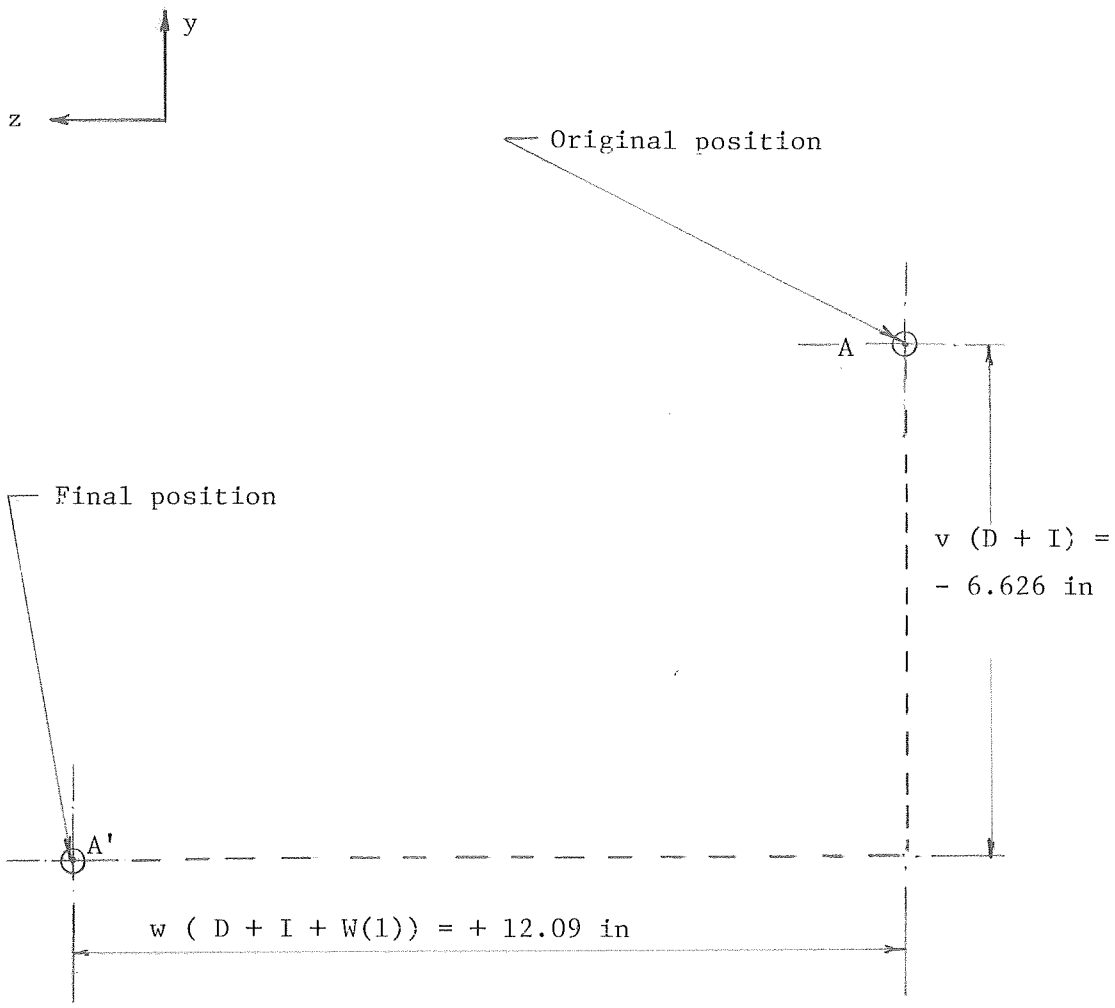

Fig. 4.9 Components of the Static Displacement for Node No. 16 (i.e. at midspan of beam)

Table 4.4

Static Forces due to D + I + W(1)
Load Combination

Elem. No.	Node No.	Axial Force (lbs)	Shear (in-pl.) (lbs)	Shear (out-of pl.)(lb)	Torsion (in-lb)	Moment (out-of-plane)	Moment (in-pl.)
1	1	-3.135E 03	2.628E 03	1.481E 03	-1.751E 04	-3.556E 05	-2.589E 05
	2	-3.135E 03	2.628E 03	1.481E 03	-1.751E 04	-2.623E 05	-9.333E 04
2	30	-3.640E 03	-2.628E 03	-2.205E 03	2.269E 04	-3.969E 05	-5.688E 04
	31	-3.640E 03	-2.628E 03	-2.205E 03	2.269E 04	-5.359E 05	-2.224E 05
3	2	-2.928E 03	2.628E 03	1.434E 03	-1.751E 04	-2.623E 05	-9.333E 04
	3	-2.928E 03	2.628E 03	1.434E 03	-1.751E 04	-1.720E 05	7.221E 04
4	29	-3.453E 03	-2.628E 03	-2.158E 03	2.269E 04	-2.610E 05	1.097E 05
	30	-3.453E 03	-2.628E 03	-2.158E 03	2.269E 04	-3.969E 05	-5.688E 04
5	3	-2.732E 03	2.628E 03	1.383E 03	-1.751E 04	-1.720E 05	7.220E 04
	4	-2.732E 03	2.628E 03	1.383E 03	-1.751E 04	-8.485E 04	2.377E 05
6	28	-3.257E 03	-2.628E 03	-2.107E 03	2.269E 04	-1.283E 05	2.742E 05
	29	-3.257E 03	-2.628E 03	-2.107E 03	2.269E 04	-2.610E 05	1.097E 05
7	4	-2.547E 03	2.628E 03	1.329E 03	-1.751E 04	-8.485E 04	2.377E 05
	5	-2.547E 03	2.628E 03	1.329E 03	-1.751E 04	-1.100E 03	4.033E 05
8	27	-3.072E 03	-2.628E 03	-2.053E 03	2.269E 04	1.101E 03	4.397E 05
	28	-3.072E 03	-2.628E 03	-2.053E 03	2.269E 04	-1.283E 05	2.742E 05
9	6	-2.628E 03	-2.371E 03	1.280E 03	1.102E 03	-4.507E 03	3.788E 05
	7	-2.628E 03	-2.371E 03	1.280E 03	1.102E 03	5.950E 04	2.603E 05
10	25	-2.628E 03	2.894E 03	-2.004E 03	1.102E 03	9.775E 04	2.652E 05
	26	-2.628E 03	2.894E 03	-2.004E 03	1.102E 03	-2.444E 03	4.100E 05
11	7	-2.628E 03	-2.221E 03	1.237E 03	1.102E 03	5.948E 04	2.603E 05
	8	-2.628E 03	-2.221E 03	1.237E 03	1.102E 03	1.337E 05	1.270E 05
12	24	-2.628E 03	2.746E 03	-1.961E 03	1.102E 03	2.154E 05	1.004E 05
	25	-2.628E 03	2.746E 03	-1.961E 03	1.102E 03	9.777E 04	2.652E 05
13	8	-2.628E 03	-2.049E 03	1.188E 03	1.102E 03	1.337E 05	1.270E 05
	9	-2.628E 03	-2.049E 03	1.188E 03	1.102E 03	2.050E 05	4.083E 03
14	23	-2.628E 03	2.574E 03	-1.911E 03	1.102E 03	3.301E 05	-5.401E 04
	24	-2.628E 03	2.574E 03	-1.911E 03	1.102E 03	2.155E 05	1.004E 05
15	9	-2.628E 03	-1.859E 03	1.133E 03	1.102E 03	2.050E 05	4.047E 03
	10	-2.628E 03	-1.859E 03	1.133E 03	1.102E 03	2.799E 05	-1.196E 05

Table 4.4 (cont'd)

Static Forces due to D + I + W(1)
Load Combination

Elem. No.	Node No.	Axial Force (lbs)	Shear (in-pl.) (lbs.)	Shear (out-of plane)	Torsion (in-lb)	Moment (out-of-plane)	Moment (in-pl.)
16	22	-2.628E 03	2.077E 03	-1.374E 03	1.102E 03	4.208E 05	-1.911E 05
	23	-2.628E 03	2.077E 03	-1.374E 03	1.102E 03	3.302E 05	-5.400E 04
17	10	-2.627E 03	-1.648E 03	1.073E 03	1.102E 03	2.798E 05	-1.186E 05
	11	-2.627E 03	-1.649E 03	1.073E 03	1.102E 03	3.506E 05	-2.273E 05
18	21	-2.628E 03	1.866E 03	-1.314E 03	1.102E 03	5.076E 05	-3.143E 05
	22	-2.628E 03	1.866E 03	-1.314E 03	1.102E 03	4.208E 05	-1.911E 05
19	11	-2.628E 03	-1.438E 03	1.013E 03	1.102E 03	3.505E 05	-2.273E 05
	12	-2.628E 03	-1.438E 03	1.013E 03	1.102E 03	4.098E 05	-3.115E 05
20	20	-2.628E 03	1.336E 03	-7.706E 02	1.102E 03	5.527E 05	-3.924E 05
	21	-2.628E 03	1.336E 03	-7.706E 02	1.102E 03	5.076E 05	-3.143E 05
21	12	-2.628E 03	-1.231E 03	9.539E 02	1.102E 03	4.098E 05	-3.115E 05
	13	-2.628E 03	-1.231E 03	9.539E 02	1.102E 03	4.656E 05	-3.835E 05
22	19	-2.629E 03	1.129E 03	-7.112E 02	1.102E 03	5.944E 05	-4.585E 05
	20	-2.628E 03	1.129E 03	-7.112E 02	1.102E 03	5.527E 05	-3.925E 05
23	13	-2.628E 03	-1.075E 03	9.073E 02	1.102E 03	4.655E 05	-3.835E 05
	14	-2.628E 03	-1.075E 03	9.073E 02	1.102E 03	4.900E 05	-4.125E 05
24	18	-2.627E 03	9.727E 02	-6.493E 02	1.103E 03	6.124E 05	-4.847E 05
	19	-2.627E 03	9.727E 02	-6.493E 02	1.103E 03	5.948E 05	-4.585E 05
25	14	-2.628E 03	-8.860E 02	8.531E 02	1.102E 03	4.900E 05	-4.125E 05
	15	-2.629E 03	-8.860E 02	8.531E 02	1.102E 03	5.514E 05	-4.763E 05
26	17	-2.628E 03	4.642E 02	-1.302E 02	1.102E 03	6.217E 05	-5.181E 05
	19	-2.628E 03	4.642E 02	-1.302E 02	1.102E 03	6.123E 05	-4.847E 05
27	15	-2.628E 03	-5.981E 02	7.713E 02	1.102E 03	5.514E 05	-4.762E 05
	16	-2.628E 03	-5.981E 02	7.713E 02	1.102E 03	6.070E 05	-5.193E 05
28	16	-2.627E 03	1.469E 01	2.063E 02	1.102E 03	6.070E 05	-5.193E 05
	17	-2.627E 03	1.469E 01	2.063E 02	1.102E 03	6.218E 05	-5.192E 05
29	5	-2.627E 03	-2.447E 03	1.301E 03	1.102E 03	-1.751E 04	4.033E 05
	6	-2.627E 03	-2.447E 03	1.301E 03	1.102E 03	-4.503E 03	3.789E 05
30	26	-2.628E 03	2.972E 03	-2.025E 03	1.102E 03	-2.435E 03	4.100E 05
	27	-2.628E 03	2.972E 03	-2.025E 03	1.102E 03	-2.269E 04	4.397E 05

The latter were obtained by simple stress analyses, using the stress resultant values.

The first point is node 16, located at the middle of the span of the beam, where the largest displacements and beam stresses were expected to occur. The second point is node 31, located at the base of the column, where a combination of bending and axial stresses are likely to control the design of the column.

The normal stresses for points 16 and 31 for different loading combinations are given in Table 4.5. It is clear that the maximum static stress occurs at the base of the column under a combination of dead plus ice plus wind loads, and is equal to 18.65 ksi. The maximum bending stress at the midspan of the beam under a combination of gravity and equivalent wind loads has been calculated as 17.30 ksi. As far as the static behavior of the structure is concerned, both of these stresses provide ample margins of safety for the structure. In particular, it is observed that the steel that is commonly used in monotube structures has a yield stress of 55 ksi. Using the AISC Specification (11), for example, this gives basic allowable stresses for circular prismatic tubular members as

(a) Gravity loads only: $F_{all} = 0.6\ F_y = 33$ ksi

(b) Gravity + Wind loads: $F_{all} = 1.33.33 = 44$ ksi

and it is seen that the allowable values are well in excess of the actual stresses. It is therefore obvious that it is not difficult to meet the strength requirements of the specifications. The current serviceability criterion is the $d^2/400$ formula; its value for the monotube structures has been commented upon and will be further discussed in Volume II (Appendix C).

TABLE 4.5
Maximum Bending Stresses (1) (KSI)

Load Combination	Midspan of Beam	At Base of Column
D	7.70	5.54
D + I	11.23	8.11
D + W	15.22	17.70
D + I + W	17.30 (2)	18.65

---

(1) Axial stresses are not included; their values are well below 1 ksi everywhere.

(2) Typically calculated with the data from Table 4.4 as

$$\frac{M}{S} = \frac{\sqrt{M_y^2 + M_z^2}}{S}$$, for point 16.

S = 46.24 in^3 = section modulus for cross section at this point on the beam; M_y = 607 k-in and M_z = 519.3 k-in for this loading case. In other words, biaxial bending is considered.

5. DYNAMIC BEHAVIOR OF MONOTUBE STRUCTURES

5.1 Description of Typical Structure

The structure that was used for the static behavior study was also used to evaluate the dynamic behavior. This facilitates a coordinated study of the static and dynamic behavior of the same structure, in order to observe the relationships between the two with respect to its response to normal loading conditions. The structure and its different structural details have been shown in Figures 4.1 to 4.4.

5.2 Modeling of the Structure

The finite element discretization that was used for the static model was also utilized to examine the dynamic behavior of the monotube structure. The original structure is shown in Figure 4.1; the FEM discretization is given in Figure 4.5.

The structure is idealized as either a plane frame or a space frame with masses lumped at the finite element nodes, depending on whether 2D or 3D modeling is to be done. The masses of the traffic-signs are lumped at the relevant nodes. In all cases, the lumped masses are assumed to have only translational degrees of freedom.

The basic finite element model with additional masses for signs is shown in Figure 5.1. The lumped masses for the bare frame are automatically generated and applied, as needed by the computer program, (23) and are therefore not shown in Figure 5.1.

5.3 Computer Program

The computer program GIFTS (23) that was used for the static analysis is also used for the dynamic evaluation. A general description of this program has been provided in Chapter 4.3.

5.3.1 Determination of natural nodes of vibration. The computer program GIFTS (23) uses the "subspace iteration method" for the computation of the eigenvalues and modes which give the natural frequencies and mode shapes. GIFTS handles the masses in lumped format in the translational directions only. For a given frame, the program generates the mass matrix for the masses of the bare frame, along with any additional lumped mass considering only the translational degrees of freedom. In this way, the program is capable of giving at the most the first ten natural frequencies and mode shapes. This is usually more than sufficient for civil engineering structures.

5.3.2 Transient response analysis. A structure subjected to time-dependent loads will have a time-dependent response. GIFTS can determine this, considering the external loads and the inertia of the

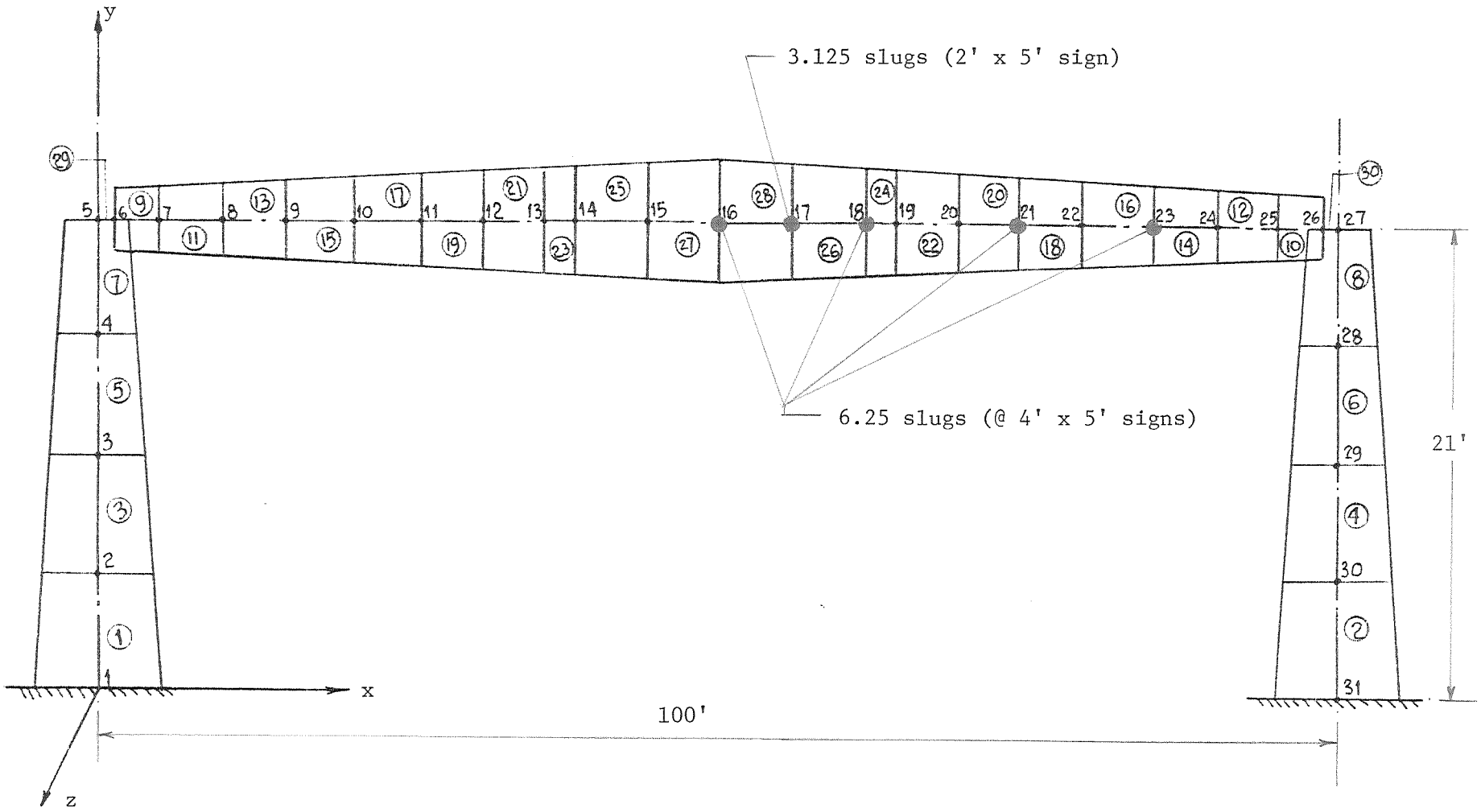

Fig. 5.1 Discretization for Dynamic Loads and Masses due to Signs

structure as well as damping forces. The transient response analysis can be performed using GIFTS through one of the five different methods. The methods are: (1) Modal Analysis, (2) Houbolt Method, (3) Newmark's Beta Method, (4) Wilson's Theta Method, and (4) Trapezoidal Rule.

The program has been used to obtain the response of the sign support structure when it is subjected to a time-dependent vortex-shedding force. This is caused by wind blowing across the plane of the frame, but the vortex-shedding occurs in-plane. A detailed discussion of the development of these loads is given in Chapter 5.4.

The computer program can compute the response of the structure under the action of the time-dependent loads at specified time steps. After obtaining the response of the structure in terms of deflections at different nodes of the finite element model, the dynamic stresses may be computed at the same time steps at which the deflections have been determined.

Modal analysis is very effective in finding the principal modes and the corresponding natural frequencies that dominate the dynamic behavior. This analysis may be performed effectively by using the first few dominant modes.

The other four methods are basically different forms of direct time integration schemes. Regarding these direct integration schemes, it can be said that the quality of the results is largely dependent upon the choice of time-step size. This depends on the dominant natural frequencies of the structure and the excitation frequency.

5.4 Loads

A stead wind blowing against a cylindrical structural member induces vibrations in the member that are perpendicular to the wind direction, due to the formation of vortices alternatively on the two sides of the member in addition to the wind itself.

The frequency Ω of the alternating vortices is determined from the equation

$$\Omega = \frac{SV}{D} \qquad (5.1)$$

where S is the non-dimensional Strouhal number, which varies with the Reynolds Number R, as illustrated in Figure 5.2 (6). V is the wind velocity and D is the diameter of the cylindrical member.

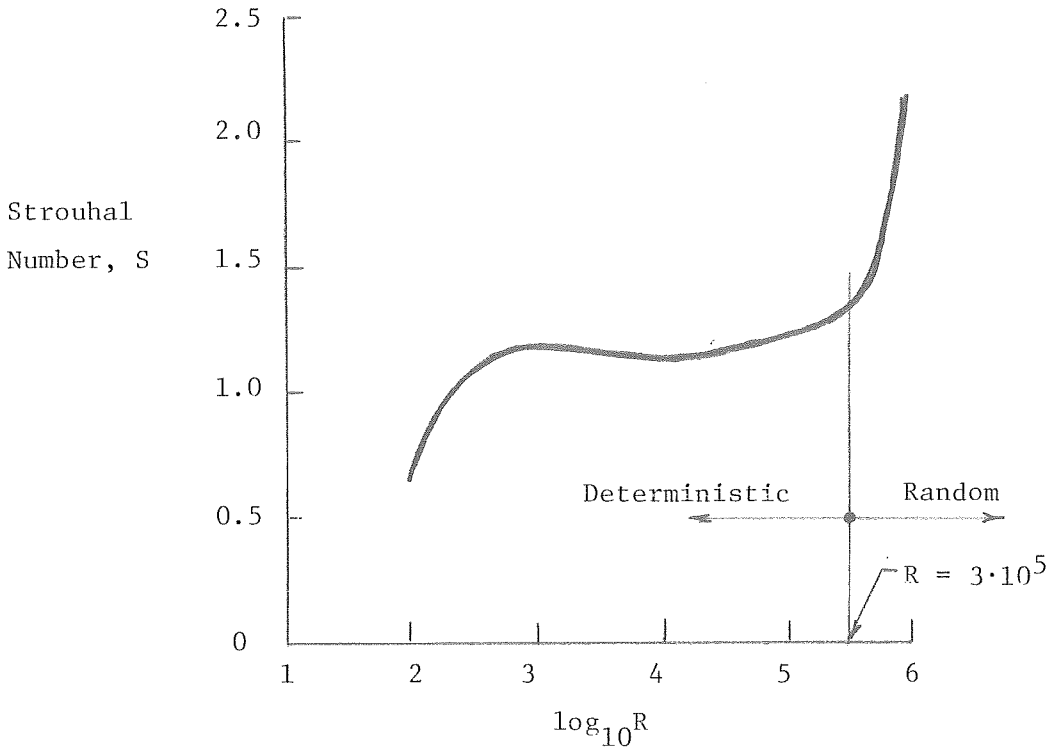

Fig. 5.2 Relationship Between Strouhal Number, S, and the logarithm of Reynolds Number, R (6).

The Reynolds Number for air is defined as

$$R = 780.5 \cdot V \cdot D \qquad (5.2)$$

where V is the wind velocity in miles per hour and D is the diameter of the cylinder in inches.

For the purpose of computing the response of an elastic system, the following two ranges of R must be considered (6):

1. For $300 < R < 3 \times 10^5$, the forcing function is sinusoidal with a deterministic frequency but a random amplitude.

2. For $R > 3 \times 10^5$, the forcing function is sinusoidal but with random frequency and random amplitude. The first range is of primary interest because most members of highway sign structures subjected to moderate wind velocities fall into this category.

Vortex shedding forces can and have been observed to cause sustained vibrations when the frequency of vortex shedding is nearly equal to the frequency of one of the natural modes of vibration of the structure (13). If the structural damping is small, as in the case of monotube structures, and if the wind remains steady, it is possible that large amplitude vibrations may develop.

For $300 < R < 3 \times 10^5$, the generally accepted expression for the alternating force is (13):

$$F(t) = \frac{1}{2} \rho V^2 A_p C_L \sin\Omega t \qquad (5.3)$$

where $F(t)$ = time dependent vortex shedding force
ρ = density of dry air
V = velocity of wind
A_p = projected area of the cylinder
C_L = force coefficient
t = time

To account for the random force amplitude, Weaver (13) has experimentally determined the root-mean-square (rms) values of C_L (denoted as $\bar{C}_L$), and using these the expression for the alternating force becomes:

$$F(t) = \frac{1}{2} \rho V^2 A_p \bar{C}_L \sin\Omega t \qquad (5.4)$$

5.4.1 Determination of F(t): Vortex shedding frequency equal to natural frequency. As an example, the vortex shedding frequency that equals the first mode natural frequency of 0.469 cps (three-dimensional) will be determined. This is an iterative procedure and is demonstrated in the following (13). It is noted that the value of the average diameter of the cylindrical members, D, has been set as 14 inches.

First Trial: V = 2 mph
From Eq. (5.2):

$$\log_{10}R = \log_{10}(780.5 \times 2 \times 14) = 4.34$$

Figure 5.2 then gives a value of S = 1.16.

From Eq. (5.1), using Ω = 0.469 cps, S = 1.16, and D = 14 inches, the value of V is obtained as:

$$V = 0.469 \times 2 \times \frac{14}{1.16}$$

$$= 2.02 \text{ mph}$$

Second Trial: V = 2.02 mph

$$\log_{10}R = \log_{10}(780.5 \times 2.02 \times 14) = 4.344$$

From the plot of S vs. $\log_{10}R$, the value of S is obtained as 1.16. Confirming that the iteration scheme has converged, using Ω = 0.469 cps, S = 1.16, and D = 14 inches, the value of V is found from Eq. (5.1) as 2.02 mph.

This trial therefore has given a wind velocity of 2.02 mph that will produce vortex shedding with a frequency equal to 0.469 cps; i.e., matching the natural frequency of the first 3D mode of structure. The forcing function, F(t), is determined from Eq. (5.4):

$$F(t) = 1/2\rho V^2 A_p \overline{C_L} \sin \Omega t$$

where ρ = 0.002378 slug/ft^3

V = 2.02 mph = 2.963 ft/sec

A_p = projected area (ft^2) for a node of the finite element model (see Fig. 5.1)

$\overline{C_L} = 1.0$

$\Omega = 2\,\pi(0.4692)$ rad/sec

Hence: $F(t) = 1/2\ (.002378)\cdot(2.963)^2\cdot A_p\cdot(1.0)\cdot\sin[2\pi(0.4692)t]$

$$F(t) = 0.01044\cdot A_p\cdot\sin[2\ \ (0.4692)t] \qquad (5.5)$$

This equation for F(t) can be used to find the individual nodal point loads due to the vortex shedding. It is important to note that for nodes on the column member, F(t) acts horizontally in-plane, whereas for the nodes on the beam member, F(t) acts vertically in-plane. Again, the vortex shedding takes place in a plane perpendicular to the wind direction and the longitudinal axis of the individual member.

5.4.2 Determination of F(t) for any wind velocity. In order to study the response at any wind velocity for Reynolds Numbers in the range of $300 < R < 3 \times 10^5$, the forcing function F(t) can be determined as shown in the following example.

As an example, a wind speed of V = 25 mph is considered. Hence, with a tube diameter of 14", this gives $\log_{10}R = \log_{10}(780.5 \times 25 \times 14) = 5.44$. From the plot of S vs. $\log_{10}R$ (see Fig. 5.2), the value of S is obtained as 1.32143.

From Eq. (5.1), using S = 1.32143, V = 25 mph = 439.99 in/sec, and D = 14 in, the value of Ω is found as:

$$\Omega = 1.32143 \times \frac{439.99}{14} = 6.61 \text{ cps.}$$

F(t) is now determined from Eq. (5.4) as

$$F(t) = 1/2\ (.002378)\ (36.67)^2\ A_p\ (1.0)\ \sin\ [2\pi\ (6.6097)t]$$

$$F(t) = 1.599\ A_p\ \sin\ [2\pi(6.6097)t]$$

where 36.67 is the wind speed in ft/sec. The nodal forces can now be found for each individual node, given the corresponding value of A_p.

5.5 Dynamic Behavior: Free Vibration of the Monotube Structure

5.5.1 General Introduction. The free natural vibration characteristics of the structure are representative of the dynamic behavior of the structure without the influence of any external load or forcing function, as the dynamic load is often called. These properties can be determined by an iterative technique, such as subspace iteration, and the structure can be treated as a distributed or lumped mass system. The

former mass distribution approach gives a structure with an infinite number of degrees of freedom; the latter, which has been used to analyze the monotube sign structure, has a number of degrees of freedom that can be given as

$$(NDF) = (NP) \cdot (NFP) - (NFP)_S \qquad (5.6)$$

where NP = number of nodal points in the structure, NFP = number of degrees of freedom at each nodal point, and $(NFP)_S$ = number of suppressed degrees of freedom. The value of NFP, therefore, takes into account whether the analysis has been based on a three- or a two-dimensional representation of the structure.

A number of studies have described the numerical procedures that can be used to obtain the free vibration characteristics of a structure; the book by Clough and Penzien (24) represents an up-to-date and practical reference. The discretization of the monotube structure is described in detail in Chapter 4.2; the numerical technique that has been used to arrive at the natural dynamic properties is described in section 4 of this chapter.

The natural vibration characteristics of a structure are particularly important when it is being subjected to a set of dynamic loads. The frequencies of the loads and those of the bare structure may be such that the actual response is a magnification of the natural vibrations. In the most unfavorable case, there is agreement between the loading frequency and that of one or more of the natural vibration modes, such that the combined effect is a structure that vibrates with ever-increasing deflections. This constitutes resonance, and is a dynamic failure criterion for the structure.

In theory, the attainment of resonance is possible, and there are a few recorded instances of actual structural failures where resonance has at least played a certain part. The celebrated failure of the Tacoma-Narrows Bridge is one such extreme example; another case is that of the wind-induced vibrations known as flutter that can be encountered in some flight structures or others where the mass-to-stiffness ratio is very low. However, under realistic conditions the resonance phenomenon is one of mathematical importance only, due to the inherent damping of the structure.

It has been pointed out that in the analysis of the single span monotube structure, the amount of damping has been assumed to be equal to zero. This is a conservative assumption insofar as the structural response to forced vibration is concerned, and must be borne in mind when the forced vibration properties are presented. These data will be discussed in detail in section 6 of this chapter.

As will be shown, complete two- and three-dimensional vibration analyses have been carried out for the structure. With a total of 31 nodal points in the frame, the resulting number of degrees of freedom will be very large. However, Clough and Penzien (24) and others have observed that for most civil engineering structures only the first few modes of vibration are practically significant. For that reason, it was decided to determine the properties only of the first 10 natural modes of vibration of the monotube structures for each of the 3D and 2D analysis schemes. It will be shown that this is well in excess of what is useful; the first five modes of vibration generally dominate the response of these structures.

5.5.2 Natural Frequencies and Modes. Table 5.1 gives the natural frequencies and the natural periods for the first 10 modes of the basic monotube structure, including 2D as well as 3D data. It is emphasized that the response for the 2D-case represents x- and y-components only, since the out-of-plane motion has been suppressed. Figure 5.3 shows the front elevation view of the 2D mode-shape for Mode 1 of the structure, and Figures 5.4 (a) to (d) give the isometric and three planar views of the 3D mode-shape for Mode 1.

The data in Table 5.1 show that the following 2D and 3D modes have identical frequencies/periods:

$$f_1\ (2D) = f_2\ (3D)$$
$$f_2\ (2D) = f_3\ (3D)$$
$$f_3\ (2D) = f_5\ (3D)$$
$$f_4\ (2D) = f_8\ (3D)$$
$$f_5\ (2D) = f_{10}\ (3D)$$

Since the 2D modes are all in-plane, the above indicates that the 3D modes f_2, f_3, f_5, f_8 and f_{10} are dominated by in-plane behavior. At the same time, the first 3D mode is an out-of-plane one that is independent of in-plane properties, and is prompted by the small out-of-plane stiffness of the beam-to-column connection.

The above data and those in Table 5.1 give one of the reasons why it eventually was decided to propose design recommendations based on independent, individual analyses of the structure in the in-plane and out-of-plane directions. Due to the static gravity loads that act on the structure, along with the in-plane vortex shedding (i.e., dynamic effects of the wind load, the in-plane loading conditions and response will govern the overall structure. However, a static out-of-plane evaluation of the beam member subjected to wind loads is also necessary. It is shown that this can be accomplished by a simple, independent check of the bending stress and the deflection produced by the static equivalent of the wind load.

TABLE 5.1
Natural Frequencies and Period for Monotube Structure*

	Natural Frequency (cps)		Natural Period (sec.)	
Mode	2D	3D	2D	3D
1	0.783	0.47	1.28	2.13
2	1.494	0.783	0.67	1.28
3	3.033	1.494	0.33	0.67
4	6.377	1.91	0.157	0.524
5	10.15	3.033	0.099	0.33
6	15.61	4.083	0.064	0.245
7	23.65	6.241	0.042	0.16
8	38.28	6.377	0.026	0.157
9	39.9	9.004	0.025	0.111
10	44.3	10.15	0.023	0.099

* Frequencies and periods are related as f = 1/T.

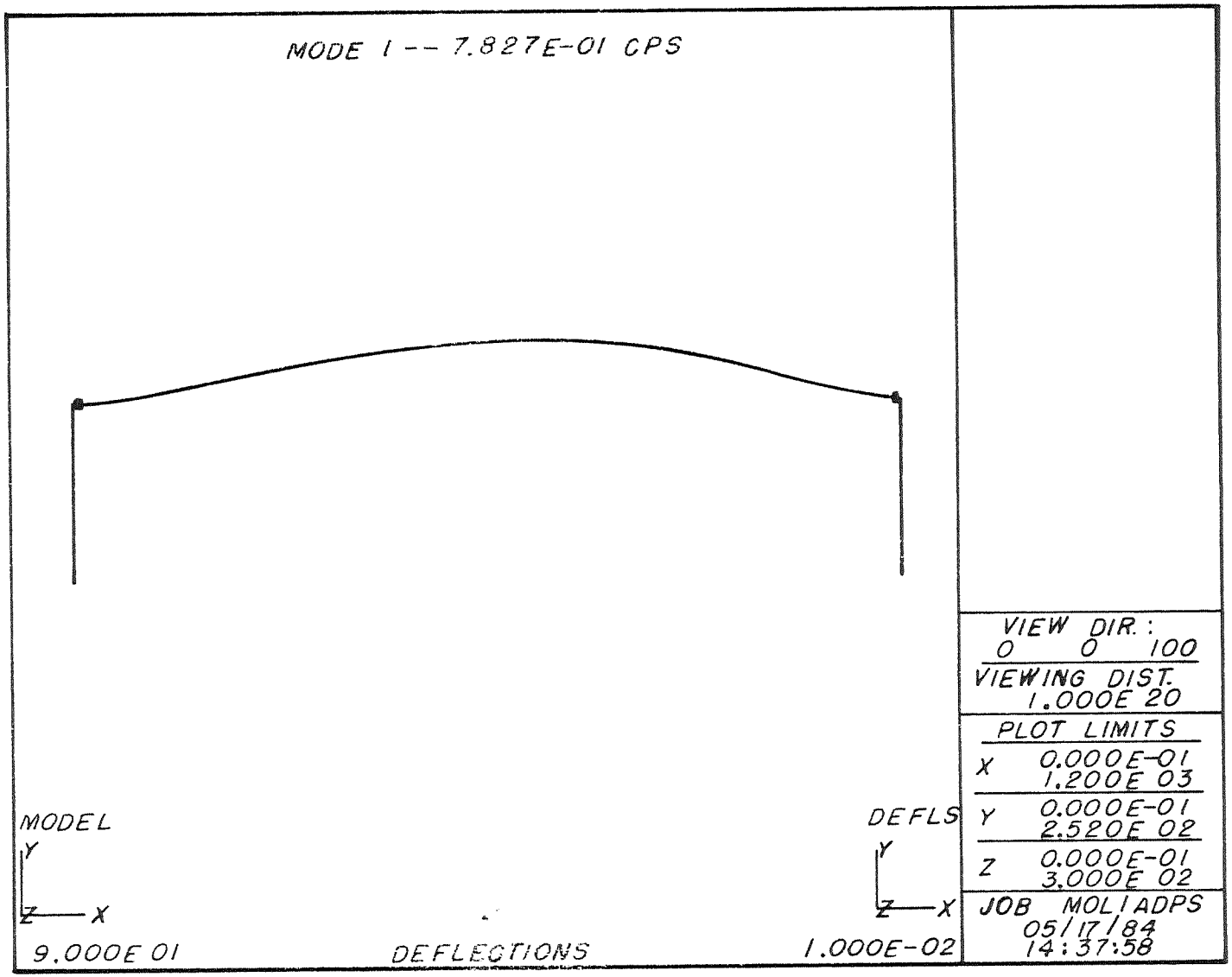

Fig. 5.3 x-y-elevation View of Mode 1 for 2D Natural Vibration

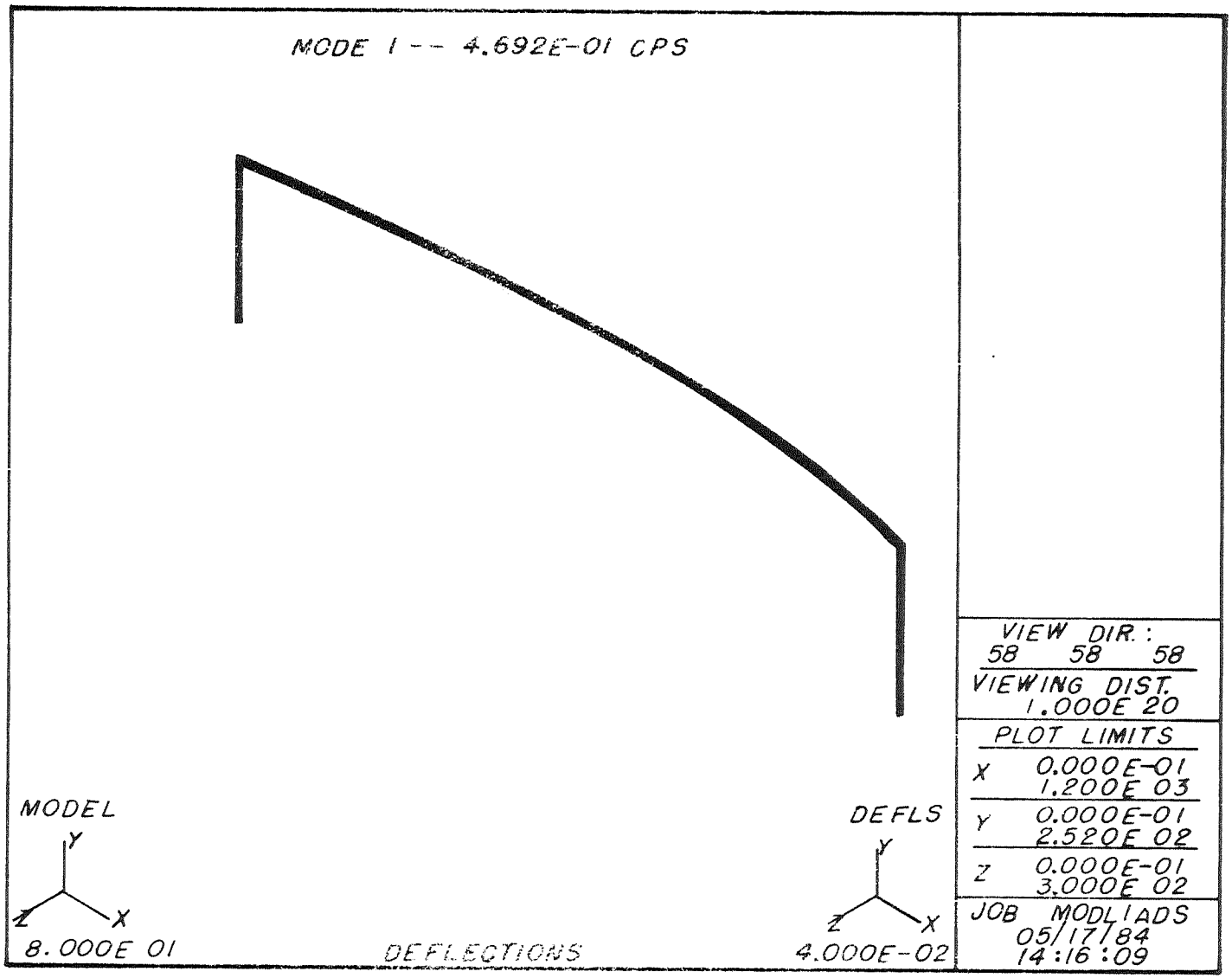

Fig. 5.4 (a) Isometric View of Mode 1 for 3D Natural Vibration

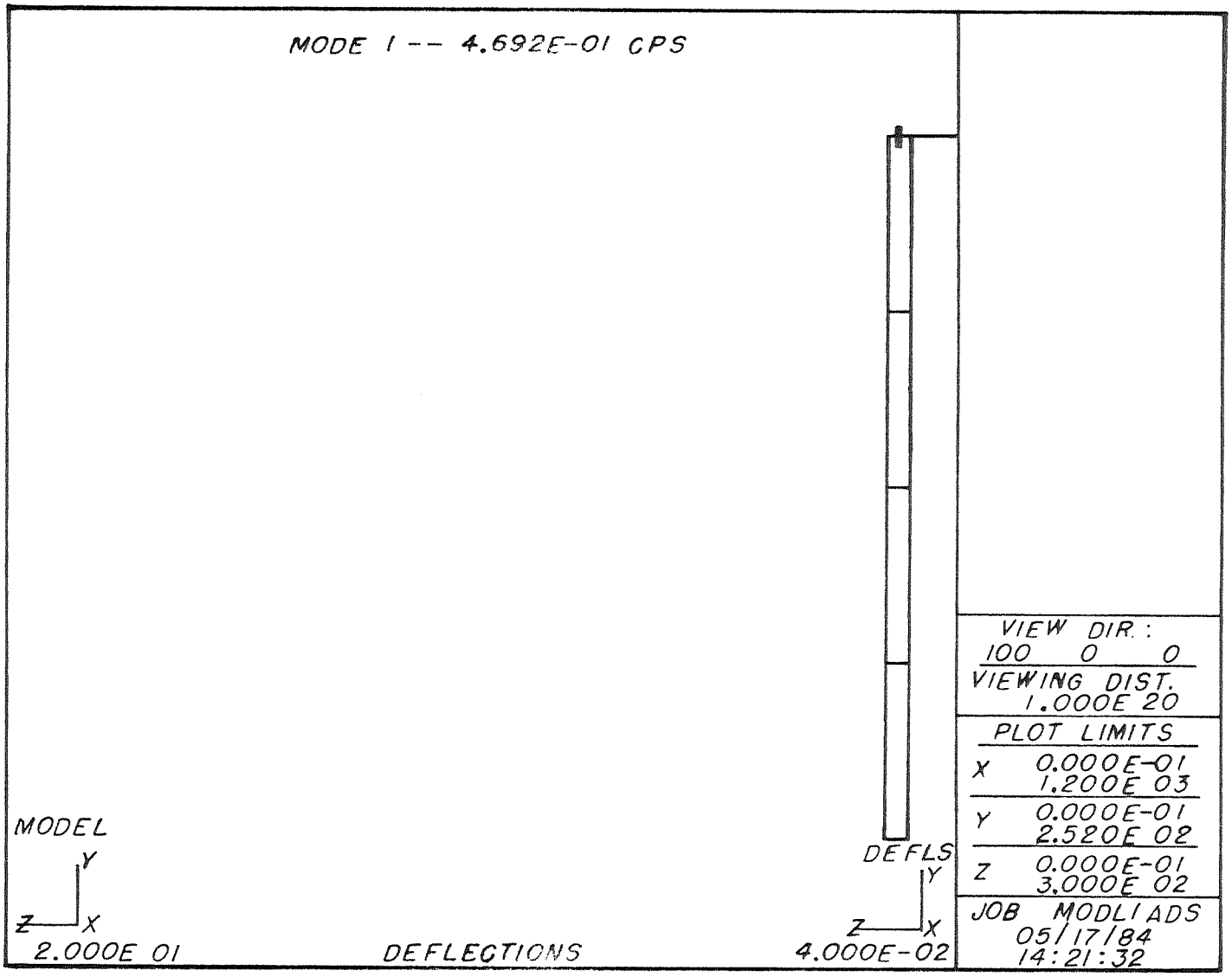

Fig. 5.4 (b) z-y-elevation View of Mode 1 for 3D Natural Vibration

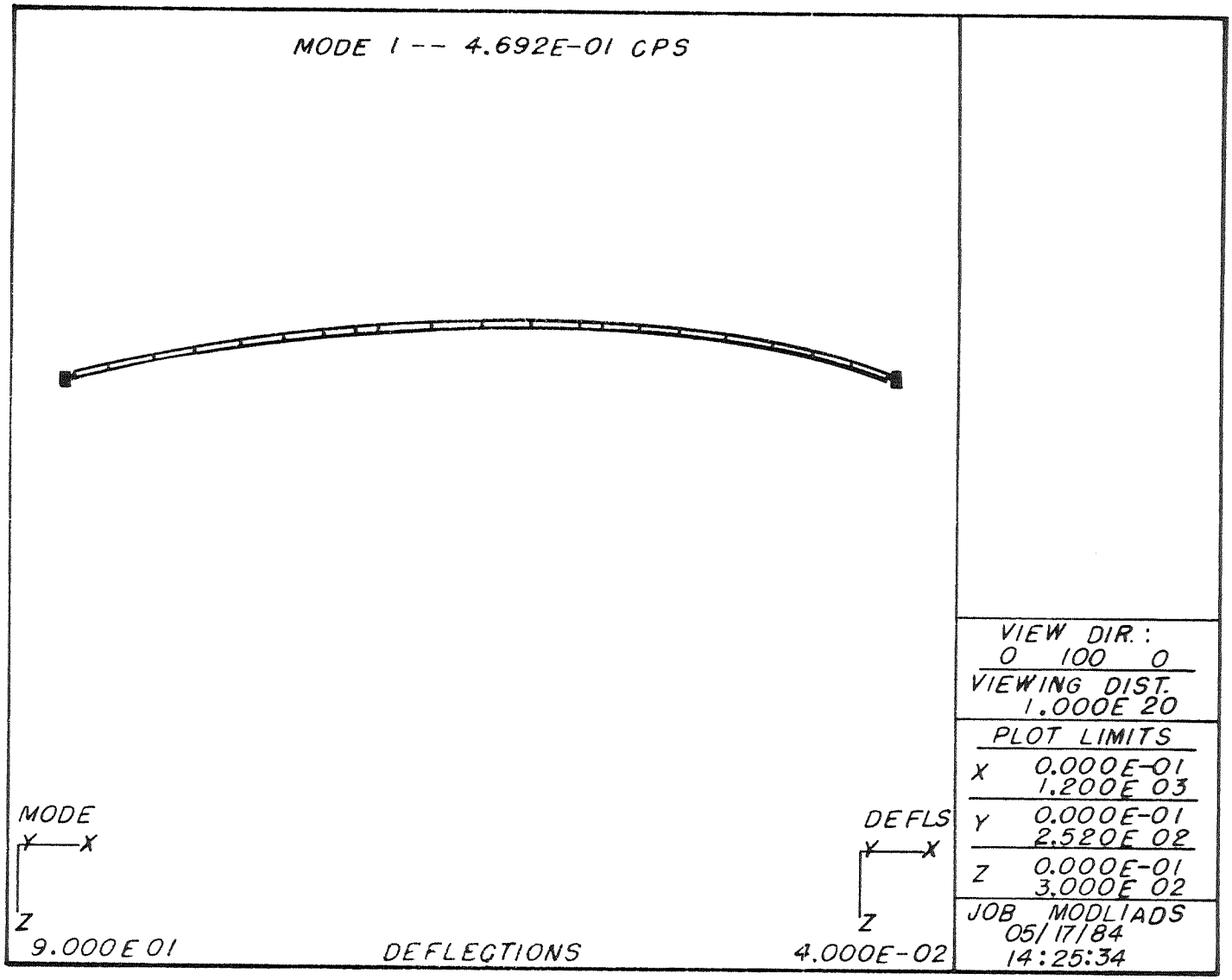

Fig. 5.4 (c) x-z-plan View of Mode 1 for 3D Natural Vibration

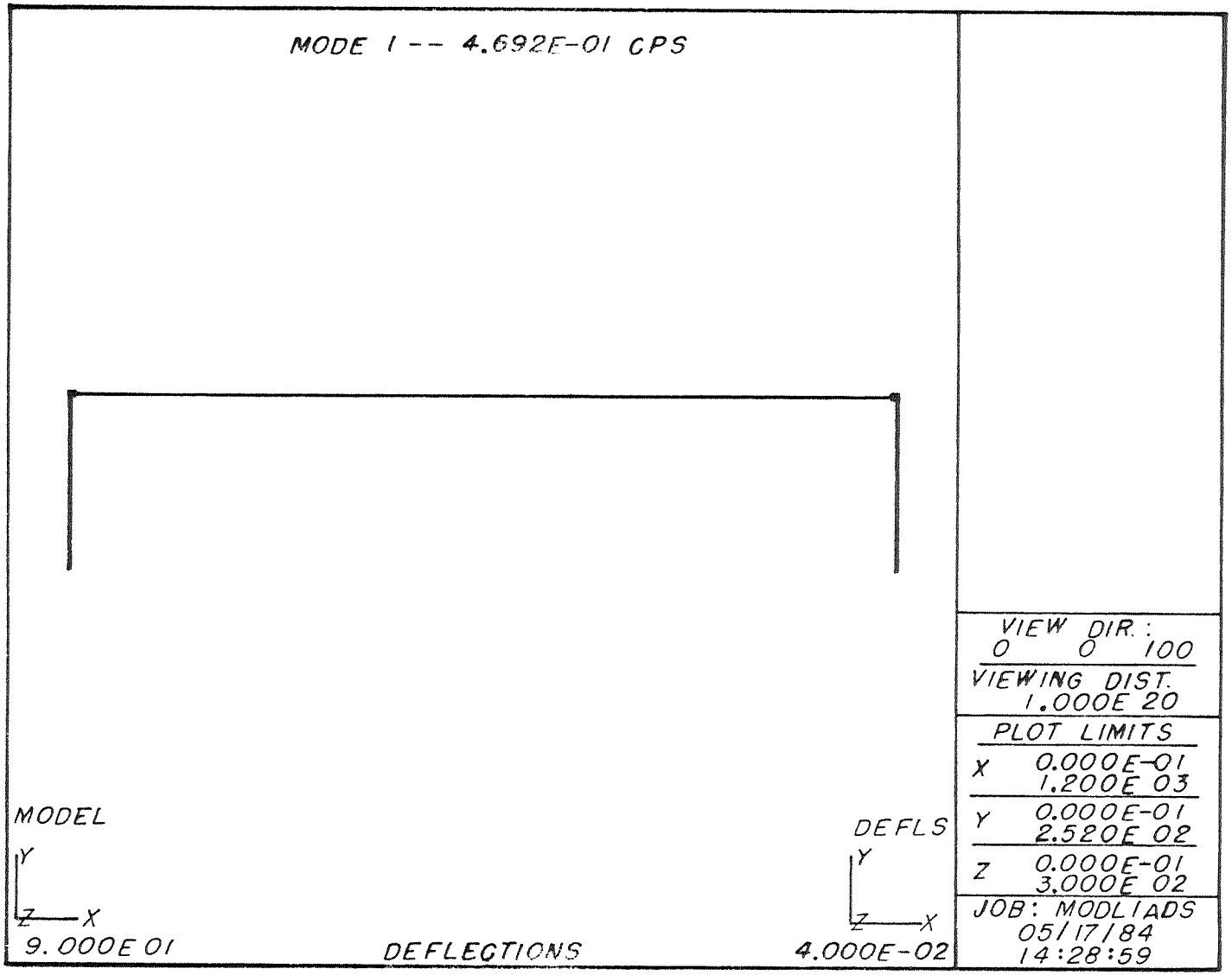

Fig. 5.4 (d) x-y-elevation View of Mode 1 for 3D Natural Vibration

The mode-shape data that were used to plot the displaced frame configurations of Figures 5.3 and 5.4 are given in Appendix A of this report, as Tables A.1 and A.11, respectively. Appendix A also gives the complete mode-shape data for the other 2D and 3D natural modes of vibration. It is emphasized that the displacements, for example, that are given in these tables, do not represent actual deflections, since the natural modes of vibration are not associated with any load. Rather, the displacements are numbers that reflect relative positions of the nodes on the deformed structure. In other words, the natural mode-shapes are used to establish the governing shapes of the vibrating structure, and to correlate these with the behavior that results when dynamic loads are applied.

5.6 Dynamic Behavior: Forced Vibration of the Monotube Structure

5.6.1 General Introduction. A detailed description of the wind loads that act on the structure has been given in Chapter 5.4, including the method that is used to determine the characteristics of the vortex shedding forces. As explained earlier, the latter produce dynamic loads that act at each node in the in-plane direction perpendicular to the longitudinal axis of the member and the direction of the wind. That is, these forces act in the vertical direction for the beam and in the horizontal direction for the columns. The vortex shedding forces therefore produce deflections that are additive to those that result from the gravity loads. In addition, careful consideration must be given to the possibility of structural resonance, as explained in Chapter 5.5.1. The determination of the wind speeds that may produce such behavior is explained in Chapter 5.4.

It is also important to note that due to the change from deterministic to random vortex-shedding behavior for Reynolds Numbers larger than 3.10^5, this study has not dealt with wind speeds larger than those corresponding to $R = 3.10^5$ for the diameters of the members of these monotube structures. This R-value reflects wind speeds of approximately 27 to 29 mph. Although actual wind speeds may exceed this value for some length of time, it is not warranted to extrapolate the deterministic model into the random behavior range. The numerical results that will be obtained if this is done are not reliable. However, as will be demonstrated by the results, realistic and practically useful data are obtained for the deterministic wind speed range.

The influence and magnitude of drag forces which act in the same direction as the wind have not been considered in this work. Due to the tubular shape of the member cross sections of the monotube structure, it is anticipated that the drag forces will be small. Furthermore, very limited data are available on the dynamic properties of these forces.

As will be seen in the presentation of the results, a choice had to be made for the length of time that the wind would be blowing at a constant speed. A duration of 32 seconds was chosen as a large multiple (approximately 16) of the longest natural period of the structure. Table 5.1 indicates that the latter is 2.13 seconds, pertaining to the first 3D mode.

It is noted that a constant wind speed duration of 32 seconds is very long, since the wind tends to gust and therefore only attain specific velocities for short periods of time. However, assuming such a long duration is conservative, especially when it comes to evaluating the resonance response. This will be discussed in detail in Chapters 5.6.2, and 6.

In the initial phase of the forced vibration analysis a numerical integration scheme was utilized to determine the response of the structure. However, due to an inherent numerical round-off error (also called numerical damping) that can only be improved upon by using very small time-steps, this computation technique was discarded in favor of modal superposition. It is noted that the latter approach is the one most commonly adopted for typical structural engineering dynamic problems.

5.6.2 Dynamic Response Due to Vortex-Shedding. The dynamic response of the monotube structures has been determined for the full range of deterministic wind speeds as outlined in Chapters 5.4 and 5.6.1. In addition to obtaining the vibration data for wind speeds where the natural and vortex shedding frequencies match, complete data have been developed for a large number of velocities. Some of the results that are presented in the following are but an example of what has been done, such as the magnitudes of nodal loads for a given wind speed and the displacement-vs-time relationships (displacement histories) for certain points in the structure. Similar data have been developed for all velocities, but only the essence of the results have been presented. That is, the relationship between the maximum in-plane displacement due to vortex shedding and the corresponding wind speed is the most useful output as far as design evaluations are concerned.

Using a mid-range wind velocity of 15 mph as an example, Figure 5.5 shows the monotube structure with the individual vortex shedding loads applied at each nodal point. Additional masses are applied at the nodes where the traffic signs are attached, as indicated. The loads are computed in accordance with the procedure that is detailed in Chapter 5.4.2. Thus, the wind speed of 15 mph corresponds to a vortex shedding frequency of 3.787 cps. Using Eq. (5.4) with $C_L = 1.0$, $\rho = 0.002378$ slugs/ft^3 and V = 15 mph = 22.0 ft/sec, this gives a general expression for the vortex shedding nodal point load of:

$$F(t) = P_{VS} = 1/2\ 0.002378\ (22)^2\ A_p\ 1\ \sin\ (2\pi \cdot 3.787)t$$

or:

$$P_{VS} = A_p \cdot 0.5755 \cdot \sin(23.78t)$$

A_p is the magnitude of the projected tributary area for any node, the forces given in Figure 5.5 reflect the actual A_p -values.

Figure 5.6 shows the displacement histories for four important points on the structure, as follows:

Nodal Point 16: Midspan of beam

Nodal Point 18: Approximately one-third of the distance between midspan and end of beam (see Figure 4.5)

Nodal Point 23: Approximately two-thirds of the distance between midspan and end of beam (see Figure 4.5)

Nodal Point 27: Top of column

These nodal points include the single most important one as far as deflections are concerned, namely, at midspan. The other two beam nodal points were included for direct comparison with midspan, as well as to give an indication of the influence of the beam-to-column connection.

The displacement histories for Points 16, 18 and 23 reflect vertical (in-plane) deflections of these points in relation to time, and the displacement history for Point 27 gives horizontal (in-plane) movement in relation to time. The maximum vertical deflection (at Point 16) equals approximately 0.2 inches; it occurs first after about 6 seconds of load duration and reoccurs roughly every 2 seconds. The response is stable, i.e., the maximum deflection does not increase with time.

As expected, the maximum horizontal deflection (at Point 27) is one order of magnitude smaller than the vertical one. It reaches a value of 0.01 inches after approximately 6 seconds, and then occurs under stable conditions every 10 to 15 seconds thereafter. It is clear that the structural significance of the horizontal in-plane deflections is limited; the only aspect of the behavior that might be affected by this may be the fatigue response of some of the structural details (beam-to-column connection; column base). However, this is a topic that is beyond the scope of this project and cannot be further evaluated here.

The maximum vertical deflection due to the dynamic load must be considered in relation to the value of the maximum static one at the

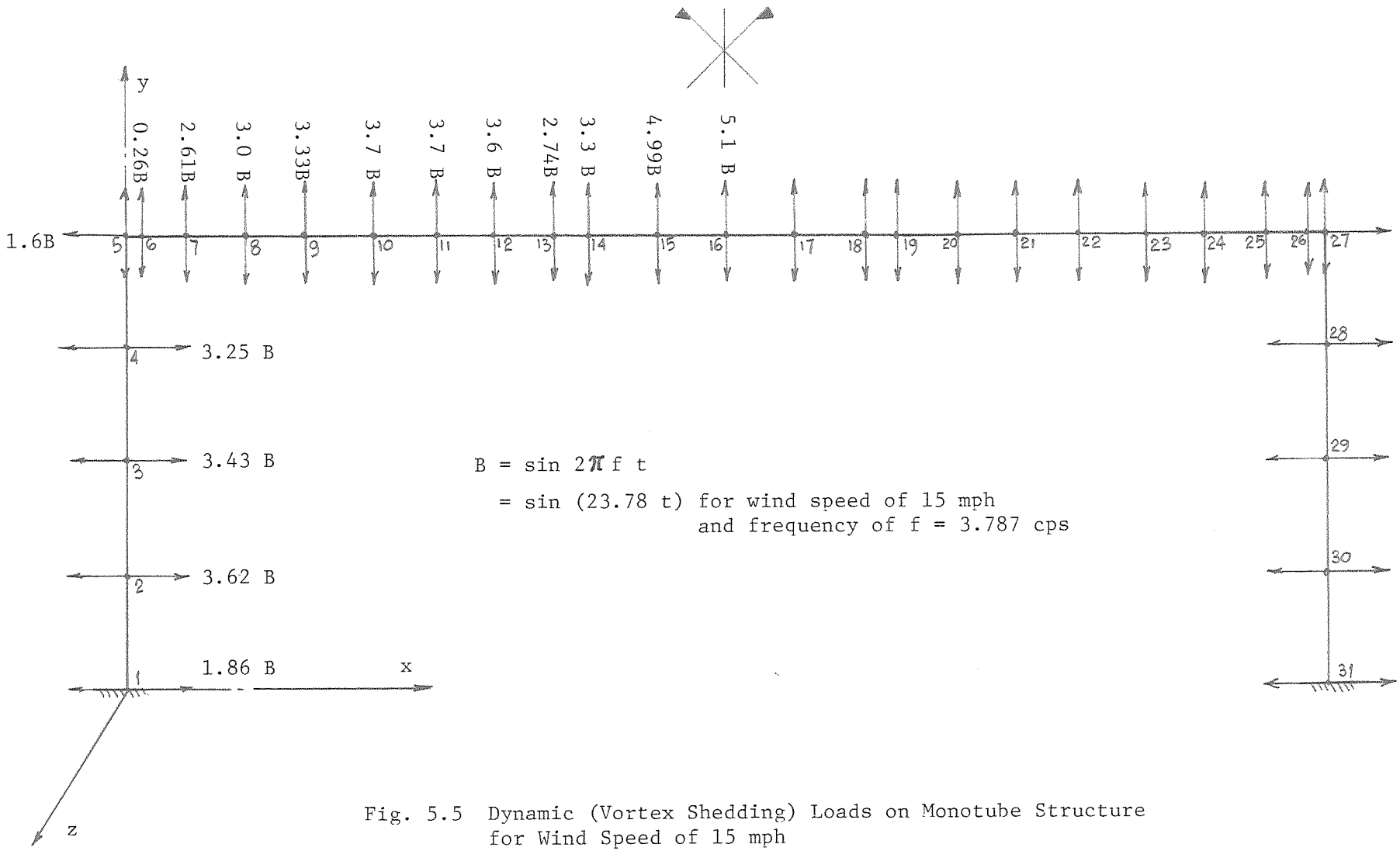

Fig. 5.5 Dynamic (Vortex Shedding) Loads on Monotube Structure for Wind Speed of 15 mph

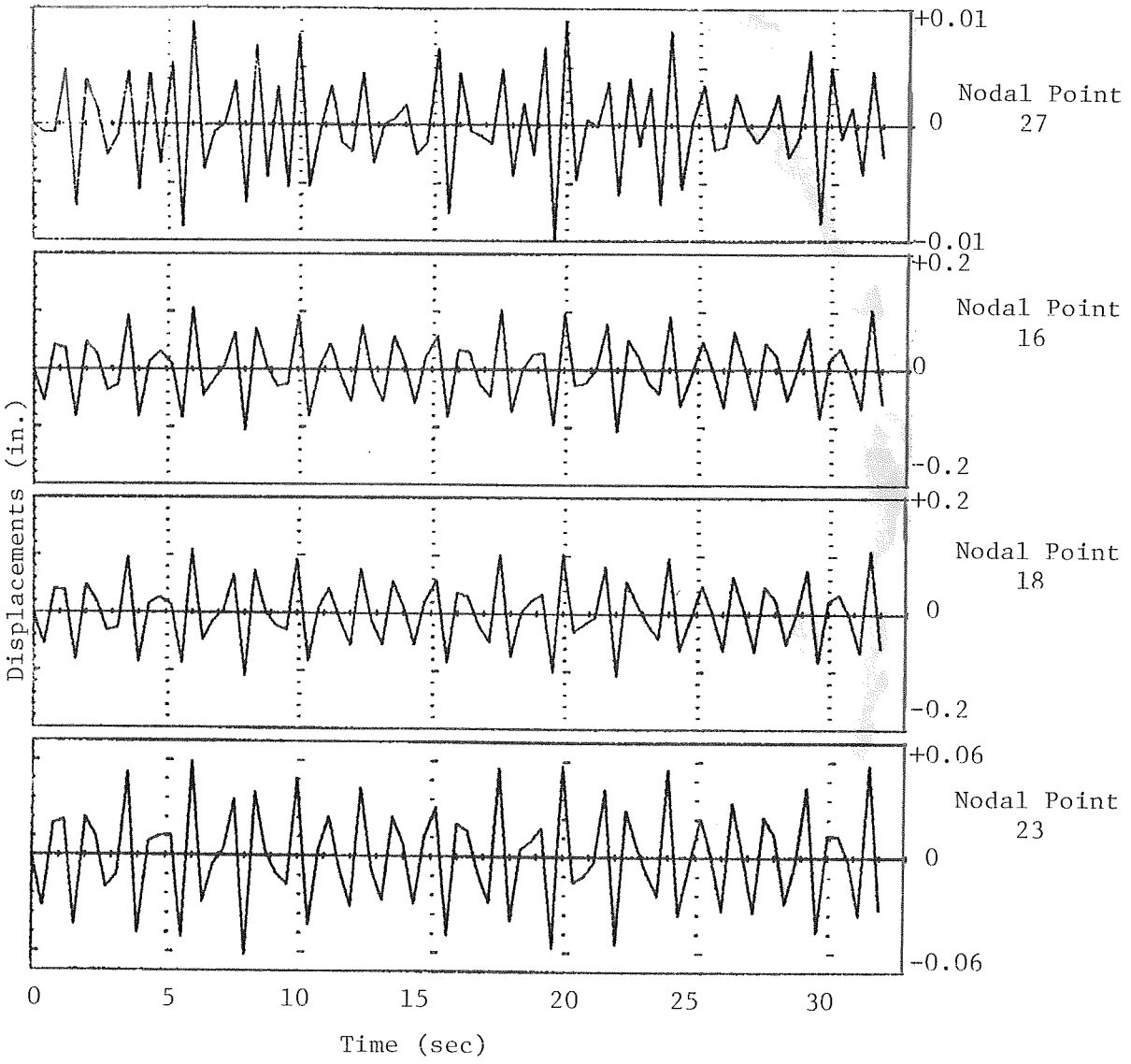

Note: For nodal point 27, the horizontal displacement is shown; for nodal points 16, 18, and 23, vertical displacements are shown.

Fig. 5.6 Displacement Histories for Nodal Points 16, 18, 23 and 27, due to a Wind Speed of 15 mph.

same point. The static displacements are given in Chapter 4; for comparison they are repeated here:

Dead Load:	Δ_{SD} = 4.56 in.
(Dead + Ice) Load:	Δ_{SG} = 6.63 in.
Dynamic (Vortex-Shedding) Load	Δ_d = 0.2 in.

The increase of the deflection due to the dynamic effect is therefore less than 5% for both dead and (dead + ice) loads. Since the allowable stresses (11, 12) are increased by one-third for the load cases that incorporate wind, it is obvious that gravity load will govern the in-plane design. This is amplified by the dynamic stress increases of 0.17 ksi and 0.22 ksi at the column base and at beam midspan, respectively.

The statically equivalent out-of-plane deflection of the beam for a wind speed of 15 mph is computed as shown in Chapter 4, namely:

$$\Delta_h\ (v = 15) \simeq \Delta_h(v = 70)\ (\frac{15}{70})^2$$

which becomes:

$$\Delta_h\ (v = 15) \simeq 0.56 \text{ in.}$$

where it is recalled that $\Delta_h\ (v = 70) = 12.09$ inches. For this wind speed the gravity load combination therefore will govern.

5.7 Correlation of Wind Speed and Maximum Amplitude

Figure 5.7 shows the relationship between the maximum dynamic vertical deflection (at Point 16) and the wind speed for the complete deterministic velocity range. Peaks are reached for velocities of 3.31 mph, 6.2 mph and 12.13 mph, corresponding to the natural frequencies for the first three 2D-modes. The maximum value of 0.3 inches occurs for the first mode; it is insignificant in comparison with the static deflections.

Large deflections appear to take place for wind speeds around 16.2 to 17.0 mph, as well as for the range of 21.0 to 23.0 mph. The peaks do not correspond to any natural frequency of the structure, but do show the tendency towards resonance for these wind speed ranges. The implications of these numbers will be explored in full in Chapters 6 and 7. However, it is emphasized here that the ranges of velocities for which resonance appears to be taking place are very narrow. At the same time, the data in Figure 5.7 have been based on a sustained wind duration of 32 seconds which is of limited practical value. It is also recalled that it has been assumed that the structure possesses no damping capability. In consequence, although large deflections are

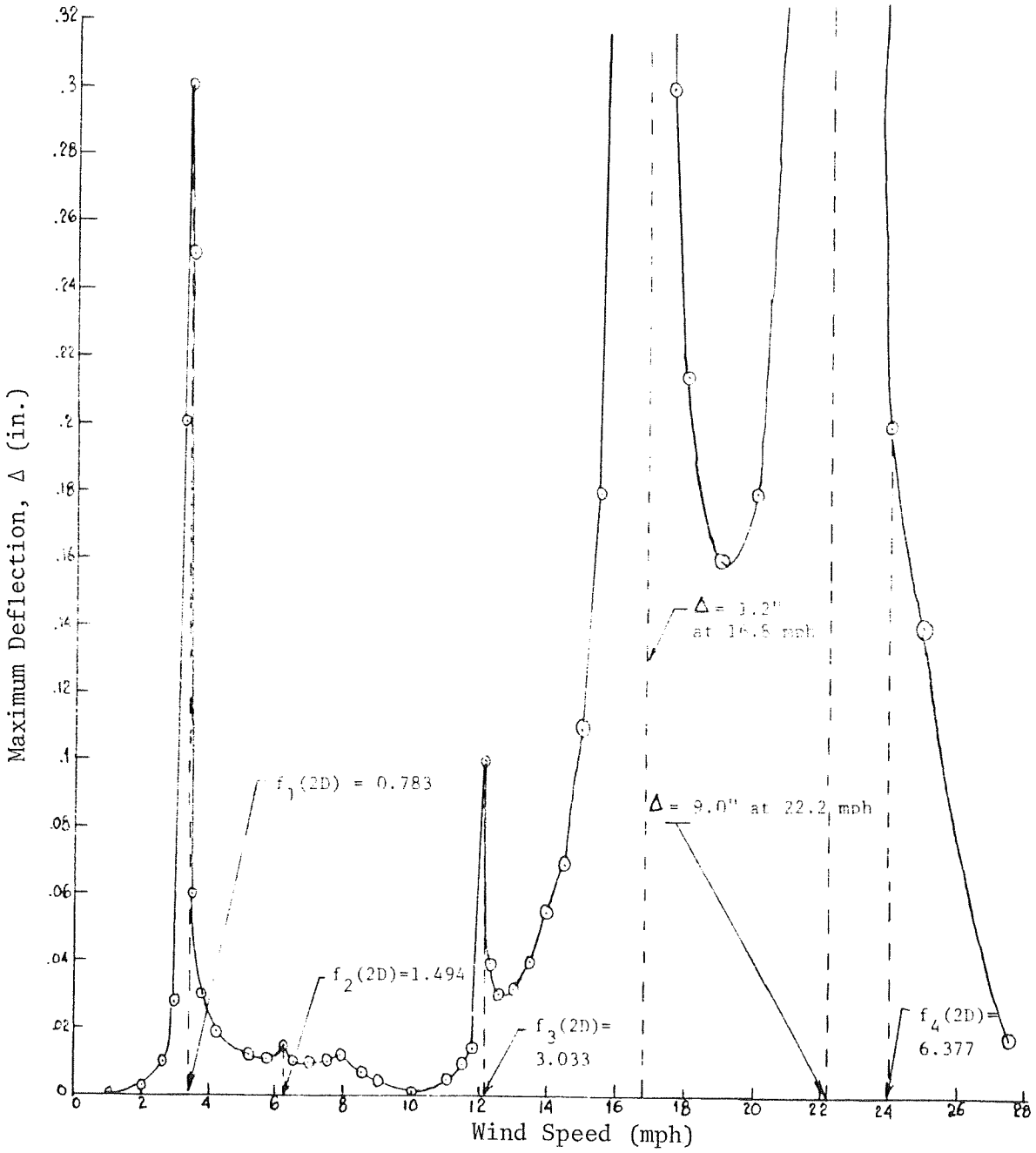

Fig. 5.7 Maximum Vertical Dynamic Deflections at Midspan of Beam for Different Wind Speeds

indicated for certain wind speeds, their practical impact is questionable.

It is also noted that at the highest wind velocity where resonance appears, i.e., V 22 mph, the statically equivalent out-of-plane deflection is found as

$$\Delta_h\ (v = 22) \simeq 12.09 \cdot \left(\frac{22}{70}\right)^2 = 1.19 \text{ in.}$$

The deflection-to-span ratio for this value is approximately 1/1000; hence, its influence on the stresses in the structure, for example, is very small.

Further evaluations of the above findings are presented in Chapter 6.

6. PARAMETRIC STUDIES

6.1 Choices of Parameters

It is clear that the behavior of monotube sign support structures depends on the stiffnesses of the columns and the beam, the span length, and the location of the traffic signs on the beam. In order to study the effect of each of these four parameters, a total of eight different models were developed and their behavior compared to that of the base model. The latter has been covered extensively in the previous chapters. For each model, only one of the four parameters was varied while the other three parameters were kept the same as the base model. The overall dimensions for all eight models are shown in Fig. 6.1.

The first parameter to be studied was the stiffness of the columns. Two different column models were developed which were identical to the base model shown in Fig. 4.5, except that in one case the moment of inertia of the column ($I_{col.}$) was 1.5 times the moment of inertia of the column in the base model, and in the second case it was selected as 1.25 times that of the base model. These two models were named Column Model 1 and 2, respectively. Because the beam stiffness, the span length, and the location of the signs were kept the same as for the base model for these two models, the influence of the column stiffness on the behavior of the structures could be determined.

There are several ways by which the stiffness of the column can be increased. However, because the wind forces are proportional to the outside diameter of the members, it was decided to increase the column stiffness by increasing the thickness of the tubes while keeping the same outside diameter as the base model.

The cross sectional properties of the two column models are listed in Table 6.1. For comparison, the properties for the base model are also given. It is recalled that the number of nodes for the two column models is the same as that for the base model, which is shown in Fig. 4.5.

The second variable to be studied was the beam stiffness. Beam Models 1 and 2 were developed by increasing the moment of inertia for the beams (I_{beam}) in the base model by 50% and 25%, respectively, without changing the column stiffnesses, the span length, or the location of the signs. The properties of the two beam models are also listed in Table 6.1.

The third parameter which was investigated was the span length, as shown in Fig. 6.1 (b). The base model had a span of 100 feet. Instead of increasing or decreasing the span of the base model by a certain percentage to obtain the span models, span lengths of 60 and 120 feet were selected on the basis of discussions with Arizona Department of

(a) Base, Beam and Column Models

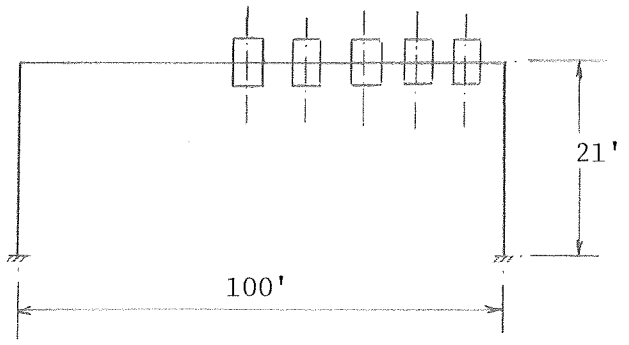

(b) Span Models

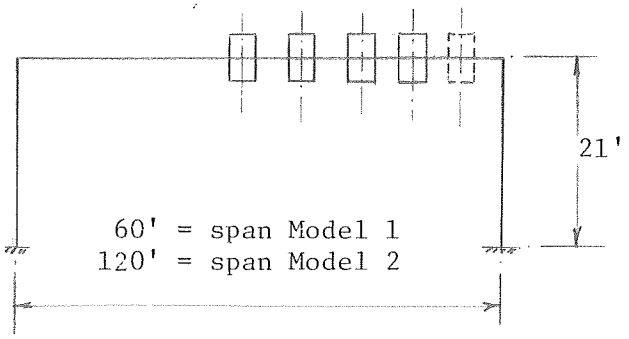

(c) Sign Models

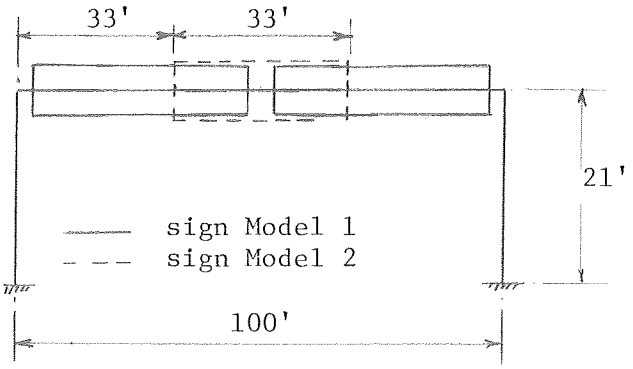

Fig. 6.1 Overall Dimensions for Base and Eight Parametric Models (for dimensions, see Tables 6.1 and 6.2)

TABLE 6.1
MEMBER CROSS SECTIONAL DATA
FOR COLUMN AND BEAM MODELS

Location	Cross Sectional Measures	Base Model	Column Model #1 (1.5 I col)	Column Model #2 (1.25 I col)	Beam Model #1 (1.5 I beam)	Beam Model #2 (1.25 I beam)
Column Base	Outer diameter at Node 1 (in)	15.0	15.0	15.0	15.0	15.0
Column	Wall-thickness for column (in)	0.188	0.287	0.237	0.188	0.188
Column Top	Outer diameter at Node 5 (in)	12.06	12.06	12.06	12.06	12.06
Beam End	Outer diameter of Node 6 (in)	11.11	11.11	11.11	11.11	11.11
Beam	Wall thickness for beam (in)	0.188	0.188	0.188	0.286	0.236
Beam Midspan	Outer diameter at Node 16 (in)	18.0	18.0	18.0	18.0	18.0

NOTES:

1. Columns are uniformly linearly tapered between base and top.

2. Beams are uniformly linearly tapered between midspan and end, and are symmetrical about midspan.

3. For locations of nodes refer to Fig. 4.5.

4. The bare frames are symmetric about the beam midspan (i.e., node 16).

Transportation personnel. The overall dimensions for these span models, Nos. 1 and 2, respectively, are shown in Figs. 6.2 and 6.3. The 60-foot and 120-foot spans are the lower and upper limits for the most typical monotube structures currently in service.

Due to the different span lengths, the number of elements and nodes used in modeling the two span models are different from the base model. The cross sectional properties of the span models are listed in Table 6.2 for comparison with the base model.

The fourth parameter to be investigated was the location of the traffic signs along the span. For the base model the signs were on one-half of the span only, as shown in Fig. 4.1. For Sign Model 1 the traffic signs were placed over the entire span of the structure with a small opening near midspan. For Sign Model 2 only the middle one-third of the span was used to support signs, as shown in Fig. 6.1 (c). The remaining parameters of the two sign models, namely, the column and beam stiffness and the span, were the same as the base model. It is emphasized that the location of the signs influences both the gravity and the wind loads and their point of application on the structure.

6.2 Results for Individual Parameters

In order to determine the influence of each parameter, the models were analyzed for static as well as dynamic forces, and the results are presented in the following sections.

6.2.1 Static Load Results. All eight models were subjected to different combinations of static loads which included the self weight of the structure, ice, and equivalent wind forces due to a wind velocity of 70 mph. In other words, the same load combinations that were used to analyze the base structure are also used here.

Table 6.3 gives the deflections at four significant points in the column models subjected to the four cases of loading. For ease of comparison, the same information for the base model is included in Table 6.3. The stresses at the midspan of the beams and the base of the columns are also given in Table 6.3.

The increase in the column stiffness reduced the beam displacements slightly. The v-component of the deflections were lower by approximately 7% and 5% for Column Models 1 and 2, respectively. This was due to the additional restraint against rotation at the ends of the beam due to the increase in the stiffness of the column. The most noticeable change occurred for the u- and w-components of the deflection at the top of the columns. U-direction displacements of the top of the column (Node Number 27) dropped by 20% and 11%, and the w-values were reduced by 33% and 20% for Column Models 1 and 2, respectively.

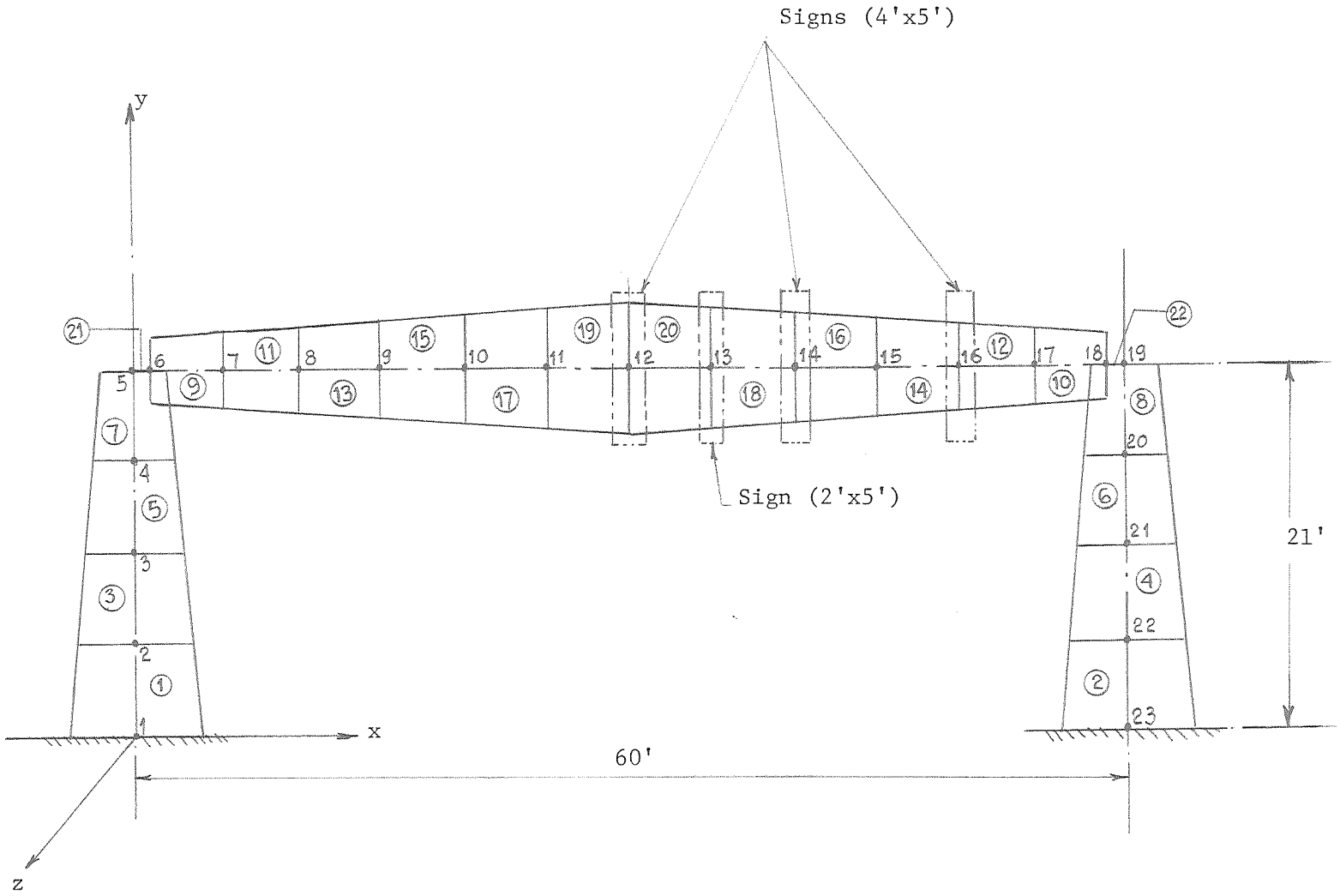

Fig. 6.2 Discretized Model of Monotube Structure for Span Model 1

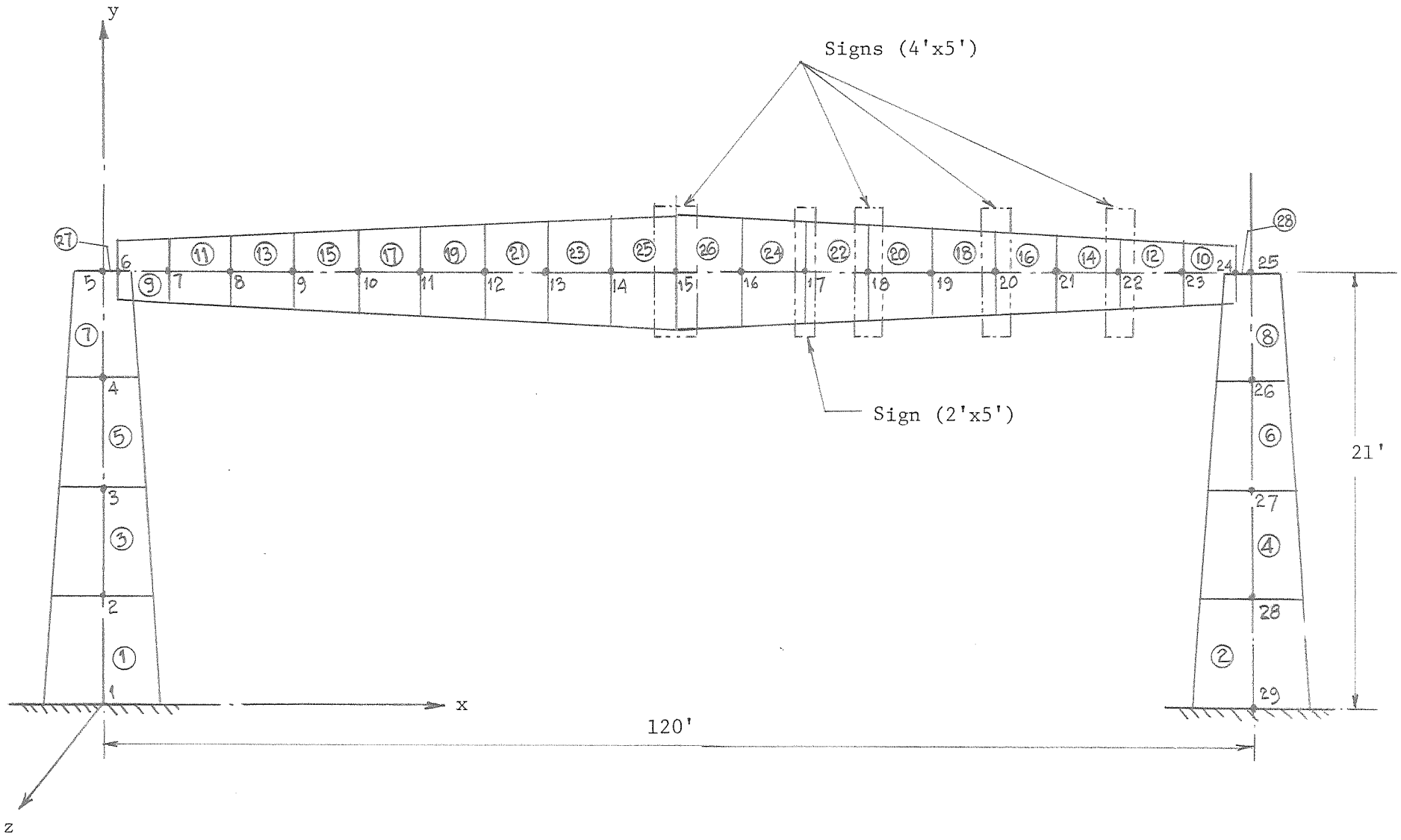

Fig. 6.3 Discretized Model of Monotube Structure for Span Model 2

TABLE 6.2
Member Cross Sectional Data for Span Models

Cross Sectional Measure	Base Model	Span Model #1 (l=60 ft.)	Span Model #2 (l=120 ft.)
Outer diameter at column base (in)	15.0	15.0	15.0
Wall thickness for column (in)	0.188	0.188	0.188
Outer diameter at column top (in)	12.06	12.06	12.06
Wall thickness for beam (in)	0.188	0.188	0.188
Outer diameter at beam midspan (in)	18.0	15.195	19.396

NOTES:

1. Columns are uniformly linearly tapered between base and top.

2. Beams are uniformly linearly tapered between midspan and end, and are symmetrical about midspan.

3. The bare frames are symmetric about the beam midspan.

TABLE 6.3

COMPARISON OF STATIC DEFLECTIONS AND BENDING STRESSES
BETWEEN THE BASE MODEL AND THE COLUMN MODELS

Deflections (in.)

Load Case	Point	Base Model			Col. Model #1 (1.5 I col.)			Col. Model #2 (1.25 I col.)		
		U	V	W	U	V	W	U	V	W
D	16	-0.065	-4.556	0.0	-0.052	-4.258	0.0	-.058	-4.38	0.0
	18	-0.066	-4.320	0.0	-0.053	-4.028	0.0	-.059	-4.148	0.0
	23	-0.068	-1.877	0.0	-0.055	-1.69	0.0	-.061	-1.767	0.0
	27	-0.070	-0.003	0.0	-0.057	-0.002	0.0	-.062	- .002	0.0
D + I	16	-0.105	-6.626	0.0	-0.084	-6.193	0.0	-.093	-6.371	0.0
	18	-0.105	-6.298	0.0	-0.085	-5.872	0.0	-.095	-6.047	0.0
	23	-0.109	-2.747	0.0	-0.088	-2.474	0.0	-.098	-2.587	0.0
	27	-0.113	- .004	0.0	-0.091	-0.003	0.0	-.010	- .003	0.0
D + W(1)	16	-0.065	-4.556	12.09	-0.052	-4.258	11.56	-.058	-4.38	11.77
	18	-0.066	-4.32	11.90	-0.053	-4.028	11.33	-.059	-4.148	11.56
	23	-0.068	-1.877	7.46	-0.055	-1.69	6.046	-.061	-1.767	7.092
	27	-0.070	-0.003	1.928	-0.057	-0.002	1.289	-.062	- .002	1.545
D + I + W(1)	16	-0.105	-6.626	12.09	-0.084	-6.193	11.56	-.093	-6.371	11.77
	18	-0.106	-6.298	11.90	-0.085	-5.872	11.33	-.095	-6.047	11.56
	23	-0.109	-2.747	7.46	-0.088	-2.474	6.846	-.095	-2.587	7.092
	27	-0.113	-0.004	1.928	-0.091	-0.003	1.289	-.010	- .003	1.545

MAXIMUM BENDING STRESSES (ksi)

Load Case	Section	Base Model	Col. Model #1 (1.5 I col.)	Col. Model #2 (1.25 I col.)
D+I	Beam $\mathcal{L}$	11.23	10.9	11.00
	Col. Base	8.113	5.7	6.68
D+I+W	Beam $\mathcal{L}$	17.3	17.05	17.13
	Col. Base	18.65	12.56	15.0

NOTE:

Wind Load W(1) is based on a wind speed of 70 mph in the + z direction.

The change in the column stiffness had almost no effect on the stresses at the midspan of the beam. However, the maximum bending stresses at the base of the column were reduced by approximately 30% and 18% due to gravity loads alone, and by 30% and 20% due to the combined effect of gravity and wind loads for Column Models 1 and 2. It is recalled that the maximum bending stresses which are listed in Table 6.3 are the resultant of the bending stress about the y- and z-axes for each node. The x-component of the moment is torsion and therefore does not influence the normal stresses in the circular cross section.

The results for the deflections and stresses of the two beam models are compared with those for the Base Model in Table 6.4. As mentioned previously, the increase in the stiffness of the beam was achieved by increasing the thickness of the tube, and thus adding to the dead weight of the structure. As a result, the v-component of the beam deflection for dead weight alone increased slightly for both beam models. The addition of ice load produced a decrease in the v-component of the deflection. However, this decrease was less than 7%. The u-component of the deflection also decreased with the additional stiffness of the beam, but in general, the magnitude of the displacements in the u-direction are so small that they can be ignored for all models. Due to the wind forces, the w-component of the deflection at the top of the column remained unchanged. However, the deflection of the beam in the w-direction was reduced by 27% and 17% for Beam Models 1 and 2, respectively.

The stresses at midspan of the beam for gravity loads alone were reduced by 12% and 7%, and for the combination of gravity and wind loads were reduced by 23% and 14% for Beam Models 1 and 2. The stresses at the base of the column due to the gravity loads increased by 15% and 8% for Beam Models 1 and 2. The larger weight of the beams produced larger moments at the top of the columns which led to larger moments at their base. When the wind forces were considered, the column base stresses for Beam Models 1 and 2 were only 3% and 2% larger than the Base Model.

As discussed previously, the numbers of nodes for the span models differed from the Base Model. The deflections and stresses for "similar" points are listed in Table 6.5. The u-components of the displacements are again very small and can be ignored. In the v-direction, the displacements were reduced by 80% for Span Model 1 and were increased by approximately 80% for Span Model 2. The out-of-plane displacement for Span Model 1 was 70% lower than that of the Base Model and was approximately 50% higher for Span Model 2.

The changes in the stresses were also significant. For Span Model 1, under the gravity loads alone the stresses at the midspan of the beam and the base of the column were reduced by 49% and 61%. Stresses at the same locations under the combined effects of gravity and wind were 43% and 33% lower than the Base Model, respectively. For Span Model 2, the

TABLE 6.4

COMPARISON OF STATIC DEFLECTIONS AND BENDING STRESSES
BETWEEN THE BASE MODEL AND THE BEAM MODELS

Deflections (in.)

Load Case	Point	Base Model U	Base Model V	Base Model W	Beam Model #1 (1.5 I Beam) U	Beam Model #1 (1.5 I Beam) V	Beam Model #1 (1.5 I Beam) W	Beam Model #2 (1.25 I Beam) U	Beam Model #2 (1.25 I Beam) V	Beam Model #2 (1.25 I Beam) W
D	16	-0.065	-4.556	0.0	-0.053	-4.655	0.0	-.059	-4.585	0.0
	18	-0.066	-4.320	0.0	-0.053	-4.403	0.0	-.059	-4.342	0.0
	23	-0.068	-1.877	0.0	-0.055	-1.984	0.0	-.061	-1.925	0.0
	27	-0.070	-0.003	0.0	-0.056	-0.003	0.0	-.063	- .003	0.0
D + I	16	-0.105	-6.626	0.0	-0.084	-6.189	0.0	-.094	-6.337	0.0
	18	-0.106	-6.298	0.0	-0.085	-5.872	0.0	-.095	-6.017	0.0
	23	-0.109	-2.747	0.0	-0.087	-2.660	0.0	-.098	-2.680	0.0
	27	-0.113	-0.004	0.0	-0.089	-0.004	0.0	-.099	- .004	0.0
D + W(1)	16	-0.065	-4.556	12.09	-0.053	-4.655	8.688	-.059	-4.585	10.05
	18	-0.066	-4.320	11.90	-0.053	-4.403	8.583	-.059	-4.342	9.914
	23	-0.068	-1.877	7.46	-0.055	-1.984	5.647	-.061	-1.925	6.375
	27	-0.070	-0.003	1.928	-0.056	-0.003	1.928	-.063	- .003	1.928
D + I + W(1)	16	-0.105	-6.626	12.09	-0.084	-6.189	8.688	-.004	-6.337	10.05
	18	-0.106	-6.288	11.90	-0.085	-5.872	8.583	-.095	-6.017	9.914
	23	-0.109	-2.747	7.46	-0.087	-2.660	5.647	-.098	-2.630	6.375
	27	-0.113	-0.004	1.93	-0.089	-0.004	1.928	-0.99	- .004	.928

MAXIMUM BENDING STRESSES (ksi)

Load Case	Section	Base Model	Beam Model #1 (1.5 I Beam)	Beam Model #2 (1.25 I Beam)
D+I	Beam ℄	11.23	9.92	10.42
	Col. Base	8.113	9.34	8.75
D+I+W	Beam ℄	17.3	13.25	14.83
	Col. Base	18.65	19.2	18.94

NOTE:

Wind Load W(1) is based on wind speed of 70 mph in the +z direction.

TABLE 6.5

COMPARISON OF STATIC DEFLECTIONS AND BENDING STRESSES
BETWEEN THE BASE MODEL AND THE SPAN MODELS

Deflections (in)

Load Case	Point			Base Model			Span Model #1 (60 span)			Span Model #2 (120' span)		
	BM	SM1	SM2	U	V	W	U	V	W	U	V	W
D	16	12	15	-0.065	-4.556	0.0	-.026	- .857	0.0	-.089	-7.936	0.0
	18	14	18	-0.066	-4.320	0.0	-.027	- .755	0.0	-.091	-7.047	0.0
	23	16	21	-0.068	-1.877	0.0	-.027	- .396	0.0	-.094	-3.752	0.0
	27	19	25	-0.069	-0.003	0.0	-.027	- .002	0.0	-.091	- .003	0.0
D + I	16	12	15	-0.105	-6.626	0.0	-.042	-1.260	0.0	-.143	-11.4	0.0
	18	14	18	-0.106	-6.298	0.0	-.043	-1.114	0.0	-.146	-10.15	0.0
	23	16	21	-0.109	-2.747	0.0	-0.43	-0.585	0.0	-.149	- 5.417	0.0
	27	19	25	-0.113	-0.004	0.0	-0.44	- .002	0.0	-.153	- .004	0.0
D + W(1)	16	12	15	-0.065	-4.556	12.09	-.026	-0.857	3.488	-.089	- 7.936	17.65
	18	14	18	-0.066	-4.32	11.90	-.027	-0.755	3.376	-.091	- 7.047	16.79
	23	16	21	-0.068	-1.877	7.46	-.027	-0.396	2.622	-.094	- 3.752	11.61
	27	19	25	-0.069	-0.003	1.928	-.028	-0.002	1.377	-.097	- .003	2.143
D + I + W(1)	16	12	15	-0.105	-6.626	12.09	-.042	-1.26	3.488	-.143	-11.4	17.65
	18	14	18	-0.106	-6.298	11.90	-.043	-1.114	3.376	-.146	-10.15	16.79
	23	16	21	-0.109	-2.747	7.46	-.043	-0.585	2.622	-.149	- 5.417	11.61
	27	19	25	-0.113	-0.004	1.928	-.044	- .002	1.377	-.153	- .004	2.143

MAXIMUM BENDING STRESSES (ksi)

Load Case	Section	Base Model	Span Model #1 (60')	Span Model #2 (120')
D+I	Beam ℄	11.23	5.64	13.58
	Col. Base	8.113	3.12	11.02
D+I+W	Beam ℄	17.3	9.8	21.7
	Col. Base	18.65	12.5	19.33

NOTE:

Wind Load W(1) is based on a wind speed of 70 mph in the +z direction.

gravity stresses increased by 21% at the midspan of the beam and by 36% at the base of the column. When the effects of the wind loads also were included, these stresses were increased by 25% and 4% compared to the stresses in the Base Model.

As shown in Fig. 6.1 (c), the signs in Sign Model 1 were placed over the entire length of the beam, while for Sign Model 2 only the middle one-third of the span was covered. A comparison of the deflections and maximum bending stresses in the sign models and the base model is presented in Table 6.6. Due to the additional weight of the signs, the dead load v-component of the deflection at midspan in Sign Model 1 was 60% higher than that of the Base Model. The same component of deflection increased by 75% when the effect of the ice loads also was included. In Sign Model 2, although the total weight of the signs was not significantly larger than that of the Base Model, because the signs were placed closer to the middle of the span, larger downward deflections of the beam were recorded. The v-component of the deflection at the midspan for Sign Model 2 was 37% higher than that of the Base Model for the case of the dead loads, and 40% larger when the dead and ice loads were combined.

The most significant increase was observed in the w- or out-of-plane direction of the beam due to the equivalent wind forces. At midspan this component of the deflection increased by 165% for sign Model 1 and by 72% for Sign Model 2. Considering the gravity loads alone, the stresses at the midspan of the beam and at the column base increased by 65% for Sign Model 1, while the same measurements showed 48% and 23% increases for Sign Model 2, respectively. The largest increase in stresses was observed when the wind loads were included. Under the combined action of gravity and wind loads the stresses at the midspan of the beam and at the column base increased by 116% and 105%, respectively, for Sign Model 1 and the same measurements increased by 70% and 23% for Sign Model 2.

6.2.2 Dynamic Load Results. All eight models were analyzed for free vibration as described in Chapter 5.3.1. Their natural frequencies and periods for the first 10 nodes in two-dimensional and three-dimensional space are given in Table 6.7. For ease of comparison, the natural frequencies and periods of the base model are also included in Table 6.7.

It is noted that for the Base Model, Column Model 2, Beam Models 1 and 2, Span Model 1, and Sign Models 1 and 2, the first through fifth natural frequencies in the 2D case correspond to the second, third, fifith, eighth, and tenth natural frequencies in the 3D case, respectively. This is basically also true for Column Model 1, except that in this case the fourth 2D natural frequency matches the seventh 3D natural frequency instead of the eighth. As discussed in detail in Chapter 5, this observation indicates that for these 3D frequencies the

TABLE 6.6

COMPARISON OF STATIC DEFLECTIONS AND BENDING STRESSES
BETWEEN THE BEAM MODEL AND THE SIGN MODELS

Deflections (in)

Load Case	Point	Base Model			Sign Model #1 (Full Signs)			Sign Model #2 (Ctrl Signs)		
		U	V	W	U	V	W	U	V	W
D	16	-0.065	-4.556	0.0	0.0	-7.685	0.0	0.0	-6.223	0.0
	18	-0.066	-4.32	0.0	-0.01	-7.148	0.0	- .002	-5.747	0.0
	23	-0.068	-1.877	0.0	- .005	-3.007	0.0	- .004	-2.324	0.0
	27	-0.069	-0.003	0.0	- .008	- .004	0.0	- .006	- .003	0.0
D + I	16	-0.105	-6.626	0.0	0.0	-11.63	0.0	0.0	-9.294	0.0
	18	-0.106	-6.298	0.0	.002	-10.82	0.0	- .002	-8.579	0.0
	23	-0.109	-2.747	0.0	.007	- 4.552	0.0	- .006	-3.46	0.0
	27	-0.113	-0.004	0.0	.012	- .006	0.0	- .009	- .004	0.0
D + W(1)	16	-0.065	-4.556	12.09	0.0	-7.685	32.08	.004	-6.222	20.75
	18	-0.066	-4.32	11.90	- .001	-7.148	30.64	-.001	-5.746	19.69
	23	-0.068	-1.877	7.46	- .005	-3.007	18.24	-.004	-2.323	11.28
	27	- .069	-0.003	1.928	- .008	- .004	4.172	-.006	- .003	2.372
D + I + W(1)	16	-0.105	-6.626	12.09	0.0	-11.63	32.08	0.0	-9.294	20.75
	18	-0.106	-6.298	11.09	- .002	-10.82	30.64	-0.002	-8.579	19.69
	23	-0.109	-2.747	7.46	- .007	- 4.552	18.24	-0.006	-3.46	11.28
	27	-0.113	-0.004	1.928	- .012	- .006	4.172	- .008	- .004	2.372

MAXIMUM BENDING STRESSES (ksi)

Load Case	Section	Base Model	Sign Model #1 (Full Signs)	Sign Model #2 (Central Signs)
D+I	Beam $\mathbb{Q}$	11.23	18.5	16.57
	Col. Base	8.113	13.38	10.02
D+I+W	Beam $\mathbb{Q}$	17.3	37.41	29.4
	Col. Base	18.65	38.44	22.9

NOTE:

Wind Load W(1) is based on a wind spend of 70 mph in the + z direction.

TABLE 6.7

Natural Frequencies and Periods for All Monotube Structure Models

Model	Mode	Natural Frequency (cps)		Natural Period (sec.)	
		2D	3D	2D	3D
Base	1	0.783	0.47	1.28	2.13
	2	1.494	0.783	0.67	1.28
	3	3.033	1.494	0.33	0.67
	4	6.377	1.91	0.157	0.524
	5	10.15	3.033	0.099	0.33
	6	15.61	4.083	0.064	0.245
	7	23.65	6.241	0.042	0.16
	8	38.28	6.377	0.026	0.157
	9	39.9	9.004	0.025	0.111
	10	44.3	10.15	0.023	0.099
Column Model #1 (1.5 I col.)	1	0.8102	0.4807	1.234	2.08
	2	1.709	0.8102	0.585	1.234
	3	3.143	1.709	0.32	0.585
	4	6.51	2.026	0.154	0.494
	5	10.31	3.143	0.097	0.32
	6	15.73	4.384	0.064	0.228
	7	23.997	6.51	0.042	0.154
	8	37.43	6.557	0.207	0.153
	9	38.734	8.99	0.026	0.111
	10	43.756	10.31	0.023	0.097
Column Model #2 (1.25 I col.)	1	0.799	0.476	1.25	2.1
	2	1.6076	0.799	0.622	1.25
	3	3.095	1.6076	0.323	0.622
	4	6.453	1.976	0.155	0.506
	5	10.23	3.095	0.098	0.323
	6	15.68	4.253	0.064	0.235
	7	23.84	6.414	0.042	0.16
	8	37.85	6.453	0.026	0.155
	9	39.25	8.999	0.025	0.111
	10	43.98	10.24	0.023	0.098
Beam Model #1 (1.5 I Beam)	1	0.8736	0.5297	1.145	1.90
	2	1.509	0.8736	0.663	1.145
	3	3.32	1.509	0.30	0.663
	4	6.725	1.99	0.149	0.503
	5	11.17	3.32	0.09	0.30
	6	17.56	3.939	0.057	0.254
	7	24.47	6.385	0.041	0.157
	8	39.4	6.725	0.025	0.149
	9	40.98	9.411	0.024	0.106
	10	46.4	11.17	0.022	0.09

TABLE 6.7 (Continued)

Natural Frequencies and Periods for All Monotube Structure Models

Model	Mode	Natural Frequency (cps)		Natural Period (sec.)	
		2D	3D	2D	3D
Beam Model #2 (1.25 I beam)	1	0.834	0.503	1.2	1.99
	2	1.505	0.834	0.664	1.2
	3	3.2	1.505	0.313	0.664
	4	6.58	1.964	0.152	0.51
	5	10.7	3.2	0.093	0.313
	6	16.72	4.01	0.06	0.25
	7	24.02	6.32	0.042	0.16
	8	38.94	6.58	0.026	0.152
	9	40.5	9.22	0.025	0.11
	10	45.7	10.7	0.022	0.093
Span Model #1 (60' span)	1	1.6035	0.853	0.624	1.17
	2	1.9066	1.614	0.524	0.62
	3	6.352	1.917	0.157	0.52
	4	13.46	3.07	0.074	0.33
	5	21.373	6.18	0.047	0.162
	6	39.76	6.383	0.025	0.157
	7	42.353	10.43	0.024	0.096
	8	47.37	13.464	0.021	0.074
	9	62.913	17.254	0.016	0.058
	10	76.38	21.47	0.013	0.047
Span Model #2 (120' span)	1	0.66		1.52	
	2	1.392		0.72	
	3	2.453		0.41	
	4	4.841		0.21	
	5	7.543	*	0.13	*
	6	11.44		0.09	
	7	17.17		0.058	
	8	27.91		0.036	
	9	34.26		0.029	
	10	39.91		0.025	
Sign Model #1 (Full Signs)	1	0.471	0.274	2.12	3.65
	2	0.8023	0.471	1.25	2.12
	3	1.36	0.8023	0.74	1.25
	4	2.94	0.84	0.34	1.19
	5	4.79	1.36	0.21	0.74
	6	8.324	2.11	0.12	0.47
	7	11.344	2.94	0.088	0.34
	8	16.76	3.623	0.06	0.28
	9	20.90	4.79	0.048	0.21
	10	24.84	6.316	0.04	0.16

*Inconsistent results; reliability is doubtful

TABLE 6.7 (Continued)

Natural Frequencies and Periods for All Monotube Structure Models

Model	Mode	Natural Frequency (cps)		Natural Period (sec.)	
		2D	3D	2D	3D
Sign Model #2 (Central Signs)	1	0.527	0.326	1.9	3.07
	2	1.165	0.526	0.86	1.9
	3	2.384	1.17	0.42	0.855
	4	7.183	1.78	0.14	0.56
	5	12.52	2.384	0.08	0.42
	6	15.61	4.84	0.064	0.21
	7	21.93	5.99	0.046	0.167
	8	33.70	7.18	0.03	0.14
	9	37.02	8.28	0.027	0.12
	10	39.76	12.52	0.025	0.08

behavior of the structure is dominated by the in-plane charactertistics. There does not seem to be any similar relationship present for span Model 2. The frequencies for the 3D case that are indicated are distinctly at odds with the 3D behavior of similar structures. These data do not appear reliable, but no rational explanation can be offered for these numbers.

Table 6.7 also indicates that as the stiffness of the structure increases, the natural frequencies for the corresponding modes do the same. In addition, this increase seems to be almost linear. Therefore, by knowing the natural frequencies of the Base Model and Column Model 1, for example, the natural frequencies of Column Model 2 can be predicted without an exact analysis of the model.

Based on the above observation and similar relationships that apply to the static deflections and stresses, it was decided to perform the remainder of the dynamic analysis with only one of the models in each category. Therefore, column model 1, beam model 1, and span model 1 were retained knowing that the behavior of the other models can be fairly accurately predicted by extrapolation.

It is emphasized that the deflections and stresses for the two sign models are significant. However, due to the large number of possible sign locations and considering the fact that for the sign models, no direct relationship exists between any two models to allow interpolation or extrapolation, it was decided to discontinue the study of this parameter for the remainder of the dynamic analysis.

A complete forced vibration analysis similar to that discussed in Chapter 5 was carried out for the Column, Beam and Span Models 1 only, assuming that the wind could blow on the structure at a constant speed for a duration of 32 seconds. The dynamic analysis of these models indicated that as long as resonance of the structure does not occur, the stresses at the midspan and the column base are very small compared to the static stresses. Therefore, the primary concern in the dynamic analysis is the maximum vertical displacement at the midspan of the beam due to vortex shedding. For this reason, plots of the maximum vertical midspan deflection versus the wind speed for the complete deterministic range of wind speeds were developed. These plots are shown in Figs. 6.4, 6.5 and 6.6 for Column, Beam and Span Models 1, respectively.

Figures 6.4 through 6.6 indicate that there is a peak corresponding to the first mode frequency of each model. Because vortex shedding displacements take place in the plane of the structure, these peaks correspond to the 2D frequencies of the models. The second and third mode frequencies also correspond to peak displacements. However, these displacements are much smaller than that of the first mode. Each model also exhibited large displacements at wind velocities which correspond

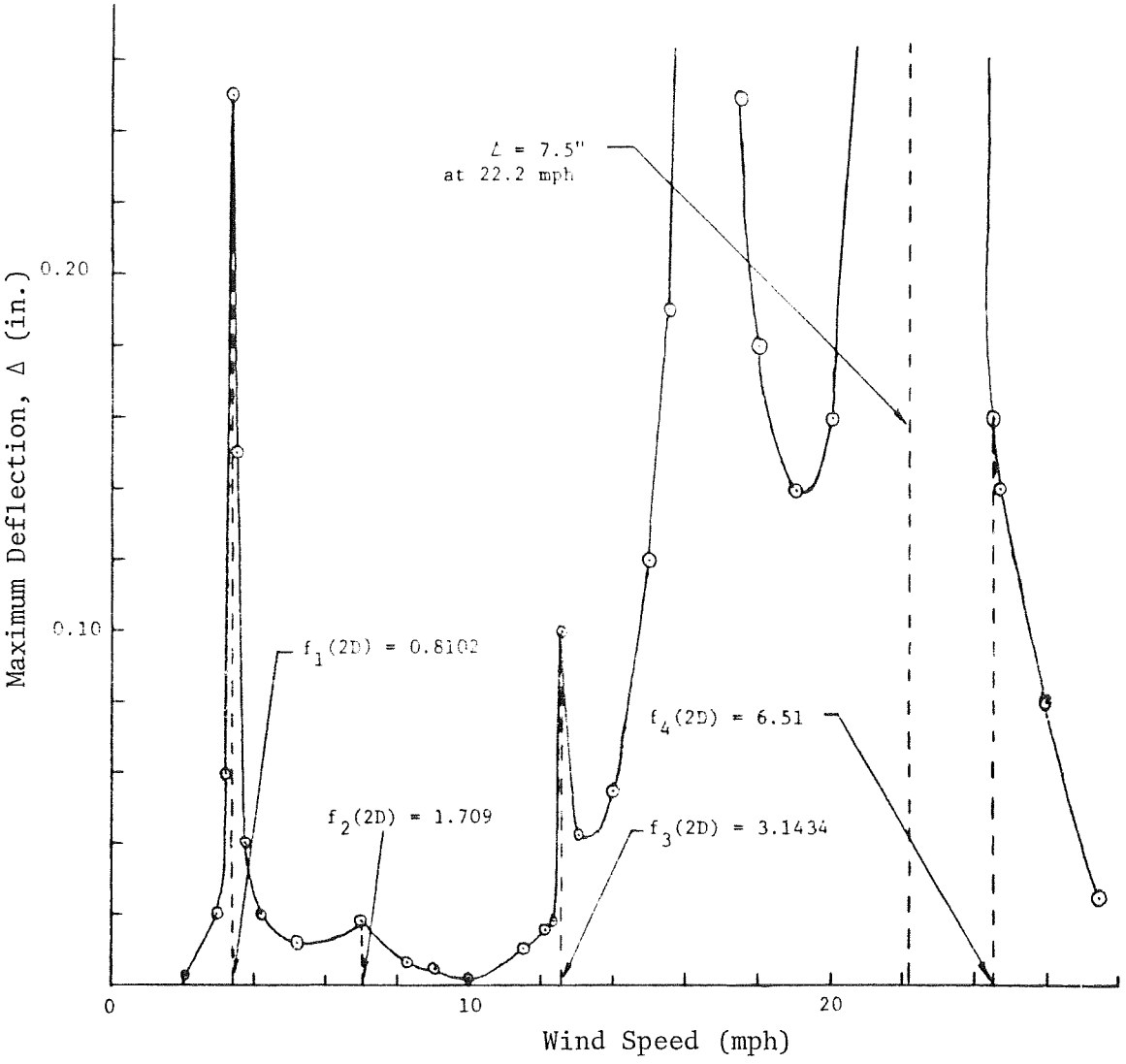

Fig. 6.4 Maximum Vertical Dynamic Deflections at Midspan of Beam for Different Wind Speeds for Column Model #1

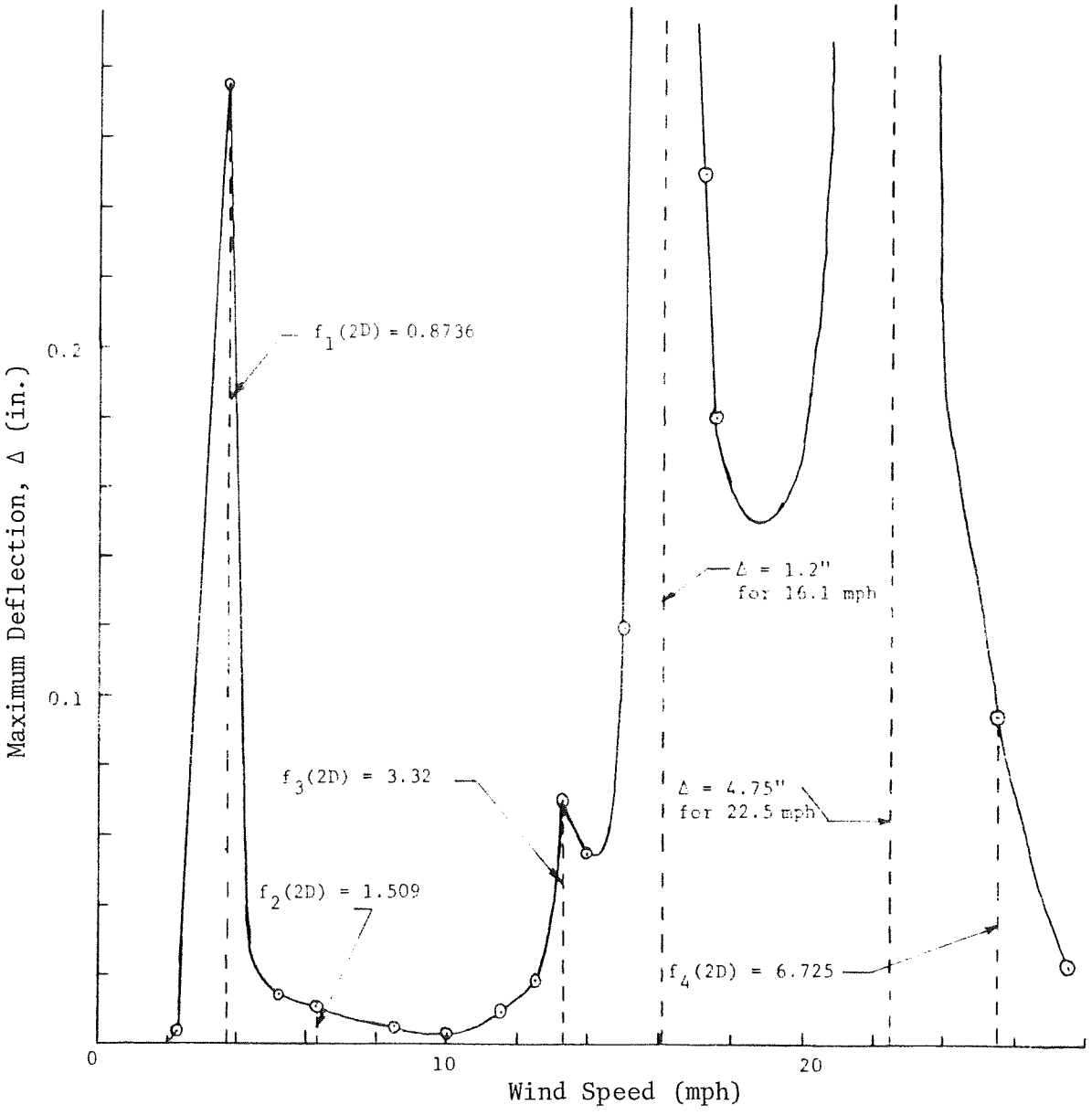

Fig. 6.5 Maximum Vertical Dynamic Deflections at Midspan of Beam for Different Wind Speeds for Beam Model #1

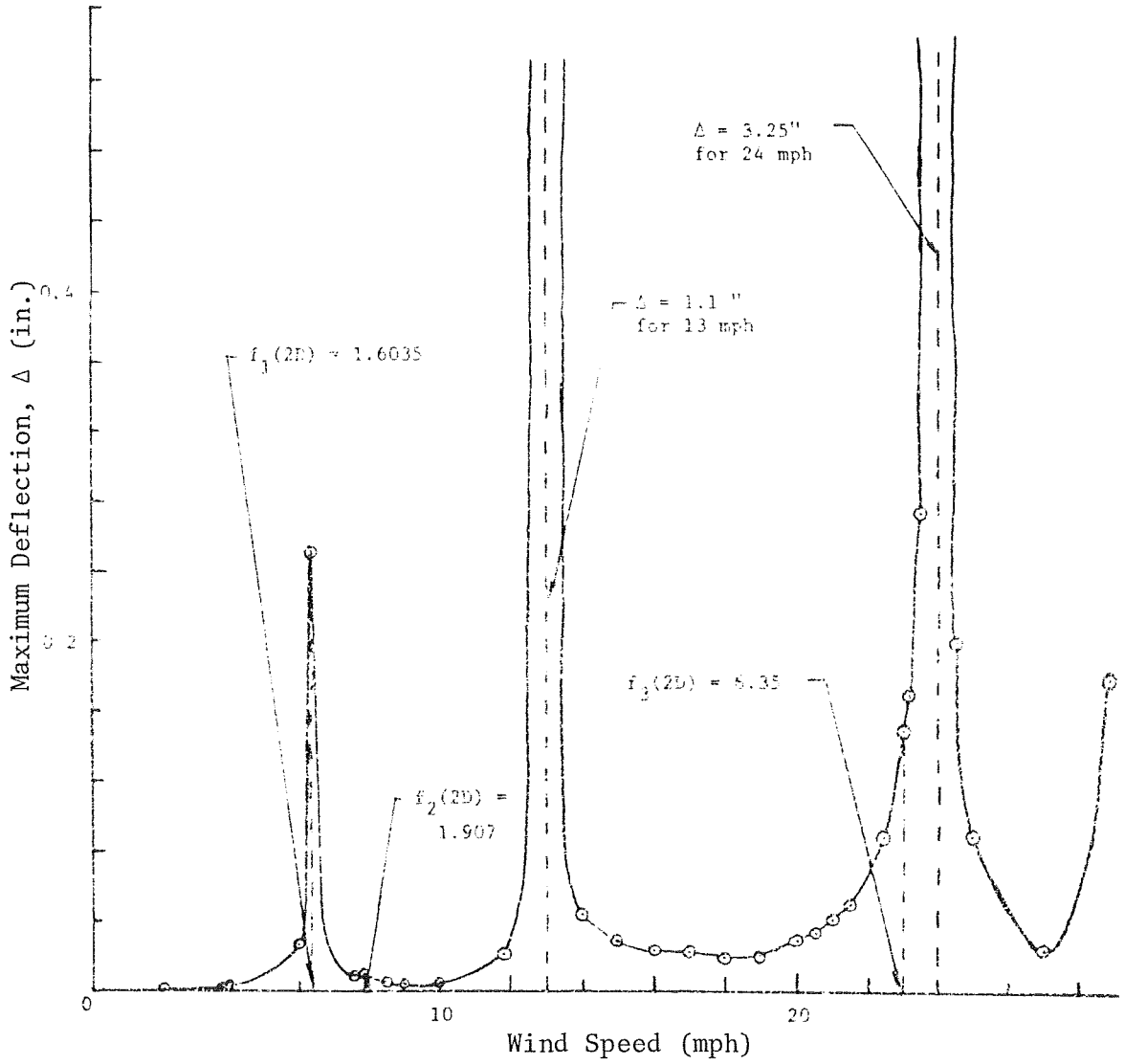

Fig. 6.6 Maximum Vertical Dynamic Deflections at Midspan of Beam for Different Wind Speeds for Span Model #1

to the resonance frequency of the structure. However, these wind speeds do not necessarily correspond to any particular natural frequency of the structure.

In order to make use of the data in Figs. 6.4 through 6.6 and 5.7, which provides the same type of information for the base model, it is necessary to define an allowable maximum displacement due to vortex shedding at the midspan of the beam. Two factors were taken into account in determining this deflection. First, it has been shown previously that the static stresses in these structures are low and well within the elastic range. Secondly, when wind forces are considered, the allowable stresses can be increased by one-third (11, 12). Based on these factors, it was decided to define the maximum allowable dynamic deflection as the deflection which would result in the same stresses. Therefore, a dynamic deflection equal to one-third of the static vertical deflection at midspan was selected as the maximum allowable value. For wind speeds causing smaller displacements, the combined gravity and wind stresses will not govern, having taken advantage of the one-third increase in the allowable stresses.

Based on the above criterion, the maximum allowable dynamic deflection for each model was calculated and the results are presented in Table 6.8. The ranges of wind speeds corresponding to these displacements were conservatively obtained from Figs. 5.7 and 6.4 through 6.6. It is important to note that the ranges of the wind speeds are very small; the largest being 1 mph (12.6 to 13.6 mph for Span Model 1).

6.3 Significance of Parameters

Based on the analyses of the models, several observations can be made with respect to the effects of the parameters in the overall behavior of the structure.

As far as the static deflections of the structures are concerned, moderate increases in the stiffness of the columns or the beam do not result in a significant reduction of the deflections. Changing the span of the structure, however, does affect the midspan deflections considerably, both for the in-plane as well as out-of-plane cases. The larger the area of the signs and the closer the signs are placed to the midspan, the larger the deflections. It must be noted that the sign location has a considerable effect on the deflections due to ice loads, as the signs will accumulate ice and further increase the midspan deflection. The detailed effects of the various sign placement locations is a subject that should be given further study.

The static bending stresses were also affected by the changes in the parameters. Increasing the column stiffness resulted in a reduction of the stresses in the column, while increasing the beam stiffness

TABLE 6.8 Static and Dynamic (Wind Vortex Shedding) Deflections at Midspan

Model	Max. Static Deflection (in)		Resonance Wind Speed (mph)	Δ_H Static at Resonance (in)	$\frac{\Delta V \text{ Static}}{3}$ (in)	Range of Wind Speed (mph) Corresponding to $\Delta V/3$	Δ_V Static + 1/3 Δ_V Static (in)	$\frac{\Delta H}{\ell}$	$\frac{\Delta V}{\ell}$	(Δ_V Static + 1/3 ΔV Static)/ℓ	$\frac{\Delta H}{\ell}$
	ΔH	ΔV									
Base	12.09	6.63	22.0	1.19	2.21	21.8-22.5	8.84	$\frac{1}{99.3}$	$\frac{1}{181}$	$\frac{1}{136}$	$\frac{1}{1008}$
Column Model #1 (1.5 I col)	11.56	6.20	22.25	1.17	2.07	22.0-22.5	8.27	$\frac{1}{104}$	$\frac{1}{194}$	$\frac{1}{145}$	$\frac{1}{1026}$
Beam Model #1 (1.5 I beam)	8.69	6.19	22.5	0.9	2.06	22.2-22.8	8.25	$\frac{1}{138}$	$\frac{1}{194}$	$\frac{1}{146}$	$\frac{1}{1383}$
Span Model #1 (60' span)	3.5	1.26	13.1 24.1	0.12 0.41	0.42	12.6-13.6 23.6-24.6	1.68	$\frac{1}{206}$	$\frac{1}{572}$	$\frac{1}{429}$	$\frac{1}{1735}$
Remarks	wind= 70 mph	(DL+IL)		$\Delta=\Delta H\ (\frac{V}{10})^2$	$\frac{(3)}{3}$		(3) + (6)	$\frac{(2)}{\ell}$	$\frac{(3)}{\ell}$	$\frac{(8)}{\ell}$	$\frac{(5)}{\ell}$

reduced the stresses in the beam. Again, significant changes in the stresses were noticed as a result of changing the span of the structure. Similarly, the location of the signs had a major role in the calculated stresses in the beam and the column. The stresses in structures supporting large areas of traffic signs can be high and must be investigated carefully. It is a question whether monotube structures are suitable for large groups of signs.

The parameters did not appear to have any influence on the dynamic displacements at the midspan of the beam as long as resonance was not occurring. For example, for all models, the maximum peak displacement corresponding to the first natural frequency was between 0.24 and 0.3 inches. All models exhibited large displacements at higher wind speeds due to resonance. However, the magnitude of these displacements for different models is meaningless, since in theory undamped resonance leads to infinite deflections.

The change in the parameters did not have any appreciable effect on the dynamic stresses either. These stresses were found to be very small (less than 1 ksi), and therefore negligible for all practical purposes.

As far as the natural frequencies of the structures are concerned, they were found to be insensitive to the changes in the column and beam stiffness. The most significant change occurred due to the change in span and the location of the signs.

All models indicated that for two wind speeds, which did not necessarily coincide with the natural frequencies, resonance would occur. Although the conditions of resonance are undesirable, several points need to be explained here. First, the structure was analyzed assuming that structural damping was equal to zero. This assumption, although conservative, is not realistic for any structure. Secondly, the resonance of the structure in many cases resulted from winds blowing at a constant speed for the relatively long duration of 32 seconds. It is improbable that this condition will be present in the field where winds usually blow in gusts and the velocity changes rapidly. Thirdly, for all parameters the range of wind speeds over which resonance occurs is very small (i.e., less than or equal to 1 mph). It is therefore highly unlikely that resonance of these structures will take place. However, to answer this question with certainty, extensive field testing of monotube structures is needed.

7. DEVELOPMENT OF DESIGN RECOMMENDATIONS

7.1 General Introduction

The preceding chapters have detailed the static and dynamic behavior of monotube structures, as well as the influence of the primary structural parameters. In addition, the two- and three-dimensional responses have been evaluated. Using the loads and load combinations that are realistic for these types of structures, the stress and deflection data that have been generated give a detailed illustration of what governs their behavior. In other words, it is now possible to present the considerations that must be made by a designer or a evaluator of monotube structures in order that they will exhibit satisfactory performance in service.

It is reiterated that the design recommendations that are given in the following do not consider fatigue in the structure, nor do they cover the design criteria for the connections that are used for typical structures. Both of these are topics for potential future research.

7.2 Static versus Dynamic Behavior

Chapters 4 and 5 give the complete data for the static and dynamic analyses of the base model monotube structure and Chapter 6 evaluates the influence of beam and column stiffnesses, beam span and traffic sign placement. In the comparison of static and dynamic behavior, only the in-plane response is of interest due to the interaction of the static and dynamic load effects. Out-of-plane characteristics are dominated by the static equivalent of the governing wind speed load, recognizing that the influence of drag forces is limited for the type of circular cross sections that are used in these structures. The beam-to-column connection also plays an important role in this respect.

It has been found that for the deterministic range of wind speeds, that is, from 0 to approximately 27-29 mph, the dynamic effect of the wind load generally will not govern the behavior of monotube structures. The dynamic effect is the vortex shedding that occurs in the plane perpendicular to the direction of the wind, as explained in Chapter 5.6.1. Although the wind blowing against the structure produces in-plane vibrations, the magnitude of the maximum amplitude is one order of magnitude less than the static displacements due to dead load and dead load plus ice load. The corresponding dynamic increases in the level of stress are therefore well below 1 ksi, and hence insignificant for the strength of the structure.

It has been shown that it is theoretically possible to attain resonance in the structure due to the vortex shedding. This, of course, cannot be found by a pure static analysis. However, the resonance was

obtained on the assumption that the wind would be blowing at a constant speed for a certain length of time. In addition, the structure was analyzed on the basis that it did not possess any damping capability. It is consequently reasoned that resonance is highly unlikely to occur under realistic wind loading conditions for actual sign structures. It is not practically justified to impose design criteria that are based on this form of behavior. Rather, the observation is made that as long as the dynamic deflection increment is less than one-third of the static value, the static behavior will govern. This occurs for all but one or two narrow wind speed ranges; due to the remote likelihood that the wind can maintain a specific velocity for anything but a short time, the static response provides the necessary design data.

The out-of-plane behavior of the monotube structure is governed by the deflection that is caused by the statical equivalent of the force of the wind blowing at a certain speed. This is not a dynamic phenomenon for these structures. It will therefore be examined in the following section of this chapter. However, the magnitude of the wind speed that is chosen is important; in this study, a velocity of 70 mph was selected from the applicable iso-tach map. This is an extreme which nevertheless may be realistic. On the other hand, design of the structure on the basis of limit states design principles, such as those that are given in the proposed Load and Resistance Factor Design (LRFD) Specification of AISC (25), would alleviate such difficulties. Thus, the appropriate wind load factor would cover the problem of the magnitude of the wind load. These problems are also discussed in the most recent edition of the loading standard of the American National Standards Institute (ANSI), A58.1-1982(26).

On the basis of the preceding evaluations, it is shown that a static evaluation of the monotube structure will be sufficient to ensure that deflections and levels of stress are satisfactory. The $d^2/400$ requirement, which stems from dynamic analyses of other sign structures, can neither be satisfied nor is it a rational design criterion for monotube structures. The gravity load deflections do not produce excessive levels of stress in the members; if a user feels that a certain dead load deflection level should not be exceeded, this can be satisfied by specifying a camber or a beam splice detail that produces the requisite camber by a suitable splice plate angle. The latter is schematically shown in Figure 7.1.

Additional details regarding the dynamic versus the static deflection levels and the corresponding wind speeds, etc., are given in Table 6.8, including the allowable deflection-to-span ratios that are obtained on the basis of the concept of the one-third increase over the static values. Vertical deflection-to-span ratios of 1/136 to 1/429 are structurally acceptable; however, it may be decided to reduce these for

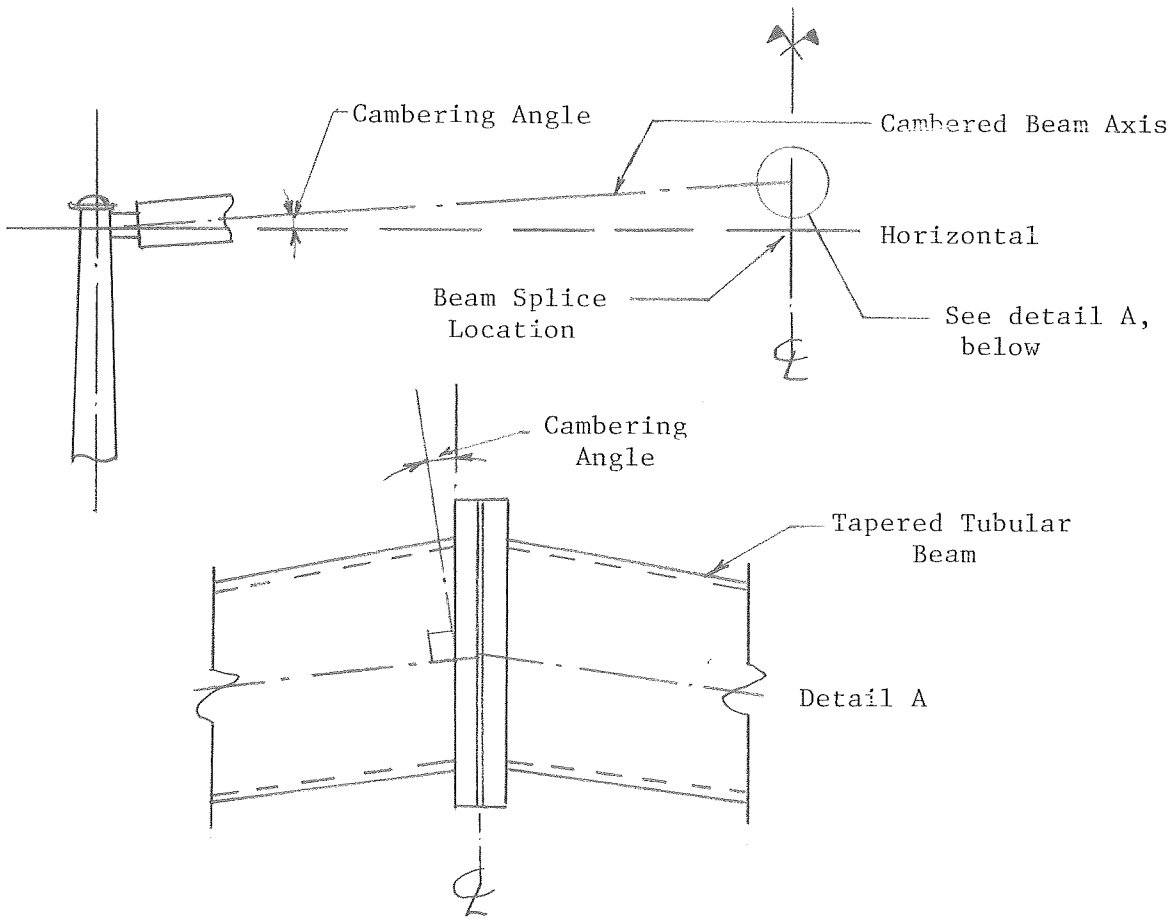

Fig. 7.1 Beam Splice Detail to Achieve Suitable Camber

aesthetic reasons. That is a choice that must be made by the owner of the structure.

7.3 Two- vs. Three-Dimensional Analysis

The results of the two- and three-dimensional static analyses have been discussed in detail in Chapter 4 and the effects of the various structural parameters are evaluated in Chapter 6. Due to the independence of the in-plane (due to gravity loads) and out-of-plane (due to wind load) deflections, it has been shown that these data may be determined separately. That is, gravity load displacements due to dead load alone and due to dead plus ice load can be computed for the in-plane response of the monotube structure, preferably by using a plane frame method of analysis. A plane frame computer program is the most convenient, because it is then possible to specify the in-plane stiffness of the beam-to-column connection. The out-of-plane behavior of the beam can be determine by analyzing the member as simply supported at the ends, due to the very small out-of-plane bending stiffness of the connection. In this direction, the beam is subjected to the static equivalent of the wind load, determined in accordance with the applicable load code (e.g., ANSI A58.1-1982(26)). However, these simple support conditions are only realistic for the type of connection that has been used for the monotube structures evaluated here. They cannot be applied in the case of connections with a measure of out-of-plane stiffness.

The above procedure is not especially complicated, although it is recognized that the out-of-plane deflection of the beam cannot be ignored. However, the ease of computation allows the designer or evaluator to incorporate three-dimensional structural behavior into a design format that is essentially based on single member evaluation.

Several limiting approaches can be utilized in assessing the in-plane stiffness of the beam-to-column connection, as follows:

(a) In-plane connection stiffness equal to zero: This treats the connection as a pin, and is conservative insofar as beam deflections and stresses are concerned. However, it will lead to an under-estimation of the stresses at the column base, and is also unconservative for the design of the connection itself.

(b) In-plane connection stiffness equal to that of a fully rigid connection: This is unconservative for the beam deflections and stresses since it will indicate values that are smaller than the actual ones. By the same token, it will produce a conservative estimate of the bending stresses at the column base. This approach is not recommended for practical use.

If a plane frame computer program is available, it is recommended that the actual elastic bending stiffness of the connection be used. This will produce accurate estimates of the in-plane (gravity load) deflections and stresses, and will also incorporate the additional normal stresses at the column base that result from the transferred connection moment.

Independent of the out-of-plane analysis of the beam, which can be realistically based on simply supported ends, the out-of-plane deflection at the top of the column can be determined by treating the column as a cantilever beam. A concentrated load equal to the reaction on the column from the beam due to wind load on the latter is applied at the level of the beam-to-column connection. This produces an out-of-plane displacement of the top of the column as well as a bending moment at the base. For example, this deflection equals 1.928 inches for the column in the Base Model of the monotube structure, as shown in Table 4.3.

The combined effect of in-plane and out-of-plane bending moments on the circular cross section is easily obtained by making a vector addition of the biaxial moments. The following may be utilized in finding the maximum stresses:

(a) Beam Stresses: The in-plane bending moment is given by M_z and the out-of-plane bending moment is M_y (refer to orientation of axes in Fig. 4.8). These are determined independently of each other, as explained earlier in this chapter. The maximum bending stress is then found as

$$\sigma_{max} = \frac{1}{S} \sqrt{M_z^2 + M_y^2} \qquad (7.1)$$

where S is the elastic section modulus of the tubular cross section.

(b) Column Stresses: The in-plane bending moment is given by M_z and the out-of-plane moment is M_x. The maximum bending stress in the cross section is then found from Eq. (7.1), replacing M_y with M_x.

Resultant deflections due to the combined effect of gravity loads and wind loads can be found as explained in Chapter 4; Fig. 4.9 gives an illustration of this as it applies to the Base Model under the combined action of dead, ice and wind loads. However, it is noted that the resultant deflection has little practical meaning. Rather, the pure in-plane and out-of-plane components are the data that are normally needed for design and design evaluations of planar structures.

7.4 Proposed Analysis Procedure

The following procedure is recommended for a detailed evaluation or design of a monotube span-type sign structure. The steps have been developed in accordance with the analyses that are described in the preceding chapters of this report.

(a) Structural Discretization: The beam and column members are discretized into a suitable number of elements. Each element is prismatic, with cross sectional and other properties equal to those at mid-length of the element. The locations of the traffic signs should correspond to specific nodes. The in-plane bending stiffness of the beam-to-column connection reflects that of the real one; a rectangular element is a good choice. The out-of-plane bending stiffness is therefore small. The column base is assumed to be fixed.

(b) Load Computation: The dead load of the structure, including the traffic signs, is distributed in accordance with the element sizes and the locations of the signs. If required in the geographical area where the structure is to serve, ice loads are computed in accordance with the AASHTO rules (1) and distributed in relation to element sizes. Wind loads are based on the statical equivalent of the wind pressure for the code-mandated speed, and are distributed in relation to element sizes and sign locations.

(c) Load Combinations: The response of the structure is to be determined for the following loads and load combinations:

(1) Dead Load
(2) Dead + Ice Load
(3) Wind Load

Combination (2) applies only if ice is a realistic expectation in the particular geographical area. The combined effect of (1) and (3), or (2) and (3), can be obtained by an appropriate addition of deflections and stresses, since these structures behave elastically under service conditions.

(d) In-Plane Response: Deflections and stresses are computed on the basis of loads (1) and (2) above. The data for the midspan of the beam are likely to be the most important. The stress levels are compared with those of the applicable material codes; it is anticipated that the requirements will be easily met. Gravity load deflection magnitudes should be compared to the span of the monotube structure that is being designed/evaluated; deflection-to-span ratios of 1/150 or less

are acceptable from strength as well as serviceability standpoints. It may be elected to camber the beam; an amount of camber on the order of the dead load deflection will be suitable. However, it is noted that this is not normally done unless aesthetic criteria require it. Stresses in the column can be easily checked. However, it is expected that in most cases these will be very small and therefore can be neglected.

(e) Out-of-Plane Response: Deflections and stresses are computed on the basis of the wind load by itself. The data for the midspan of the beam and the base of the column are likely to be the most important, although the deflection at the top of the column also merits consideration.

(f) Combined Structural Response: The maximum bending stresses in the structure are determined by a vector addition of the biaxial moments from (d) and (e) above. In-plane and out-of-plane deflections are not combined; rather, their individual values are compared with the performance criteria (i.e., serviceability) of the governing specification. The $d_2/400$ requirement is not applicable to monotube structures.

7.5 Simplified Criteria for Structural Evaluation

The following criteria and procedures are recommended for use by agencies and other organizations when a particular monotube structure is to be evaluated for acceptability.

(a) Material Data: Detailed data must be provided by the designer/manufacturer on the types and grades of steel that are to be used.

(b) Loads: The sizes of the members and the traffic signs must be provided, along with ice loads, if any, and the applicable maximum wind speed.

(c) Method of Analysis: The designer/manufacturer must supply details on the method of analysis that has been used, including assumptions regarding support conditions, structural discretization, and so forth. These details are needed for the evaluation of the results that are given.

(d) In-Plane Deflections and Stresses: The designer/manufacturer must supply detailed data for dead load and dead plus ice load (if applicable) deflections and stresses for the members; in particular, the maximum values for the beam. The stress levels are not likely to govern; rather, a maximum beam

deflection-to-span ratio of 1/150 is preferred. If deemed unsightly, the beam may be cambered for dead load. The dynamic response of the structure will be adequately accounted for if deflections as above are obtained.

(e) Out-of-Plane Deflections and Stresses: The out-of-plane deflections and stresses due to the static equivalent of the wind load must be available for evaluation. The deflections due to this extreme wind load should be regarded only as indicative of the behavior rather than being taken as absolute magnitudes. This also applies to the wind load stresses. If meteorological data are available for wind speeds and directions, a more realistic evaluation of deflections can be based on a sustained, lower wind velocity, such as, for example, 15 to 25 mph.

(f) Combined Stresses: The bending stresses due to the biaxial bending of the beam and the column are vector additive to indicate a maximum probable level.

(g) Method of Design Evaluation: Due to the serviceability characteristics of the monotube structures, it is generally preferable to utilize a limit states design (LRFD) approach. However, at this time the available design specifications are based on allowable stress principles. This will be satisfactory as long as it is recalled that stiffness, rather than strength, governs the design.

8. CONCLUSIONS AND RECOMMENDATIONS

8.1 Conclusions

The following findings have been made in this study of the behavior of monotube span-type sign structures.

1. The static response of the structure can be determined separately for in-plane and out-of-plane loads. That is, the deflections and stresses due to gravity loads are not influenced by those due to wind loads.

2. For the type of monotube structure that has been evaluated here, the best method of structural analysis for gravity loads will be that of a regular two-dimensional plane frame. This should be able to model the beam-to-column connection as well.

3. The beam-to-column connection model should have shear force and bending moment capacities that are approximately the same as the real connection. An element with a rectangular cross section was used in this study, providing some in-plane capacity, but essentially acting as a pin in the out-of-plane direction.

4. Dead and ice (if applicable) loads should be determined on the basis of material weights, including traffic signs and local codes. Wind load should be based on meteorological wind speed data, and the static equivalent can be determined as illustrated by codes.

5. Due to the independence of the in-plane and out-of-plane responses, a three-dimensional analysis of the monotube structure is not needed.

6. Out-of-plane deflections due to the static equivalent of the wind load can be computed by assuming that the beam is simply supported. The out-of-plane deflections at the top of the columns can be found by analyzing these as cantilevers fixed at the base and subjected to a concentrated load at the top.

7. The monotube structures are not able to satisfy the current AASHTO dead load deflection requirement known as the $d^2/400$-criterion. The actual in-plane deflections are significantly larger than those indicated by $d^2/400$.

8. The stress levels associated with the actual deflections are well below the magnitudes of the allowable stresses, even though the maximum deflection is much larger than the $d^2/400$-level.

9. The out-of-plane deflections associated with the maximum wind speed, which was set equal to 70 mph for this study, vary from 3.5 to 12.1 inches for monotube structures with spans from 60 feet to 100 feet. The largest deflection-to-span ratio (horizontal) was approxiamtely 1/100. It is emphasized that this is a hypothetical condition which occurs if a constant wind of a speed of 70 mph is acting on the structure.

10. The combined effects of the in-plane and out-of-plane (i.e., biaxial) bending did not produce stresses larger than the allowable value for any load combination and any structure.

11. The design of monotube structures is governed by stiffness (i.e., deflection) rather than strength (i.e., stress) criteria. Allowble stresses were never exceeded, even though large deflections were recorded.

12. The study investigated the influence of varying beam and column stiffness by 25% and 50% over the base model. The beneficial effects of this were limited, and the cost of same appears to rule out such a device if reduced deflections are sought.

13. The study examined the behavior of monotube structures of spans equal to 60, 100 and 120 feet. Although some of the deflections were large, the stress levels were not above the allowable.

14. The most extreme structure that was examined had a span of 100 feet and 5 feet high traffic signs placed along the full span. The largest beam and column stresses for combined dead, ice and wind loads were 37.4 and 38.4 ksi, respectively. This compares to an allowable stress of 44 ksi (including wind) for the common grade of steel that is used for these structures (F_y = 55 ksi). The net horizontal (i.e., out-of-plane due to wind of speed 70 mph) deflection for the beam of this case was (20.75-2.37) = 18.38 inches. This gives an extreme deflection-to-span ratio of approximately 1/65. This is not acceptable by itself, but the extreme nature of the loads and the structure must be borne in mind.

15. The dynamic behavior under vortex shedding conditions was examined in detail for all of the different monotube structures that were considered. The wind speeds were limited to those producing a deterministic response implying Reynolds numbers less than 3×10^5 and wind speeds of less than 27-29 mph.

16. Dynamic responses due to wind drag forces were not investigated, both because of the limited amount of data as well as the fact that tubular cross sections offer little resistance to drag.

17. The dynamic deflection increments that were produced by the vortex shedding were one order of magnitude (or more) smaller than the static values for almost all wind speeds. Their influence on stress and deflection levels is therefore not important, especially when it is recalled that the allowable stress is increased by one-third for any load combination that involves wind. (It is noted that vortex shedding produces in-plane displacements when the wind acts perpendicularly to the plane of the structure.)

18. Resonance was found to occur for certain frequencies of vortex shedding that did not match exactly any natural modes of vibration of the structures. However, this phenomenon was found to occur only when the wind speed was maintained at a constant value for a longer period of time. In addition, the resonance-producing wind speeds were all within very narrow ranges: the largest range was 1 mph.

19. It is believed that the resonance condition is not serious, for several reasons. They are as follows:

    (a) Wind speed must be maintained within a narrow range and for a prolonged period in order for resonance to occur.

    (b) The structural analysis was performed on the assumption that the monotube structure does not possess any damping capability.

    (c) The apparent strength of the material increases with the rate of loading.

20. Analysis and design evaluation criteria are presented for use by designers and agencies that utilize monotube sign structures. It is observed that stress levels are normally easy to satisfy. Deflections should not be limited to the $d^2/400$-value; rather, if aesthetic reasons call for reduced deflections, this can be attained by specifying the use of a cambered beam.

21. Analysis and design can follow the criteria of any suitable design specification. Only static evaluations are needed, and the in-plane and out-of-plane responses can be dealt with indpendently.

8.2 Recommended Future Studies

This study has been the first major investigation of monotube sign support structures subjected to static and dynamic (wind) loading. As is the case for most first studies, time and budgetary constraints did not permit a detailed investigation of all aspects of the problem. To identify the areas of needed research, and to provide an indication of some of the limitations of the design recommendations presented in Chapter 7, the following gives a description of additional topics that are in need of study:

1. Analytical Modeling and Field Testing: In developing the analytical models for this study, many assumptions were made with respect to the damping characteristics of the structure, the degree of fixity at the beam-to-column connection and the column base, and the speed and duration of the wind blowing at a constant velocity. Extensive field monitoring of monotube structures is needed to verify or modify these assumptions. In particular, the analytical study has been limited to wind speeds of approximately 27-29 mph, as explained in Chapter 5. Field testing is imperative in determining the behavior of monotube structures at higher wind velocities.

2. Evaluations of Fatigue Characteristics: The theoretical study presented here was based on the magnitude of the calculated stresses, which for most of the common types of monotube structures are relatively low. However, the ranges of these stresses are considerable as the direction and the speed of the wind changes. Although the design recommendations that are presented in Chapter 7 are in most cases governed by limitations on static deflections, a failure in such structures may be caused by fatigue. The results of the field testing will provide some information on the range of stresses in such important regions as the beam-to-column connection and the base of the column. Additionally, laboratory testing of these elements is recommended in order that their load carrying capacity and fatigue behavior under different stress ranges can be determined. Such tests should be conducted on full-scale connection and base details, utilizing the relevant stress ranges that have been observed in the field and through analytical studies. This will permit the classification of the connections and their details according to the AISC and AASHTO fatigue categories.

3. Behavior of Cantilever Structures: This study addresses the design of span-type structures where the beam is supported at both ends by columns. Sign-supporting cantilever structures, however, represent a major category of structures that have not

been considered. These are commonly designed as either a one-piece column with a continuous curved portion at the top to form the beam, or as a two-piece member where the straight beam is rigidly connected at one end to the top of the column. While both of these designs will develop bending and torsional moments at the column base, the latter requires additional attention to the connection of the beam to the column and of the base detail. It is expected that fatigue will be of greater concern in these structures due to the lower degree of redundancy. It is likely that the stress range at the column base will be larger than that in the span-type structures.

4. Use of Non-Circular Member Cross Sections: The monotube structures investigated in this study were constructed of circular tubular members. More recently, construction of sign support structures utilizing square or rectangular tubes has gained popularity. These structures differ in several ways from their circular counterparts. First, it is expected that drag forces will be a more severe problem with rectangular tubes and may not be ignored. Secondly, depending on the fabrication techniques, residual stresses and cold-working effects may be important for the rectangular tubes. This could play a major role for the life expectancy of these structures under fatigue conditions. Thirdly, the connections of the beam to the column for these structures are different from those used for circular tubes. This could have a significant effect on the static as well as the dynamic behavior of the structure.

9. REFERENCES

1. American Association of State Highway and Transportation Officials (AASHTO), "Standard Specifications for Structural Supports for Highway Signs, Luminaires, and Traffic Signals," AASHTO, Washington, D.C., 1975 (Revised 1978 and 1979).

2. American Society of Civil Engineers (ASCE), "Wind Forces on Structures," ASCE Transactions, Part II, Vol. 126, 1961.

3. Hayus, F., "Drag Measurements on One Square Section and Two Rectangular Sections with Different Corner Radii," CIDECT Report No. 1-NK-I-68-41, Brussels, Belgium, September, 1968.

4. Hay, J. S., "Forces on a Sign Gantry in Normally Directed Winds," Transport and Road Research Laboratory Monograph, England, 1978.

5. Zell, J. B., "Vehicle-Induced Gust Loads on Aluminum Overhead Sign Structures," New York DOT, Engineering Research and Development, Albany, New York, 1977.

6. Fung, Y. C., An Introduction to the Theory of Aeroelasticity, John Wiley and Sons, Inc., New York, 1955.

7. Mirza, J. F. and J. C. Smith, "State-of-the-Art Study of Tubular Members in Highway Structures," School of Engineering, North Carolina State University, January, 1970.

8. Illinois Department of Transportation, "Evaluation of a Louvered Panel for Use as Freeway Sign Background,"Bureau of Traffic, IDOT, August, 1971.

9. Sherman, D. R., "Tentative Criteria for Structural Applications of Steel Tubing and Pipe," American Iron and Steel Institute, Washington, D.C., August, 1976.

10. U. S. Steel Corporation, "Design and Construction Guide: Structural Steel Supports for Outdoor Advertising Signs," November, 1968.

11. American Institute of Steel Construction (AISC), "Specification for the Design, Fabrication and Erection of Structural Steel for Buildings," AISC, Chicago, Illinois, November, 1978.

12. American Iron and Steel Institute (AISI), "Specification for the Design of Cold-Formed Steel Structural Members," AISI, Washington, D.C., 1978.

13. Weaver, W., "Wind Induced Vibrations in Antenna Members," Journal of the Engineering Mechanics Division, ASCE, Vol. 87, No. EM1, January, 1961, pp. 141-165.

14. Kumar, V., C. Tung, J. Mirza, J. Smith, "Wind-Excited Vibrations for Tri-Chord Overhead Sign Support Structures," Transportation Research Board (TRR), N488, 1974.

15. Lengel, J. S. and M. L. Sharp, "Vibration and Damping of Aluminum Overhead Sign Structures," Highway Research Board, HRB No. 259, 1969.

16. Mirza, J. F., C. C. Tung and J. C. Smith, "Static and Dynamic Behavior of 'Tri-Chord Truss' Overhead Sign Support Structures," Highway Research Program, North Carolina State University, September, 1975.

17. Pelkey, R. E., "New Design Approach to Long-Span Overhead Sign Structures," Highway Research Record, HRB No. 34b, 1971.

18. Parcello, W. H., R. D. Seitz and B. F. McCollom, "Study of Fatigue Damage in Overhead Sign Supports and High Light Towers," Kansas DOT, January, 1981.

19. Parcell, W. H., "Study of Fatigue Damage in Overall Sign Supports and High Light Towers, Final Report, Kansas DOT, January, 1981.

20. Stoker, J. R. and J. P. Dusel, "Fatigue Characteristics of A307 and A325 Bolts," Transportation Laboratory, California DOT, 1982.

21. Mike, C., J. Fisher, and R. Slutter, "Fatigue Behavior of Steel Light Poles," Fritz Engineering Laboratory Report, No. 200.81.714.1, Lehigh University, December, 1981.

22. Seitz, R. D. and E. L. Utter, "Study of Fatigue Damage of Overhead Sign Supports and High Light Towers," Kansas DOT, Ongoing Study.

23. Kamel, H. and and R. R. Nagulpally, "GIFTS Primer: A First Introduction to the GIFTS-5 System," AME Department, The University of Arizona, Tucson, Arizona, December, 1983, Revised.

24. Clough, R. W. and J. Penzien, "Dynamics of Structures", McGraw-Hill, New York, 1975.

25. American Institute of Steel Construction (AISC), "Proposed Load and Resistance Factor Design Specification for Structural Steel Buildings", AISC, Chicago, Illinois, September 1, 1983.

26. American National Standards Institute (ANSI), "Minimum Design Loads for Buildings and Other Structures", ANSI Standard No. A58.1-1982, New York, March 10, 1982.